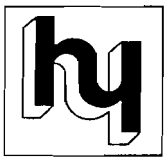

HR Wallingford

SINGLE LAYER ARMOUR UNITS FOR BREAKWATERS

NWH Allsop & DM Herbert

Report SR 259
March 1991

Address: Hydraulics Research Ltd, Wallingford, Oxfordshire OX10 8BA, United Kingdom.
Telephone: 0491 35381 International + 44 491 35381 Telex: 848552 HRSWAL G.
Facsimile: 0491 32233 International + 44 491 32233 Registered in England No. 1622174

FUNDING SUPPORT

This report describes work funded in part by the Department of the Environment under Research Contract PECD 7/6/107 for which the nominated officer was Dr R P Thorogood. The work was carried out in the Maritime Engineering Department of Hydraulics Research, Wallingford, under the management of Dr S W Huntington.

This work has also been supported by the Single Layer Armour Research Club formed by:

Coode Blizard	G Maunsell & Partners
Kirk McClure & Morton	Posford Duvivier
Shephard Hill & Co	Soil Structures (to 9/90)
Hydraulics Research	University of Bristol
South-West Polytechnic	States of Jersey

All members of the research club contributed to the project.

Further support was given by research grants from the Science and Engineering Research Council to the University of Bristol and South-West Polytechnic.

This report is published on behalf of the Department of the Environment and the Single Layer Armour Research Club, but any opinions expressed in this report are not necessarily those of the funding organisations.

Published by permission of the Controller of Her Majesty's Stationery Office, and on behalf of the Department of the Environment.

SINGLE LAYER ARMOUR UNITS FOR BREAKWATERS

Report SR 259 March 1991

CONTENTS

		Page
1.	INTRODUCTION	1
	1.1 Project objectives	1
	1.2 Project organisation	1
	1.3 Outline of report	2
2.	CONCRETE ARMOURING FOR BREAKWATERS	3
	2.1 Introduction	3
	2.2 Strength of concrete armour units	5
3.	OUTLINE OF RESEARCH CLUB	6
	3.1 Membership	6
	3.2 Objectives	7
4.	NUMERICAL MODELLING OF WAVE ACTION	8
	4.1 SLACWAVE	8
	4.1.1 Model development	8
	4.1.2 Validation	11
	4.1.3 Recommendations	12
	4.2 WENDIS	13
	4.2.1 Model development	13
	4.2.2 Validation	15
	4.2.3 Recommendations	16
5.	FIELD DATA ACQUISITION	17
	5.1 Study design	17
	5.1.1 La Collette breakwater	17
	5.2 Instrument deployments	18
	5.2.1 Initial trials	18
	5.2.2 Second deployment, January to May 1988	19
	5.2.3 Third deployment, September 1989 to June 1990	19
	5.3 Measurement results	22
	5.3.1 Wave run-up	22
	5.3.2 Wave pressures	23
	5.4 Conclusions	26

CONTENTS (cont'd)

		Page
	5.4.1 Instrumentation	26
	5.4.2 Analysis	26
6.	PHYSICAL MODELLING OF ARMOURED SLOPES	27
	6.1 Cob armoured section, wave flume tests	27
	6.1.1 Model design and construction	27
	6.1.2 Wave run-up	29
	6.1.3 Wave reflections	31
	6.1.4 Wave pressures	32
	6.1.5 Wave forces	33
	6.1.6 Armour unit and underlayer movement	34
	6.2 SHED armoured section, wave flume tests	34
	6.2.1 Model design and construction	34
	6.2.2 Wave run-up	35
	6.2.3 Wave reflections	35
	6.2.4 Wave pressures	36
	6.2.5 Wave forces	37
	6.3 SHED armoured roundhead, wave basin tests	37
	6.3.1 Model design and construction	37
	6.3.2 Wave run-up	38
	6.3.3 Wave pressures	39
	6.3.4 Wave forces	39
7.	CONCLUSIONS AND RECOMMENDATIONS	40
	7.1 Conclusions	40
	7.1.1 Wave forces	40
	7.1.2 Wave pressure	41
	7.2 Recommendations for future work	41
	7.2.1 Limitations of work to date	41
	7.2.2 Proposals for future work	41
8.	ACKNOWLEDGEMENTS	42
9.	REFERENCES	43

TABLES

5.1 Run-up levels on La Collette, second deployment

FIGURES

2.1 Tetrapod, Stabit, Dolos and Accropode armour units.
2.2 Cob and Shed units.

CONTENTS (cont'd)

FIGURES (cont'd)

4.1 Mathematical model definitions, SLACWAVE
4.2 Comparison of model elevations with those of Kobayashi et al (Ref 12)
4.3 Comparison of model velocities with those of Kobayashi et al (Ref 12)
4.4 Layout for physical model tests, calibration stage 2
4.5 Comparison of elevations for physical and numerical models
4.6 Comparison of velocities for physical and numerical models
4.7 Comparisons of relative run-up levels calculated by SLACWAVE and by empirical equations (Ref 14)
4.8 Comparisons of relative run-up levels on armoured slopes calculated by SLACWAVE and by empirical equations (Ref 15)
4.9 Bathymetries used to test WENDIS
4.10 Calibration of friction factor in WENDIS, B_c = 0.75
4.11 Calibration of friction factor in WENDIS, f = 0.01
4.12a&b Inshore wave height comparisons, m = 1/20
4.13 Inshore wave height comparisons, m = 1/500
5.1 Location map, La Collette
5.2 Instrumentation layout
5.3 Sample pressure record, 1st deployment
5.4 Location of pressure transducers
5.5 Sample pressure record, 2nd deployment
5.6 La Collette breakwater showing instrumentation details
5.7 Location of pressure transducers, 3rd deployment
5.8 Section through column of Cobs showing run-up gauges
5.9 Wind and waves during third deployment
5.10 Run-up on La Collette, 2nd deployment
5.11 Typical raw pressure record (500Hz)
5.12a,b&c Typical time series of tidally reduced pressures during rising tide on 28/01/91 - Sensor 1
5.13a,b&c Typical time series of tidally reduced pressures during rising tide on 28/01/91 - Sensor 4
5.14 Significant pressures versus tidal elevation
5.15 Peak pressures versus tidal elevation
5.16 Number of impact events during 5 minute period versus tidal elevation
5.17 Mean period of pressure events versus tidal elevation
5.18 2 percentile exceedence pressures versus tidal elevation
5.19a&b Major impact events on 28/01/91
5.20 Major impact events identified
5.21 Distribution of major pressure event rise times
6.1 La Collette breakwater, section 1.
6.2 Positioning of the force transducers, section 1.
6.3 Positioning of the pressure transducers, section 1.
6.4 Positioning of the run-up gauges, section 1.
6.5 Run-up data, upper gauge, section 1.
6.6 Run-up data, middle gauge, section 1.
6.7 Run-up data, bottom gauge, section 1.
6.8 Run-up period data, section 1.
6.9 Run-up data, upper gauge, sections 2 and 3
6.10 Run-up data, middle gauge, sections 2 and 3
6.11 A comparison of significant run-up data, section 1.

CONTENTS (cont'd)

FIGURES (cont'd)

6.12 A comparison of 2% run-up data, section 1.
6.13 Reflection coefficient data,section 1.
6.14 Pressure data, section 1, upper limb.
6.15 Pressure data, section 1, bottom limb.
6.16 Pressure data, section 1, side limb.
6.17 Underlayer movement.
6.18 Shed breakwater, section 4.
6.19 Reflection Coefficient data, section 4.
6.20 Pressure data, upper transducer, free surface, section 4.
6.21 Pressure data, middle transducer, free surface, section 4.
6.22 Pressure data, lower transducer, free surface, section 4.
6.23 Pressure data, upper limb, hypodermic, section 4.
6.24 Pressure data, side limb, hypodermic, section 4.
6.25 Pressure data, lower limb, hypodermic, section 4.
6.26 Variation in impact pressures, similar elevation, section 4.
6.27 Example of pressure exceedence, section 4.
6.28 Example of Gaussian pressure distribution, section 4.
6.29 Example of Log-normal pressure distribution, section 4.
6.30 Example of Rayleigh pressure distribution, section 4.
6.31 Example of force time series, section 4.
6.32 Relative magnitude of non-dimensional drag force, section 4.
6.33 Relative magnitude of non-dimensional lift force, section 4.
6.34 Location plan of Complex Sea Basin, showing test section 5.
6.35 Cross-section, test section 5.
6.36 Location of force transducers, test section 5.
6.37 Location of pressure transducers and run-up gauges, test section 5.
6.38 Variation in significant relative run-up, test section 5, trunk.
6.39 Variation in significant relative run-up, test section 5, roundhead.
6.40 Comparison of horizontal pressure transducers, test section 5.
6.41 Comparison of vertical pressure transducers, test section 5.
6.42 Comparison of upper transducer pressures, test sections 4 and 5.
6.43 Comparison of middle transducer pressures, test sections 4 and 5.
6.44 Comparison of lower transducer pressures, test sections 4 and 5.
6.45 Relative magnitude of non-dimensional drag forces, test section 5.
6.46 Relative magnitude of non-dimensional lift forces, test section 5.
6.47 Relative magnitude of non-dimensional transverse forces, test section 5.

APPENDICES

1. Single Layer Armour Research Club - Timetable of main events, June 1986 to April 1991
2. Bibliography of papers and reports

1. INTRODUCTION

1.1 Project objectives

Rubble mound breakwaters are widely used to protect harbours and coastal areas from the effects of wave action. Rubble stuctures dissipate much of the wave action in voids within the armour layer(s), underlayers and core. Concrete armour units may be used to form armour layers of controlled thickness and density.

Such structures are very expensive. A recently constructed breakwater in the UK cost around £30-40 million/km. Yet these structures appear to be particularly vulnerable to damage. Studies by a PIANC working group (PIANC PTC2, WG 12) suggest that most conventional breakwater designs have a 40% chance of severe damage during their design life. The reconstruction costs of such structures after damage often exceed the original construction costs.

During previous research for the Department of Environment under contract PECD 7/6/52, and the Ministry of Agriculture Fisheries and Food under commission CSA 557, a study was conducted of the performance of many types of concrete armour units (Ref 1). This study identified the methods available to determine the strength of concrete armour units, and the loads to which they might be exposed. That study did not however deal with the class of high-efficiency hollow cube units that are laid in a single layer. A separate research project was initiated "to identify and develop techniques to allow the quantitative evaluation of hydro-dynamic effects and loadings on single layer concrete armour units to rubble mound breakwaters and sea walls".

1.2 Project organisation

The research work in this project may be considered under three main headings;

a) Hydro-dynamics of armoured slopes
b) Structural performance of armour units
c) Field data collection.

The principal researchers were Hydraulics Research, Wallingford, who were mainly concerned with a) and c); the University of Bristol, who were mainly concerned with b); and South-West Polytechnic, who concentrated on the development of new field instruments for use in c).

The project also required considerable input from the other members of the Research Club. Regular review meetings were held to receive progress reports; to discuss and modify the programme; and to agree and account for members contributions to the Research Club. The organisation of the Club is described in Chapter 3 of this report.

1.3 Outline of report

Much of the work of the Research Club was described in internal reports during the course of the project. Many of those reports contain material that was later superceded or modified. Some work at the University of Bristol and South-West Polytechnic, funded under separate contracts from the Science and Engineering Research Council, is reported separately. This report therefore seeks to summarise the results of the work conducted by Hydraulics Research, Wallingford, including details of work by other members of the Research Club where possible.

A brief description of the use of concrete armour units for rubble breakwaters is given in Chapter 2. The reasons for the development of this project are described. The objectives and organisation of the Single Layer Armour Research Club are outlined in Chapter 3. Chapters 4, 5 and 6 then summarise the main areas of the research by Hydraulics Research, Wallingford, on this project. For convenience each of the main areas of work are described seperately.

The development of two numerical models of wave action at and on a coastal structure is described in Chapter 4. The numerical model SLACWAVE simulates the action of a wave running up and down smooth or armoured slopes. WENDIS calculates the height of waves at the toe of a structure where the water depth is shallow, and incident conditions are dominated by wave breaking.

Field measurement instruments were deployed on three occasions, two during the life of this research contract. These experiments are described in Chapter 5.

Considerable effort was devoted in this project to measuring the hydro-dynamic performance of breakwater sections armoured with hollow cube units. Tests were conducted in a random wave flume on sections armoured with Cobs, and later Sheds. A final series of tests explored the influence of 3-dimensional effects at a breakwater roundhead. The results of these physical model experiments are described in Chapter 6.

2. CONCRETE ARMOURING FOR BREAKWATERS

2.1 Introduction

Breakwaters, and some sea walls, may be constructed as armoured rubble mounds, protected against wave attack by rock or concrete armour. Such structures dissipate wave energy by flows within the voids in the armour layer(s), underlayer(s), and core. This reduces the wave energy reflected from the structure. Generally optimum hydraulic performance and stability are given where the structure is as permeable as possible, with a gradual decrease in permeability from the armour inwards.

Natural rock may often provide an economical armour, if it can be produced and handled in the unit sizes and gradings required to face local wave conditions. Rock is seldom available in sizes above about 15 tonne, and in many areas local rock of acceptable quality is restricted to a few tonnes. This has often restricted the wave conditions that could be faced.

A wide range of concrete armour units have been developed to overcome these restrictions. Cubes and rectangular blocks gave little or no improvement in hydraulic performance or stability over rock, simply allowing larger sizes to be used. Like rock, cubes are laid in two, or more, unit thickness.

More complex forms have been developed to reduce the unit size needed, and to improve the hydraulic performance. The improved resistance to wave action is achieved by increasing the permeability of the armour layer, thus reducing down-rush drag forces, and/or by increasing the restraining forces acting on any individual armour unit. Complex units include the Tetrapod, Stabit, Dolos, and Acccropode (Fig 2.1). Of these, the Tetrapod and Dolos are generally laid in two layers, the Stabit and Accropode in a single layer. All rely on interlock between adjoining units to generate the additional restraint required for stability. Their shapes do not however allow units to be placed with precisely controlled position and orientation. Interlock between adjoining armour units often varies considerably, depending on placement pattern and density. Some units may be little restrained by those around them. In a long breakwater a few units may be removed under relatively low wave conditions. This may in turn allow the armour layer to lose interlock further. The armour layer strength therefore varies stochastically in time and space.

Some of the limitations of these types of armour were overcome with the development of pattern placed high efficiency units, such as the Cob. This is a hollow cube placed in a single layer to closely controlled limits. These units fit together in a very regular pattern. This produces a very open armour layer, in which flow is concentrated in the voids formed within the units, rather than between the armour units.

The Cob (Fig 2.2) was developed by Coode & Partners in the late 1960s, and was used by them to armour the La Collette breakwater at St Helier, Jersey, in 1973-4. A second hollow cube unit, the Shed, was developed by Shephard Hill around 1981, and was first used to armour a rubble sea wall around a reclamation at St Helier, Jersey. The development and use of these units has been described previously by Wilkinson & Allsop, and Dunster, Wilkinson & Allsop (Refs 2 and 3).

Historically the stability of concrete armour units has been described by the relative size of the armour unit for the onset of armour displacement. Armour displacement alone is not a useful concept in the design of hollow cube armour units, as will be shown below. This relationship does however give a simple demonstration of the stability of this type of unit. The size of an armour unit may be conveniently given by the nominal diameter, D_n, defined in terms of the unit mass, M, and density of concrete, ρ_c:

$$D_n = (M/\rho_c)^{1/3}$$

The relative size of armour unit may then be given by $H_s/\Delta D_n$ where the bouyant density, Δ, is defined in terms of the densities of concrete and (salt) water, ρ_c and ρ_w: $\Delta = (\rho_c / \rho_w) - 1$. Values of $H_s/\Delta D_n$ have been derived from the results of hydraulic model tests for various armour units at the onset of armour movement. Example values may be summarised:

Armour unit	$H_s/\Delta D_n$ for no damage
Rock	1.0 - 1.5
Cube	2.0
Dolos	2.8
Accropode	3.7
Cob/Shed	4.8

These may be used to estimate armour unit sizes required for no damage under a wave condition of H_s = 5m, with concrete of density ρ_c = 2400kg/m³ in water of ρ_w = 1030 kg/m³:

Armour unit	D_n(m)	M (tonne)
Cube	1.9	16.5
Dolos	1.3	5.8
Accropode	1.0	2.5
Cob/Shed	0.8	1.2

For production purposes, it has been argued that there is no advantage in reducing the size of the Cob or Shed below 2 tonnes, so for this example 2 tonne hollow cube units would offer considerable increase in safety.

2.2 Strength of concrete armour units

Historically the main response process addressed in the design of a rubble mound breakwater or sea wall was the displacement of armour units, often termed damage. Due to the variable strength of armour layers, some damage (typically 2-5%) was permitted under the design wave condition. The main parameter addressed was the minimum size, or mass, of the armour unit required to give damage less than the prescribed limit under the design condition. The main tools used by designers to determine this size were hydraulic model tests; empirical formulae relating armour size to wave height; and experience of other structures. None of these methods however gave any direct information on the loads applied, or on the strength of the units.

The armour units themselves were almost invariably unreinforced. The developers of some of the units conducted ad hoc tests of their strength in simple trials. These usually involved dropping the unit onto a prepared slab. This situation persisted late into the 1970s. The fragility of slender armour units was dramatically illustrated by major damage to the breakwater at Sines in Portugal in February 1978, by waves believed to be less than the design condition. Many factors contributed to the failure, but the most important is generally accepted as the breakage of the 42 tonne Dolos units (Ref 4).

Following this, many breakwater failures involving breakage of concrete units were reported. In 1980 the breakwater at Arzew el Djedid in Algeria was damaged. The breakwater at Tripoli, Libya, was hit by a large storm in January 1981, again causing much damage. These problems were not confined to Europe and the Mediterranean. Significant storm damage was also caused at Diablo Canyon, California; Cleveland, Ohio; and at a number of sites around Canada. Most involved

the failure of Dolos or Tetrapod units. Outline details are summarised by PIANC (Ref 5).

Analysis of these failures has led to re-appraisal of the design standards used for breakwaters. Considerable research effort has been devoted to the development of new design methods, particularly on the stresses induced in armour units in service. Work in the USA and Denmark has concentrated on the Dolos. A major field experiment at Crescent City has generated data from twenty instrumented Dolos on an outer section of the breakwater. In the Netherlands, a consortium of researchers, contractors, and government agencies have addressed the design of Tetrapod and Cube armour units. They have used drop and impact tests and hydraulic model tests.

In the UK a research club has been set up to extend the design methods available for hollow cube and related single layer units. Phase 1 of this project, completed in March 1991, is described in this report.

3. OUTLINE OF RESEARCH CLUB

At an early stage in the development of the proposals for this project, it became clear that a wide range of skills would be required to address the full range of problems described in Chapter 2. Studies on the strength of the armour units would require test facilities and numerical modelling methods only available in a university concrete laboratory. Data on loadings at full scale could only be measured in the field, and would require the assistance of a contractor, and probably a breakwater owner or owners.

Hydraulics Research therefore decided to assemble a "Club" of other researchers, and industrial practitioners, to support the research.

3.1 Membership

Considerable effort was expended in discussing possible membership of the Research Club. A presentation on the research requirements was made at the Concrete Society conference in London on Marine Concrete in September 1986, and an article was subsequently published in the magazine Civil Engineering, December 1986. Between May 1986 and the formal start of the project in April 1987, 10 different companies, organisations or groups were approached directly. From those approached, 4 consulting engineers, 2 contractors, 2 academic

institutions, and an owner, expressed willingness to contribute to the project by the provision of resources in kind and/or by direct funding. This group, calling itself the Single Layer Armour Research Club, was formed by:

Coode Blizard	G Maunsell & Partners
Kirk McClure & Morton	Posford Duvivier
Shephard Hill & Co	Soil Structures (to 9/90)
Hydraulics Research	University of Bristol
South-West Polytechnic	States of Jersey

During the period of this project, the club met regularly to review research progress, and to organise and approve the use of supporting resources. To assist in this work, the club appointed an independent consultant, JE Clifford, to represent industrial members, and to chair its meetings. A summary of main meetings and activities is given in Appendix 1.

3.2 Objectives

The main purposes of the project have been summarised in Chapter 1. The principal aims of the research club were to provide technical guidance and practical support for the project within the overall objectives. During research club meetings, more detailed objectives for some areas of work were identified, and a statement of practitioners requirements was prepared. In setting down objectives, it was realised that it might well not be possible to meet all of them in the first phase, and that some would be changed as a result of research findings.

The detailed areas identified early in the project may be summarised:

a) Hydrodynamic stability for various sea states, breakwater slopes, underlayer properties, and arrangements of units;
b) Wave run-up and run-down levels;
c) Forces, and pressures, acting on units;
d) Wave reflection properties of example slopes;
e) The influence of angled wave attack on armour stability, and on forces acting on units;
f) Stresses induced in units by static loads, handling and transport, and in service;
g) Guidance on the interaction of armour layers with the underlayer and/or core.

These objectives were principally addressed in the design of the hydraulic model tests, Chapter 6, and the stress modelling at Bristol.

4. NUMERICAL MODELLING OF WAVE ACTION

Two numerical models of wave action near or on armoured slopes have been developed for this project. SLACWAVE is a simple 1-dimensional wave model (Ref 6). Its purpose is to calculate run-up levels, and uprush and downrush velocities/pressures. It is a developed from the simple 'wave bore' model originally developed by Professor Peregrine's team in the Mathematics Department at the University of Bristol.

The second mathematical model, WENDIS, calculates wave conditions in the nearshore zone, where wave breaking has a significant influence on the local wave height (Ref 7). The model uses empirical breaking criteria that have been checked against sets of laboratory data. The model can also calculate breaking wave conditions using Goda's method (Ref 8), which may be useful for those situations where the bathymetry can safely be represented by a single slope angle.

4.1 SLACWAVE

The mathematical model SLACWAVE solves the non-linear shallow water wave equations in one dimension with a term for frictional dissipation. Wave elevations and depth-averaged velocities are calculated at regular time intervals for fixed grid points. The model is used to derive run-up levels and reflection coefficients on sloping coastal structures. Versions of the model have been developed to run regular or random waves.

The wave elevations and velocities calculated by the model have been compared with measurements on smooth and rough impermeable slopes in a wave flume, and with published results for other models. The model is potentially suitable for waves of low steepness, and structures where surging waves are of more concern than plunging waves.

4.1.1 Model development

The model was developed in two main stages, (Refs 9 and 10). In the first stage, a regular wave model was derived for smooth slopes, and results were compared with flume data and other models. In the second stage, a 'random wave' version was developed for smooth and rough impermeable slopes, and results were compared with measurements from the wave flume.

Model formulation

The basic technique used in the mathematical model is to solve numerically the non-linear shallow water wave equations. Boundary conditions allow reflection and run-up at a steep slope to be incorporated. The set of equations which are solved contain a term to describe frictional dissipation on a rough slope. The model is based on a method originally developed for beach slopes, Packwood and Peregrine (Ref 11). Clearly many structural slopes will be considerably steeper than typical beach slopes, and the extension of the original method to include steeper slopes has been described by Kobayashi et al (Ref 12) and is also addressed by Thompson (Ref 13).

The layout and co-ordinate system used in the mathematical model are shown in Figure 4.1. It should be noted that the x' co-ordinate is taken to be positive in the landward direction, with x' = 0 at the toe of the slope. The z' co-ordinate is taken to be positive upwards with z' = 0 at the toe of the slope. The water depth is denoted by h' and the depth averaged velocity by u'. The local angle of the slope is Θ'. The elevation of the slope above Z' = 0 for X' > 0 is given by S'. The slope is assumed horzontal for x' < 0.

The incident wave train is specified at the toe of the slope, where the water depth below SWL is given by h_o. It is assumed that the slope is impermeable, waves are non-breaking and that no overtopping occurs. Vertical pressure is taken to be hydrostatic and the vertical fluid acceleration is assumed to be negligible. This is a reasonable assumption for a relatively mild slope, ie $\tan\Theta' \ll 1$.

The governing equations may then be expressed in dimensionless form as:

$$\frac{\partial h}{\partial t} + \frac{\partial}{\partial x}(hu) = 0 \qquad (4.1)$$

$$\frac{\partial}{\partial t}(hu) + \frac{\partial}{\partial x}(hu^2 + \tfrac{1}{2}h^2) = -\Theta h - f|u|u \qquad (4.2)$$

where

$h = h'/a'$, $\quad u = u'/(ga')^{1/2}$

$t = t'/T'$, $\quad x = x'/(T'(ga')^{1/2})$

$\Theta = T'(g/a')^{1/2} \tan\Theta'$ and $f = \tfrac{1}{2}T'(g/a')^{1/2}f'$.

Here f' is an empirically determined constant friction factor associated with the slope, a' is the incident wave amplitude, T' is the incident wave period and g is acceleration due to gravity. For the initial mathematical model tests, the incident wave train was taken to be sinusoidal.

In addition to the governing equations, initial and boundary conditions also need to be specified. At time t = 0 the fluid is assumed undisturbed giving initial conditions:

$$h = h_o - s, \quad u = 0 \text{ at } t = 0, \quad x > 0$$

The seaward boundary conditions are derived from a characteristics based argument in which it is assumed that waves reflected from the structure do not modify the incident wave. The derivation of the seaward boundary condition used in the model is described by Beardsley et al (Ref 9). At the landward boundary it is assumed that both the water depth on the slope and its velocity are zero at the leading edge of the wave.

The governing equations are presently solved using a Lax Wendroff finite difference scheme. This has the advantage of being relatively easy to apply, and is numerically stable provided the Courant condition is satisfied

$$(gh_o)^{\frac{1}{2}} \frac{\Delta t}{\Delta x} \leq 1$$

where Δt and Δx are the time and space steps. This scheme has been found to provide a reasonably efficient and robust method for solving the differential equations for waves of moderate steepness. For steeper waves there will be inaccuracies introduced by using this finite difference scheme, and the adoption of an alternative method may be necessary. The alternatives which have been examined are Roe type schemes, which are widely used in aerodynamic problems.

In the second stage of development the model was adapted to calculate flow conditions on both smooth and rough impermeable slopes, and to run a random wave train, rather than a simple series of regular waves. The model was also modified to separate numerically the minimum water depth defining the leading edge of the wave from that used to calculate run-up levels. This last overcame some detail problems with the definition and calculation of run-up levels.

During the second stage of development, further attempts were made to explore the performance of Roe type numerical schemes. It was hoped that these schemes would allow the model to calculate conditions for steeper waves. A number of cases were run with some success, but the lower degree of damping permitted numerical perturbations to propagate back from the shoreward boundary. This problem was not overcome, and the Lax-Wendroff scheme was used in all subsequent versions.

4.1.2 Validation

Calibration of the model was conducted in three stages. In the first, comparisons were made between results from the initial version of SLACWAVE and results from other models, principally that of Kobayashi et al (Ref 12). SLACWAVE was run for one of the cases discussed by Kobayashi in Reference 12. The comparisons of elevations and velocities are shown in Figures 4.2 and 4.3. Generally good agreement is shown. Discrepancies were mainly ascribed to machine rounding errors, as running SLACWAVE at either 250 or 400 time steps per wave had no significant effect on the velocities calculated. It may be noted that 2000 steps per wave were used by Kobayashi et al.

In stage 2 of the calibrations, wave elevations and depth-averaged velocities were measured in regular wave tests. Initally a simple smooth impermeable slope of 1:2 was used, with a sea bed slope of 1:50 (Fig 4.4). The wave surface was measured by an array of vertical wave probes, supplemented by a run-up gauge suspended above the surface of the slope. Depth averaged velocities at a given probe position were calculated from the change of the cross-section area of the wave landward of that probe. Comparisons were generated by running SLACWAVE to calculate elevations and velocities at positions corresponding to each wave probe on the slope. For tests with a smooth slope, a friction factor of 0.01 was used. Comparisons are shown in Figures 4.5 and 4.6 for waves of steepness $s = H/L = 0.014$, where H is the incident wave height and L is the wavelength. This steepness corresponds to an Iribarren number $Ir = 4.2$. Relatively good agreement is shown between numerical and physical model results.

The final stage in the calibrations concentrated on comparing wave run-up levels on smooth and armoured slopes under random waves with results derived in previous work at HR (Refs 14 and 15). The numerical model was run for a relatively short sequence of waves, around 120 in each case. The results of run-up measurements in the physical model had been previously characterised by the significant and 2% exceedance

run-up levels, R_{us} and $R_{u2\%}$. Simple empirical formulae related these levels to the incident wave conditions, using the modified Iribarren number. The modified Iribarren number, Ir_p, had been expressed in terms of the peak wave period, T_p:

$$Ir_p = \tan\alpha \; / \; s_p^{1/2} \qquad (4.3)$$

where $s = 2\pi H_s / gT_p^2$
α is the structure slope angle to the horizontal and H_s is the significant wave height.

For smooth slopes, and wave conditions in the range $3<Ir_p<6$, relative run-up levels measured in model tests were described:

$$R_{us}/H_s = 2.13 - 0.09Ir_p \qquad (4.4)$$

$$R_{u2\%}/H_s = 3.35 - 0.18Ir_p \qquad (4.5)$$

Run-up levels predicted by equations 4.4 and 4.5 are compared with levels calculated by SLACWAVE in Figure 4.7. The scatter of numerical model predictions is generally no more than the scatter of the orignal data used to give the empirical equations (Ref 14).

Run-up levels had also been measured on a permeable slope covered by a single layer of SHED units (Ref 15). Simple empirical prediction equations had been derived from this model data for R_{us} and $R_{u2\%}$, again in terms of Ir_p and covering the range of wave conditions on a 1:2 slope given by $3<Ir_p<6$. These may be written simply :

$$R_{us}/H_s = 1.33 \qquad (4.6)$$

$$R_{u2\%}/H_s = 2.78Ir_p \; /(Ir_p + 1.4) \qquad (4.7)$$

SLACWAVE was adjusted to calculate run-up levels on rough slopes by using modified friction factors. It was not however possible for the numerical model to take any account of the permeable nature of the model slope used in the wave flume tests. Run-up levels predicted by equations 4.6 and 4.7 are compared with levels calculated by SLACWAVE in Figure 4.8. The scatter of numerical model predictions is again little more than the scatter of the orignal data used to give the empirical equations (Ref 15).

4.1.3 Conclusions

The SLACWAVE numerical model uses very simplified descriptions of the wave processes. It gives no

information on variations of water velocities with depth, nor will it deal with plunging waves. It is also limited to impermeable slopes. Despite these significant limitations, run-up levels and depth-averaged velocities calculated by the model give surprisingly good agreement with data measured in hydraulic model tests.

4.2 WENDIS

Present mathematical models enable predictions of offshore wave conditions to be transformed to a nearshore point using a refraction model. Traditional refraction models do not allow for wave breaking, and therefore the nearshore prediction point must have sufficient water depth so that significant wave breaking does not occur. A simple model is needed to transform waves from nearshore to inshore.

WENDIS has been developed to allow dissipative effects for normally incident waves in shallow water to be reproduced (Ref 16). The main purpose of the model is to represent wave effects in the region where wave breaking, bed friction and shoaling are significant, but refraction effects are negligible.

4.2.1 Model development

The physical processes of shoaling, bed friction and energy dissipation due to wave breaking are represented in the model.

Shoaling is represented by calculating the shoaling coefficient, K_s, from the slope between neighbouring grid points:

$$K_s = (C_{gi} / C_{go})^{1/2} \qquad (4.8)$$

where C_{gi} and C_{go} are the wave group velocity at inshore and offshore points, and C_g is calculated:

$$C_g = (C/2) [1+ \{(4\pi h/L) / \sinh (4\pi h/L)\}] \qquad (4.9)$$

where: C is the wave speed, L/T;
T is the wave period;
h is the water depth.

The wave height at the previous grid point is then multiplied by the shoaling coefficient to give the wave height at the current point due to shoaling.

Bed friction is modelled using a method derived from the work of Hunt (Ref 17) and Bretschneider & Reid (Ref 18). This calculates the wave height reduction between neighbouring grid points due to the effect of

bed friction on a sloping bed. The expression used is based on a combination of Hunt's formulation for laminar friction, and Bretschnider and Reid's work on frictional damping due to a rough turbulent boundary layer. To the first order these two can be reconciled to give the coefficient, K_f, for change in wave height due to frictional effects between neighbouring grid points in constant depth as:

$$K_f = 1 - \frac{k^2 \Delta x}{(2kh + \sinh 2kh)} \left(\frac{\nu e}{\pi f}\right)^{\frac{1}{2}} \qquad (4.10)$$

hence: k is the wave number (=2π/L)
f is the wave frequency (= 1/T)
Δx is the distance between adjacent grid points

and $\nu e = \nu$ for $Re \leqslant Re_{trans}$

or $\nu e = \nu \frac{Re}{Re_{trans}}$ for $Re > Re_{trans}$

where ν is the kinematic viscosity of water
and Re is the amplitude Reynold's number.

The amplitude Reynolds number is given by:

$$Re = \frac{\omega H^2 (1 - \Theta^2)}{4 \nu \Theta^2}$$

where H is the wave height
$\omega = 2\pi/T$
and $\Theta = \omega^2/gk$.

Also $Re_{trans} = \frac{1}{2} \left(\frac{3\Pi}{8F}\right)^2$

Here F is the non-dimensional friction factor used by Bretschnider and Reid. Assigning this value to Re_{trans} is a device to reconcile the two formulations, but it can be considered as defining the point at which the transition from a laminar to a turbulent boundary layer takes place. In practice the value of F is determined empirically, and for WENDIS a default friction coefficient of 0.01 is derived from calibration tests.

Energy dissipation due to wave breaking is assumed to be a quantifiable loss over the entire bathymetric grid. Wave breaking is modelled using the empirical formulation of Weggel (Ref 19). This gives the ratio of the wave height to water depth at breaking as:

$$(H/h)_b = b \; / \; [\; 1 + (ah/gT^2) \;] \qquad (4.11)$$

where: $a = 43.75 \; (1 - e^{-19m})$
$b = 1.56 \; / \; (1 + e^{-19.5m})$

and m is the seabed slope.

WENDIS is a mono-frequency model (ie a single wave height and period are input and there is no calculation of either a time series or spectrum). The wave height corrected for breaking is determined assuming a Rayleigh distribution about the RMS wave height, H_{RMS}:

$$P(H)dH = (2H/H_{RMS}^2)\ e^{-H^*}\ dH \qquad (4.12)$$

where P(H) is the probability of wave heights not exceeding H, and $H^* = H^2 / H_{RMS}^2$

The breaking wave height H_b is calculated from Weggel's expression. H_{RMS} corrected for breaking is calculated by integrating this equation.

$$H_{RMS} = \{H_{uRMS}^2 - B_c\ (H_{bRMS}^2 + H_{uRMS}^2)\ e^{(-H^{**})}\}^{1/2} \qquad (4.13)$$

where $H^{**} = H_{bRMS}^2 / H_{uRMS}^2$,

H_{bRMS} is the breaking RMS wave height,
H_{uRMS} is the RMS wave height un-corrected for breaking and B_c is the specified breaking coefficient. B_c represents the fraction of energy above breaking height which is dissipated.

Calculations in WENDIS are performed using depth values spaced at equal horizontal intervals. The model provides a flexible method of specifying the depth grid data. Both regular and irregular depth grids are interpolated using an unclamped cubic spline. The interpolated chainage increment Δx, is calculated by the program as 1/8 of the wavelength. For the offshore incident wave condition:

$$\Delta x = L_p/8$$

where $L_p = gT_p^2/2\pi$, and T_p is the period of peak spectral energy.

When breaking losses become significant, Δx is determined from the local wavelength at the point of significant breaking, and is therefore a function of the water depth. The point of significant breaking is defined in the model as the point when the RMS wave height, uncorrected for breaking, reaches the breaking RMS wave height calculated using Weggel's method.

4.2.2 Validation

Results from the numerical model were compared against wave conditions measured in a random wave flume at HR. Wave conditions were measured over three different sea

bed bathymetries (Fig 4.9). Bathymetry 1 was formed by a 1:10 slope which met a horizontal bed. For Bathymetry 2 the bed slope in the flume changed from 1:10 offshore through 1:20 to 1:50 and finally 1:45, before again terminating in a horizontal slope. For Bathymetry 3 the bed sloped upwards at 1:20 from the inshore point before intersecting an existing bed profile, a somewhat atypical profile.

The purpose of the calibration tests was to recommend default friction and breaking coefficients by comparing WENDIS with the measured results. The data from these tests were grouped according to the peak wave steepness s_p. WENDIS was tested against data within the steepness ranges:

$$s_p \leq 0.025$$
$$0.025 < s_p < 0.04$$
$$s_p \geq 0.04$$

The procedure used was to assume a fixed value for the breaking coefficient $B_c = 0.75$, and run the model varying the friction coefficient (Fig 4.10). Later the recommended friction coefficient for smooth slopes, 0.01, was used when calibrating the breaking coefficient (Fig 4.11).

Wave conditions calculated by WENDIS were also compared with data obtained using alternative methods of calculating inshore wave heights (Figs 4.12 and 4.13):

a) simple prediction curves derived by van der Meer using the ENDEC wave energy decay model(Ref 20);
b) analytical equations proposed by Goda (Refs 8 and 21).

4.2.3 Conclusions

The WENDIS model has been calibrated against a wide range of wave conditions using three different bathymetries. These tests gave a recommended value for the friction coefficient over smooth bathymetry $f = 0.01$, and for the breaking coefficient $B_c = 0.75$.

For the bathymetries tested, WENDIS gave over-predictions of significant wave heights up to 15%, but any under-prediction was limited to less than 5%. There was good agreement between results from the ENDEC curves, Goda's equations and WENDIS for $0.02 < s_p < 0.05$, and bed slopes between 1:20 and 1:50. The different methods did not compare so well for s_p around 0.01, or for bed slopes shallower than about 1:100. WENDIS is not recommended for use for bed slopes shallower than 1:100 without further study.

5. FIELD DATA ACQUISITION

5.1 Study design

Physical and numerical models are often limited in their accuracy and in the range of conditions for which they give reliable results. Scale effects influence the application of some of the measurements that may be made in physical models. Numerical models are limited to the fundamental equations by which the processes are simulated. The extent and importance of these limitations can often be identified by comparing results with other models or simulation techniques, but some comparisons require detailed information at full scale. This particularly related to wave impact pressures on the armour units. Such measurements are most conveniently made in a very large wave flume, capable of generating waves around H_s = 2m or greater.

Access to either of Europe's large wave flumes was not possible in this project, but owners of two breakwaters offered access to their structures for monitoring: La Collette breakwater at St Helier, Jersey; and Pickie Breakwater at Bangor, Co Down.

The field measurements were made in three successive deployments, all made on the La Collette breakwater at St Helier, Jersey. The primary objective was to collect data on wave pressures acting on a Cob armour unit. Where possible, measurements were made to describe other aspects of the structure performance.

5.1.1 La Collette breakwater

La Collette breakwater is situated towards the eastern end of St Aubin Bay on the southern side of the island of Jersey (Fig 5.1). The breakwater forms part of the outer defence for the port of St Helier, which is also protected by the Hermitage breakwater. La Collette breakwater is founded on rock with the principle axis running ESE/WNW. Details of the structure are given in Reference 22. Rocky outcrops which are exposed at low tide lie immediately to the south of the breakwater.

La Collette breakwater is exposed to direct wave attack from between 110 to 240°N, although local rocky outcrops cause attenuation in the sector 110 to 140°N. The large tidal range (9.8m on mean spring tides) significantly influences the wave conditions in the vicinity of the breakwater. Typical tidal levels may be summarised:

	Elevation (m CD)
Highest astronomical tide	12.3
Mean high water springs	11.1
Mean high water neaps	8.1
Mean tide level	6.2
Mean low water neaps	4.1
Mean low water springs	1.3

Wave conditions off Jersey are routinely monitored using a Waverider buoy 2.7km SSW of La Collette. The wave conditions observed at the buoy will be modified by shoaling, refraction, diffraction and breaking as they propagate inshore, so they must be adjusted to take account of these processes to give the wave conditions at the breakwater.

5.2 Instrument deployments

5.2.1 Initial trials

The coastal environment is hazardous by its very nature. Large storms frequently erode beaches, breach sea walls, and damage breakwaters. The use of potentially fragile instruments to measure the effects of storm waves on an exposed breakwater is likely to be rewarded by wrecked equipment, and little data. The design of any field data collection was therefore approached with considerable care.

Before this research project started formally, Hydraulics Research and University of Bristol supported a trial deployment of field instruments on La Collette in February and March 1987 (Ref 23) to explore:

a) whether surface mounted strain gauges could be mounted on exposed (wet) concrete units in situ;
b) the practicality of securing an instrument cable to the upper limbs of Cob armour units, and the liklihood of the cable surviving winter storms;
c) the posibilities of using modified CB radios to carry data signals from submerged or semi-submerged positions;
d) whether a standard soil pressure cell (Kulite 0234) could survive in such an environment.

The location of the breakwater at La Collette is shown in Figure 5.1. The general layout of the instruments, signal cable, and recording equipment, for the first deployment is shown in Figure 5.2.

Much was learnt from this deployment. The strain gauges remained stuck to the armour unit, but gave no

useful signals, probably due to the very small changes of strain occuring in relation to the (high) level of signal noise level. The main instrument cable proved easy to secure to a column of armour units, and survived the rest of the winter well. Luckily this obviated the need for the radio link, which had not worked well. The Kulite pressure cell appeared to give good pressure signals, Figure 5.3.

5.2.2 Second deployment, January to May 1988

A second deployment in January to May 1988 (Ref 24) was more successful. Five pressure cells, modified by their supplier to improve waterproofing, were bolted to a single Cob (Fig 5.4). A wire run-up gauge was secured just above a column of units. Data was logged onto an analogue tape recorder. This had to be operated manually, a very expensive requirement. It was hoped that it would be possible to record for about ½ hour each day. Tapes were returned to Wallingford, where the signal was digitised at 500Hz and processed on a Compaq 286 PC.

A number of problems were encountered during this deployment. The wire run-up gauge was subject to abrasion and impact damage, and its failure was not surprising. More surprising was that all five pressure cells failed from corrosion and/or failure of the waterproofing. Some useful data was however collected. Whilst operating, the run-up gauge appeared to give good results, and some comparison was possible with wave heights measured at an offshore wave buoy. The pressure records showed the significant influence of relative water level on the frequency and severity of wave impacts. Example impacts are shown in Figure 5.5.

5.2.3 Third deployment, September 1989 to June 1990

During the first two deployments, data logging had required manual operation. This was no longer possible, and automated logging equipment was required to operate for long periods (3-4 weeks) without attention. The fast sample rates needed to capture impact events, typically up to 500 samples/second per transducer, meant that continuous logging would require unrealistically large data storage. A system was developed that recorded only when impact events were possible. The logging system was programmed to check the water level and/or wave action before triggering the recorder. The measurements were recorded for processing later, as this allowed the processing software to be modified in the light of signal quality, and the frequency of events of

interest. The logging procedure had to allow flexibility in the analysis stage, as the frequency and form of impact events could not be defined in advance.

The data logger, developed by Ship and Marine Data Systems Ltd for Hydraulics Research, includes processing hardware from a personal computer, and an 8mm video tape data recorder with a capacity of 2.3 Gigabytes per tape. The logger has a maximum throughput of 4000 samples/second, enabling up to 500 samples/second/channel to be collected on 8 channels. The logger is not powered directly from the mains, but from a 12v battery that is continuously float charged, ensuring that it can operate for up to 24 hours. The logger includes a battery powered real-time clock set to GMT. After any power failure lasting longer than 24 hours, all software is re-loaded, the computer is synchronised with the real-time clock, and the system is restarted.

Operationally, the logger is controlled by two triggers. The logger monitors an allocated channel, and only records data when a preset level is exceeded. If the primary channel fails, a second channel is used in the same way. The tidal output from the wave/tide gauge was used as the primary trigger. The lowest of the pressure transducers was designated as the secondary trigger.

All data were scaled and converted to digital form using a series of amplifiers and A-D converters, then recorded on video cassette. These amplifiers could be adjusted for the instrument being used. The logger also provided power to each instrument. The logger was designed to allow differential sampling rates. A high sampling frequency, 500Hz, was necessary to capture wave impacts. Wave or tide elevations and run-up levels requires a lower sampling rate. The logger was programmed to use 17Hz for these. With these rates, each cassette tape lasted a month.

Instruments

Problems had been encountered with signal quality during the previous deployment. There was significant noise on the signals, possibly caused by mains 'pick up' or earth leakage in the overall circuit. In an attempt to rectify this problem, a 4-20mA current drive was used for all instruments. This was expected to reduce the susceptibility to interference. The instruments deployed at La Collette, Figure 5.6, may be summarised:

a) four pressure transducers, designed to measure wave impact pressures;
b) two resistance type run-up gauges running through the middle and on top of a column on units;
c) a wave/tide gauge based on a pressure transducer, sited on the toe beam at the bottom of the breakwater.

The equipment was deployed from 17th September 1989 and recording was completed in June 1990. The equipment was recovered on 16th October 1990. A fuller description of the deployment, and of the data analysis is given by Ryder et al (Ref 25).

Pressure transducers

The previous deployment had used Kulite 0234 pressure cells. These proved to be particularly susceptible to corrosion, and all five pressure cells failed. It was uneconomic to modify them to include the required changes, and alternative transducers were purchased (Schaevitz P1787/0001 intended to operate over 0-2Bar).

Four transducers were attached to a Cob in the fourth row from the toe beam, just below mean low water neap tide level. Two transducers were sited in the upper limb, one on a side limb and a further transducer on the bottom limb (Fig 5.7). The elevations of the transducers were determined:

Transducer	Level (mCD)
1	8.78
2	8.78
3	8.61
4	8.39

Each transducer was housed in a plastic cone anchored to the Cob. The performance of these new transducers was excellent. Output signals exhibited little noise. No corrosion could be found when the equipment was reclaimed after nearly 10 months. Two transducers were still working, the other two transducers had failed, but only because of cable breakages late in the deployment.

Wave/tide Gauge

Wave conditions and tidal level were measured using a current driven Druck pressure transducer, measuring up to 10m head. The output was filtered by the logger using high and low pass filters to separate the wave

and tidal components. The wave conditions recorded at this gauge will have included the effects of both incident and reflected waves. The gauge was clamped to the toe beam. The instrument did not appear to suffer damage due to rock impacts, corrosion, etc, but the signals were unreliable after January 1990.

Run-up Gauges

Two run-up gauges were deployed in the same column of units as the pressure transducers. The gauges used thin high-resistance nichrome wire attached to nylon cable. One was positioned through the middle, and the other along the top of the Cob units, Figure 5.8.

The reliability of these run-up gauges was poor. Although they calibrated well in the laboratory, they did not give reliable readings in service. Both gauges were destroyed during the first four months. Similar failures had been experienced with a different design in the previous deployment. It was concluded that wire run-up gauges are not sufficiently reliable for long term deployments in severe wave conditions, and in any future work, an alternative device should be considered.

5.3 Analysis of results

About 20 Gigabytes of data was collected during the monitoring period, but only that collected during larger storms was analysed. Major storms occurred between 25th January and 15th February 1990, when most of the records analysed are taken. Wind and offshore wave records in the recording period are shown in Figure 5.9. Data from 13 tides were analysed.

The size and character of wave impact events are strongly influenced by the water level in relation to the instrument. Each record was divided into short periods which were analysed separately to identify the influence of local water level. Tidal levels in Jersey rise by as much as 0.4m/minute, so five minutes was the maximum time over which tidal levels could be considered constant. This gave around 50 pressure events in each five minute segment.

5.3.1 Wave run-up

Some measurements of wave run-up were made during the early part of the second deployment. The initial analysis of this data was not very conclusive (Ref 24). Data was derived for the significant run-up, corrected for tidal level changes. Inshore wave conditions were not known, as the inshore wave gauge

was not operational at the time, but records from the offshore wave buoy were summarised, Table 5.1. Some preliminary analysis can be conducted by calculating the relative run-up, on this occasion based on the offshore wave height, and comparing with the Iribarren number, again based on the offshore wave height, see Figure 5.10. These results cannot be compared directly with those from the physical model tests, due to the use of offshore wave conditions in the parameters calculated.

Analysis of output from both of the run-up gauges in the third deployment indicated that both gauges were functioning immediately following the deployment. By the first major storm on 20th January, they had both failed, and no run-up records were analysed.

5.3.2 Wave pressures

Data from the second deployment showed typical shock wave pressures of up to 6m (sea water) on the upper limb of the Cob unit, when the still water level was between 0.3m below and 0.1m above the transducer. No significant impact events were observed on the other limbs. These conclusions were based on few observations, and signal noise limited the temporal resolution of the pressure measurements to greater than 20 milliseconds.

A typical signal from the third deployment, digitised at 500Hz, is shown in Figure 5.11. There is some noise, typically under 0.1m, but the overall quality is much improved over the previous deployment. The higher quality of the signal allowed some simplification of the analysis methods. Each five minute segment of record was considered separately:

a) The raw pressure record was calibrated to give a head of seawater using the pre-deployment calibration.
b) The mean pressure was estimated over the first 2.5 minutes of the record. This 'set-up' was then subtracted from subsequent values.
c) A zero-crossing analysis was performed, using up-crossings, to identify pressure 'events'.
d) For each pressure event, the peak pressure in the 5 minute record, p_{5max}, and peak 1/10 second average pressure were calculated, and the event was identified as 'impact' or 'quasi-hydrostatic'.
e) The 33% exceedance, $p_{33\%}$; median, $p_{50\%}$; and 2% exceedence, $p_{2\%}$, pressures; and mean pressure event period, T_{pres}, were calculated.

f) Major impact events were extracted and rise times and peak impact pressures were calculated.

Before any analysis of wave impacts can be conducted, a simple unambiguous definition of an impact event is required. In general such events show an increase in pressure that is very much faster than would be caused by the passage of a wave over a submerged pressure cell. Rise times observed in the second deployment were generally of the order of 100 milliseconds, although the signal quality severely limited the resolution. In this analysis an impact event was defined as an increase of pressure greater than 0.5m over a period shorter than 100 millisecond. Using this definition, very few impact events were observed once the sensor was submerged, indicating that it provides a reasonable separation of impact and quasi-hydrostatic events.

Effect of sensor position/attitude

The effect of transducer position/attitude on the frequency of impacts was very marked. Pressure sensor 1 was positioned on the centre of the upper limb of the armour unit (Fig 5.7), and sensor 2 was positioned to one side at the same level. Sensor 4 was on the lower limb of the Cob, and was therefore angled upwards, pointing away from the wave front. Example records of the 1/10 second average pressures from sensors 1 and 4 on 28th January 1990 are shown in Figures 5.12 and 5.13. Tidal variation has been subtracted from the record. The records from sensors 1 and 4 have markedly different forms. Data recording began at a time when the still water level was 1.5m below sensor 1. At this time only the highest waves are reaching sensor 4 with maximum pressures of 0.75m. Sensor 1, despite being located 0.39m higher on the breakwater, shows much higher and sharper pressure events, indicative of wave impacts.

Variation with tidal level

The magnitudes of the wave pressures recorded, the mean period of pressure events, and the number of impact events, all varied with still water level. These effects are illustrated in Figures 5.14 to 5.17 for the 33% exceedance pressure, $p_{33\%}$; maximum pressure in the five minute record, p_{5max}; the number of impact events in the five minute record, N_5 ; and the mean event period, T_{pres}, at each of the four sensors. The level of each sensors is indicated on the graph. For all of these parameters, the sensors on the upper limb (1 and 2) give similar results. Pressures for sensors 3 and 4 on the side and lower limbs show similarities with each other, but differ from those for 1 and 2.

The 33% exceedance pressure, $p_{33\%}$, for all sensors rises as the tidal level increases and more waves hit the Cob. Once the sensors are submerged, similar pressures are observed at each sensor, with $p_{33\%}$ in the range 1.5 to 2.5m for the storms analysed. Peak pressures, p_{5max}, for sensors 1 and 2 are highest when the still water level lies around 1 to 1.5m below the sensors. The peak pressures show large but infrequent impact events. A maximum peak impact pressure of p_{5max} = 8.0m was observed, but peak pressures of over 4.0m were infrequent. Assuming an incident wave height of 2m, these represent peak pressures equivalent to 2 to 4 H_s.

Impact events are also most frequent when the water level is between 1m and 1.5m below the sensor. Up to 15 impact events occur during a 5 minute interval (Fig 5.12). Few impact events are recorded once the water level reaches the sensor.

Probability distribution of peak pressures

In the storm events analysed, the impact events represent around 30-50 events in each 5 minute period. The peak values used earlier are therefore based on relatively few events, and are probably rather unstable measures of the distribution of impact pressures. To reduce this uncertainty, probability density distributions were fitted to the pressure events in each record, and these distributions were used to estimate 2% exceedence values.

Four distributions were considered: Normal; Weilbull; log-normal; and Raleigh. Of these the least worst description of the upper end of the distribution was generally given by the Weibul distribution. The 2% exceedence pressures derived using the Weibul distribution, shown in Figure 5.18, are generally similar to the peak values over the 5 minute record, Figure 5.15.

Major impact events

Impact events with peak pressures of over 3.0m have been considered in greater detail to determine typical impact rise times, for comparison with the natural frequency for stress waves within the Cob.

Impacts on sensors 1 and 2 only were considered, as significant impacts were only observed on the upper limb of the unit. Each major impact peak on 28/01/90 for both sensors is shown in Figure 5.19. These impact events were previously identified on the time series for sensor 1 (Fig 5.12). The comparison of these results demonstrates considerable variation between pressures measured at sensors only 0.5m apart.

The similarities between records do however give reasonable confidence in the ability of the instrumentation adopted, and the processing and analysis methods used, to resolve events of the short durations and/or rapid rise times observed.

Other impact events giving $p_{5max} > 3.0m$ for 25 and 26 January 1990 are shown in Figure 5.20. Over the 13 records analysed, a total of 43 independent events were identified, some of which were observed on both sensors on the upper limb. Events with $p_{5max} > 3.0m$ can be classed in three groups: fast impacts with rise times of 0.02 seconds or less; slow impacts with rise times typically 0.05 seconds; and quasi-hydrostatic events. Three events gave $p_{5max} > 5.5m$.

5.4 Conclusions

5.4.1 Instrumentation

The overall data return for the third field exercise was much more satisfactory than for the previous deployments. The Schaevitz P1787/0001 pressure transducers performed excellently. The only failures were due to cable breakage between the instruments and logger near the end of the deployment. Similarly the wave/tide pressure transducer performed well, up to its failure after five months deployment.

The performance of the run-up gauges on the other hand was very poor, with both gauges failing shortly after the deployment. Problems have now been experienced with two designs of run-up gauge. The development of a reliable system for measuring wave run-up in the field remains an outstanding requirement. It may be more useful to revert to using a large number of pressure cells placed regularly up the slope.

The data logging system performed satisfactorily in the field. The very large volume of data, and low access times of the Exabyte tape recorder made the analysis of the data time-consuming. Recent developments in optical compact disk storage media, and/or intelligent logging may significantly improve this situation.

5.4.2 Analysis

Wave pressures on the units generally follow wave run-up levels, but some waves give impact pressure up to 3-5 times higher. Impact events often show rise times as short as 5 to 20 milliseconds. On any particular armour unit, such impacts may be quite frequent when the water level is close (within about 1m) to the measurement unit. At La Collette these impacts occured at up to once in 20 to 60 seconds, corresponding to an impact event every 3-8 waves.

6. PHYSICAL MODELLING OF ARMOURED SLOPES

The design of any rubble mound structure protected by concrete armour units requires data on the hydraulic characteristics of the armoured slope, and on wave pressures and/or forces acting on the armour units. These responses are most conveniently and reliably derived from measurements in hydraulic model tests. Three series of model tests were conducted in this project:

a) 2-dimensional tests on Cob armoured slopes at 1:1.33 and 1:2.0, based on the breakwater at La Collette;
b) 2-dimensional tests on a simplified Shed armoured slope at 1:1.33;
c) 3-dimensional tests on a simplified Shed armoured roundhead and trunk section with a slope of 1:1.33.

6.1 Cob armoured section, wave flume tests

6.1.1 Model design and construction

Introduction

Physical model tests were undertaken to further the hydraulic understanding of Cob armoured structures, by describing the effects of waves and water level on wave-induced loadings on an armour unit. Run-up and reflections were also measured to extend the existing, somewhat limited, data set. The model was loosely based on La Collette breakwater at St Helier in Jersey. These tests were completed in the deep random wave flume at HR, at a scale of 1:31.25, set by the size of model Cob units available. The tests are discussed in more detail in Reference 26.

Design variables

The bathymetry is extremely complex at La Collette. A simple representative cross section was formed in cement mortar in the flume with an average slope of approximately 1:50. The model breakwater was constructed to the cross section illustrated in Figure 6.1. The underlayer and core material were scaled to reproduce the correct permeability using the method by Jensen & Klinting (Ref 27). The toe beam, spacer block and the crown wall were not scaled for stability, but were held rigidly in place. This

enabled instrumentation to be secured firmly in the model.

Most of the tests used the model of La Collette breakwater (Section 1), but two limited series of tests were also completed on modified structures (Sections 2 and 3). La Collette has a relatively permeable underlayer which dissipates considerable energy in its internal flows. The permeability of the underlayer was expected to influence the forces imposed on the armour units, and the performance of the structure as a whole. A less permeable underlayer might dissipate less energy and increase the forces imposed on the armour layer, but it could also be easier to obtain and place, hence reducing costs. A limited series of tests on Section 2 were completed using a substantially smaller underlayer equivalent to about 10-30 Kg. Otherwise this section was identical to Section 1.

Finally, in order to investigate the effect of slope angle, some tests were completed for a 1:2 slope (as opposed to the 1:1.333 slope at La Collette) using the less permeable underlayer. This was termed Section 3.

A wide range of random wave conditions were derived, allowing the independent variation of significant wave height, H_s, and mean wave period, T_m. A standard spectral shape, in this case JONSWAP, was used throughout testing. It was important to investigate how wave-induced forces varied with the relative position of the armour unit to still water level (the freeboard). Three force gauged units were deployed in the model. Three different water levels were employed during the model tests to obtain a wide range of freeboard conditions. These corresponded to 11.1m CD, 9.0m CD and 7.9m CD at La Collette.

Instrumentation

A new force transducer was developed to measure the rigid body wave forces on selected armour units. Each force gauged unit measured forces parallel to the slope in the direction of wave travel (drag), and perpendicular to the slope (lift). These units were isolated from the surrounding armour and underlayer, ensuring that only loads caused by wave action were measured. Three instrumented units were deployed in the physical model. The position of the force transducers is illustrated in Figure 6.2.

Six pressure transducers measured both wave impact and quasi- hydrostatic pressures. These were sited in two

groups of three on the upper limb of the armour unit (the farthest up the slope in the outer plane of the armour), on the lower limb (the limb farthest down the slope in the outer plane of the armour) and on one of the two side limbs (the limbs which connect the upper and lower limbs). The pressure transducers were buried deep in the breakwater core. They were connected to the surface of the armour units by a water filled hypodermic tube down which all pressures imposed on the surface of the armour unit were transmitted, shown in Figure 6.3.

Further instruments were also deployed in the model to measure wave run-up levels, and wave reflections. Three capacitance run- up gauges were installed, one on the surface of a column of armour units, another through the central void of a column of units, and the last at the interface between underlayer and core, illustrated in Figure 6.4. An array of three wave probes were placed seawards of the breakwater to measure wave reflections.

Signals from all the instruments were recorded on a Compaq micro- computer, and analysed using various software packages. Ideally each type of instrument would be logged at a different rate. An adequate description of wave heights and run-up in the model is possible using digitisation rates of approximately 10Hz, but forces and pressures need substantially higher rates. The acquisition system did not easily allow differential sampling rates, so run-up and wave gauge data was collected at the high digitisation rates required for forces and pressures.

An investigation was completed to determine the most appropriate digitisation rates for recording forces and pressures. Data was collected at rates between 100 and 2000 Hz. Analysis of these time series indicated that a digitisation rate of 400 Hz should be used to avoid problems with aliasing and attenuation of the impact peaks. At this digitisation rate, however, both force and pressure transducers exhibited high frequency oscillations. It was therefore necessary to employ a 50 Hz low pass Chebychev filter to filter all the force and pressure data prior to digitisation.

6.1.2 Wave run-up

Values of the significant run-up level, R_{us} and the 2% run-up level, $R_{u2\%}$, were calculated for each of the three run-up gauges. A run-up event was defined as a crossing of the mean run-up level recorded during the test. This threshold was used,

rather than still water level (SWL), because wave set-up on the slope was often such that run-down seldom fell below SWL. Although all events were defined by a crossing of the mean water level, they were measured relative to SWL.

The significant, R_{us}/H_s, and 2%, $R_{u2\%}/H_s$, relative run-up levels are plotted against the modified Iribarren number, Ir_p, for the three run-up gauges on Section 1 in Figures 6.5 - 6.7. Relative run-up levels may be described by an empirical equation using the modified Iribarren number. A variety of equations were considered, see Reference 26. That selected was:

$$R/H_s = A\ Ir_p/(Ir_p + B)$$

where R is the relevant run-up level and A and B are empirical coefficients.

A regression analysis was used to identify this equation as best describing the data in this instance. These lines of best fit are illustrated in Figures 6.5 - 6.7. Although the correlation coefficient indicates the line of best fit, it does not directly aid the designer in taking account of the scatter in data values. A standard deviation was therefore determined for each line of best fit allowing the calculation of confidence limits for the data.

A comparison between run-up levels from each of the gauges indicates that run-up within the units is marginally less than on top of the units. The overall shape of the lines of best fit for these two gauges were similar, not really surprising when the proximity of the gauges and the permeability of the units are considered. Run-up levels in the underlayer were approximately half those experienced by the upper gauge. This indicates the difficulty in large run-up events penetrating the underlayer, which limits the amount of water entering and leaving the mound.

The ratio of the mean period of run-up, T_r, to the mean wave period, T_m, is plotted against the modified Iribarren number, Ir_p in Figure 6.8. At large Ir_p, ie long period waves, all three gauges exhibited similar period ratios of approximately one. Under these conditions the underlayer has time to drain down below the threshold before the onset of the next wave. However, as the wave period shortens, ie Ir_p decreases, the period ratio increases for all gauges, the threshold level is not consistently crossed for each incident wave. This increase is particularly marked for the gauge inside the

underlayer which exhibited a mean run-up period over one and a half times the mean wave period for 3 < Ir_p <4.

Run-up parameters were also calculated for the tests with the less permeable underlayer at a slope of 1:1.333, Section 2, and at 1:2, Section 3. Data obtained from the upper and middle gauges are illustrated in Figures 6.9 and 6.10. As was observed for Section 1, there is marginally less run-up through the centre as opposed to the top of the units.

The lines of best fit for Sections 1, 2 and 3 are compared with data obtained by Allsop (Ref 15) in Figures 6.11 and 6.12. Allsop measured run-up on a Shed armour placed on granular underlayer on a permeable support board. The omission of a rubble core in these tests would have decreased the wave set-up, thus reducing measured run-up levels. All three data sets exhibited similar 2% run-up levels, suggesting that run-up levels are governed chiefly by dissipation of wave energy in the voids in the units, rather than by the permeability of the underlayer and core. The data for the significant run-up showed considerable variability. The data obtained from slope 1 and that presented by Allsop suggest significant run-up levels are almost independent of Ir_p, although there is approximately 20% difference in levels.

6.1.3 Wave reflections

An overall reflection coefficient, C_r, was calculated for each test condition using a method developed by Gilbert and Thompson (Ref 28) based on the work of Kajima (Ref 29). The reflection coefficients obtained from the model tests were plotted against the modified Iribarren number and are illustrated in Figure 6.13. The data exhibited considerable scatter. However, an analysis of several empirical equations found that the data set was best described by:

$$C_r = a.Ir_p^{\,b} \qquad (6.2)$$

A standard deviation of 0.060 was calculated thus enabling confidence limits to be applied to the line of best fit.

A comparison was made between the reflection characteristics of Cobs and alternative armour units (Ref 30). This comparison is illustrated in Figure 6.13. The data for these alternative units was again obtained using a permeable backboard instead of a

core. This was likely to produce lower reflections than if a rubble core had been used. Also the data sets were somewhat small and so were combined for similar types of unit. Results indicated that all the alternative units exhibited smaller reflection characteristics than Cobs. This is not really surprising in the cases of Tetrapods or Stabits, since they are placed in thicker layers allowing substantial dissipation of wave energy in the voids between the armour units.

Alternative single layer armour units such as the Shed or Diode also exhibited slightly better reflection coefficients than the Cob. However, it is unclear if this is simply coincidental or because the shape of a Cob is marginally less efficient in dissipating wave energy. It should be noted that the alternative data was only available for $Ir_p < 6$ and the lines on Figure 6.13 have been extrapolated for higher values of Ir_p. In practice, for $Ir_p > 6$, these lines will probably be much steeper, closer to the line of best fit for the Cob data.

6.1.4 Wave pressures

The typical pressure series obtained during the model tests exhibited both short duration impact and much longer duration quasi-hydrostatic pressures. Many of the impact events, which had rise times in the order of 10-20 milliseconds, were smaller in magnitude than some of larger quasi-hydrostatic events. Attempts were made to isolate these impacts and analyse them independently, but proved unsuccessful at the time. The pressures were therefore analysed without differentiation between impact and quasi-hydrostatic events.

The pressure data was analysed using a statistical method. A threshold level equal to 0.75 x the signal mean was derived. This ensured that the threshold was above the noise level associated with the ambient pressure, but below the level of significant wave loading. The amplitude of the maximum peak between successive zero up-crossing periods was recorded and an exceedance probability distribution completed on the dataset.

The analysis was concentrated on the upper end of the exceedance curve, particularly the 2% and the maximum value (equivalent to about the 0.7% exceedance value for this length of test).

Previous fieldwork data (Ref 24) had suggested that wave impact events were strongly dependent on tidal

elevation, and so a non- dimensionalised freeboard, FREE(P)*, was defined as:-

$$FREE(P)^* = Freeboard_p/H_s \qquad (6.3)$$

where $Freeboard_p$ is the distance of the top of the transducer above still water level.

The ratio of the maximum impact pressure to significant wave height, p_{max}, and the 2% impact pressure to significant wave height ratio, $P_{2\%}/H_s$ are plotted against the non-dimensionalised freeboard in Figures 6.14 - 6.16 for transducers positioned on the upper, lower and side limbs. These graphs indicated that the most frequent and largest impacts occurred on units positioned close to the water level. Impact events were generally limited to the three units sited around SWL for the range of wave heights used in this study . The side and upper limbs sustained maximum impact pressures equivalent to approximately $3.5H_s$, whereas that on the bottom limb was equivalent to only $2H_s$. This illustrated the importance of limb orientation in determining the magnitude and frequency of wave impact events. The transducer in the side limb sustained the greatest number of large impact events (those greater than $2H_s$). However, there was a lack of data for the upper limb for $-0.2 < FREE(P)^* < 0.05$. In practice the upper limb may be expected to sustain the greatest number of impacts.

6.1.5 Wave forces

The wave force data was analysed using a threshold crossing technique similar to that performed on the pressure data. An exceedance probability curve was then derived for the maximum and minimum values of each event.

The forces imposed on the units were found to be independent of slope angle. It was also discovered that the permeability of the underlayer had a negligible effect over the range of conditions studied. However, as with impact pressures, the forces were dependent on dimensionless freeboard. The largest forces occurred on units sited around SWL and were dominated by the up- slope drag force. This force was approximately twice as large as the in-slope lift force. The large up-slope drag and in-slope lift forces were caused by waves impacting on the slope. The maximum out of slope lift and down-slope drag forces were imposed during run-down and were of much longer duration. The out of slope lift force was generally about 60% of the in-slope force. The

down-slope drag force was relatively small in comparison with the other forces.

6.1.6 Armour unit and underlayer movement

No armour units were displaced during this series of tests. There was, however, some slight settlement of the armour layer, possibly caused by compaction of the core and movement of underlayer. For the more permeable underlayer tested in Section 1, some slight intermittent rocking of the smaller sizes of the material was observed during the tests.

The smaller underlayer tested in Sections 2 and 3 exhibited significant movement when subject to wave attack. A flow vortex was formed in the central void of the unit during wave uprush, and this transported material positioned under the void, trapping it behind the lower bottom limb (see Figure 6.17). Some material was also moved during downrush, but this was less common. Although there was considerable underlayer movement, the large velocity vectors capable of transporting the material did not point in the right direction to enable any particles to escape through the central voids of the armour units. This suggests that underlayer material smaller than the void in the unit (in this case the underlayer material was approximately half the size of the void) might be used in the construction of hollow cube armoured structures, but only if underlayer movement can be tolerated.

6.2 Shed armoured section, wave flume tests

6.2.1 Model design and construction

Introduction

Two-dimensional model test were undertaken to determine the performance of Shed armour units. These tests were completed at a scale of 1:32.5, again set by the size of model Shed units. Measurements were made of wave-induced forces on isolated units, wave impact pressures, wave run-up and wave reflections. These test are discussed in Reference 31.

Design variables

A simplified approach bathymetry of 1:50 was moulded into the wave flume. A base section for the breakwater was also formed in cement mortar. This increased the water depth at the test section,

allowing larger waves without breaking, and supported the armour units instead of a toe beam, illustrated in Figure 6.18. The model Shed armoured breakwater had a slope of 1:1.333 and was topped with a parapet wall. A relatively impermeable core material was used in the model. The underlayer was based on that at La Collette breakwater. The structure was tested for a wide range of random wave conditions using the JONSWAP spectra to describe the spectral shape. All testing was completed using a water depth of 0.4m at the structure toe.

Instrumentation

A new 3-axis force transducer was developed to measure wave forces perpendicular to the slope (lift), parallel to the slope in the direction of wave travel (drag), and parallel to the slope but perpendicular to the wave (transverse). Three of these units were deployed at various elevations in the model. Six pressure transducers were also deployed, three placed in the voids of units with their diaphragms open to direct wave attack. The remainder were positioned in the core and connected to the upper, side and lower limbs of a unit by water filled hypodermic tubes as before. The position of the force and pressure transducers, which were concentrated around SWL, is illustrated in Figure 6.18. Run-up gauges and wave gauges designed to measure wave reflections were deployed in similar positions as on the Cob armoured structure.

All data was collected using Compaq micro-computers. Force and pressure data was digitised at 300 Hz and then filtered using a 100 Hz Chebychev low pass filter. A 20 Hz digitisation rate was used for the run-up gauges and wave gauges.

6.2.2 Wave run-up

There was considerable uncertainty in the wave run-up data. The measurements exhibited considerable scatter and did not appear reliable. It was considered that the high number of overtopping waves experienced by the structure caused spurious run-up events to be recorded. No results are therefore presented for wave run- up.

6.2.3 Wave reflections

The wave reflections measured during testing are presented in Figure 6.19. The reflection coefficients appeared to be considerably larger than those measured in earlier experiments, possibly due to the omission

of the toe beam, but inclusion of a crown wall. These results were therefore not considered to be typical of the behaviour of a Shed armoured slope.

6.2.4 Wave pressures

The wave pressure measurements were analysed using the same techniques as outlined in Section 6.1.4. Figures 6.20 - 6.25 illustrate the variation in the maximum impact pressure to significant wave height ratio and the 2% impact pressure to significant wave height ratio with wave steepness, $s_p = 2\pi H_s/g.T_p 2$. No dependence on wave steepness could be determined. The largest wave impacts were measured on the upper limb and in the void of the unit positioned at SWL. For these gauges the maximum impact pressure was up to twice as large as the 2% value. Maximum impacts were equivalent in size to 2-3 H_s. Wave impact events on the side and bottom limb and in the voids of units sited away from SWL were small.

The performances of the two different types of pressure measuring device were compared. Figure 6.26 illustrates the variation in impact pressures measured by different transducers at similar elevations. The open transducer positioned at SWL generally gave similar pressures to those measured by the hypodermic situated in the upper limb of a unit. Pressures measured by hypodermics in the side and lower limbs were somewhat lower. It was therefore concluded that the transducers placed in the void of a unit gave a good indication of the pressure measured on the upper limb of a unit.

The magnitude of wave impacts was generally slightly less than measured in the Cob armoured structure tests. It was considered that the number of waves breaking on to the structure was diminished in the present study because of the increased water depth and the absence of a toe beam. An example exceedance curve for all six transducers is shown in Figure 6.27. Large wave impact events were rare, and this is characterised by the steep increase in the size of wave impacts at the lower end of the curve for certain gauges. For the other gauges, where impact events were consistently small, the exceedance curve is relatively flat.

The distribution of impact pressures was investigated. Fuhrboter (Ref 32) has reported wave pressure measured on a 1:4 slope at prototype and 1:10 scales. Fuhrboter concluded that a log-normal distribution best described the impact events. Three distributions

were fitted to the pressure data; the Gaussian, log-normal and Rayleigh distributions. Examples of these three distributions are given in Figures 6.28 - 6.30. In general it was found that the Gaussian distribution gave the best fit and the log-normal distribution the worst. This disagreement may be partly explained by Fuhrboter's definition of an impact event as being the largest pressure recorded by an array of pressure transducers.

6.2.5 Wave forces

Wave forces on the Shed units were similar to those measured during the tests on the Cob armoured slope. The dominant forces were found to be the up-slope drag and the in-slope lift forces. Transverse forces, caused by vortex shedding as the wave travels up the slope, were extremely small. A typical time series trace is illustrated in Figure 6.31. This trace shows that the maxima in the up-slope drag and in-slope lift forces are coincident. The orientation of the wave appears to determine the relative magnitude of these forces with plunging waves imposing large in-slope lift forces, but small up-slope drag forces. Surging waves reversed this effect.

The relative magnitude of the non-dimensionalised drag and lift forces are illustrated in Figures 6.32 and 6.33. The method of non-dimensionalising the forces is outlined in Reference 31. The up-slope drag and in-slope lift force exhibit considerable scatter, with the largest forces occurring on units at or just above SWL. The out of slope lift force, usually of overriding concern to designers, was largest on the unit situated just below SWL. The head difference across the armour will be greatest for units just above the position of maximum run-down. For units above SWL, out of slope lift forces were small as the incoming wave permeates into the mound. The down-slope drag force is approximately constant whatever the unit elevation and incident wave conditions.

6.3 Shed armoured roundhead, wave basin tests

6.3.1 Model design and construction

Introduction

Three-dimensional model tests were completed to determine the performance of Shed armour units under angled wave attack, and on a breakwater roundhead.

The 3-axis force-gauges were deployed on the trunk and roundhead. Further instrumentation deployed in the model included pressure transducers and run-up gauges. All testing was completed in the complex sea basin at HR at a model scale of 1:32.5. The tests are discussed in depth in Reference 31.

Design variables

A Shed armoured breakwater roundhead was constructed at an angle of 45° to the direction of wave travel (see Figure 6.34). The armour layer was again supported by a moulded section at the bottom of the breakwater (see Figure 6.35). The breakwater trunk and roundhead were laid at a slope of 1:1.333. There was no increase in the radius of the roundhead. A JONSWAP spectra was used to describe a wide range of random wave conditions. All tests were completed using a water depth of 0.5m at the structure and a flat approach bathymetry.

Instrumentation

Similar instrumentation to that deployed in the 2-D Shed armoured model was used in the 3-D tests. Four force transducers were deployed at the waterline on the breakwater trunk and roundhead, illustrated in Figure 6.36. The model also included five pressure transducers, without hypodermic tubes, and six run-up gauges, shown in Figure 6.37. All run-up gauges were sited on the top of the armour layer. Data was collected on Compaq micro- computers using the same digitisation rates as before.

6.3.2 Wave run-up

Figures 6.38 and 6.39 show the variation in the significant relative run-up level, R_{us}/H_s, with modified Iribarren number, Ir_p, for the gauges deployed in the model. Gauge 6 failed early in the testing and so no results have been presented. The gauge on the roundhead facing the incoming waves (gauge 4) showed little dependence on Ir_p, with R_{us}/H_s around 1.4. This was less than that measured in the 2-d tests on Cobs, where R_{us}/H_s was approximately 1.6. This is not surprising since there are preferential pathways on the roundhead for the incoming wave front to the left and right of the gauge.

The run-up gauges situated at the end of the breakwater trunk (gauges 1 and 2) gave broadly similar results. They indicated a linear relationship between the relative significant run-up, R_{us}/H_s, and

Ir_p. The waves experience a much flatter slope than the 1:1.333 structure slope suggests, and hence the effective Iribarren number is less than that given In Figure 6.38. The relationship between relative significant run-up and Ir_p may be similar to that reported by Delft Hydraulics (Ref 33). Run-up levels at gauge 3 on the trunk appeared to be affected by the proximity of the roundhead. The relative run-up R_{us}/H_s was again independent of Ir_p and was approximately equivalent to 1.6.

Observations of the wave diffracted around the breakwater roundhead suggested that run-up levels diminished as the wave travelled around the roundhead. These observations were supported by gauge 5 which exhibited lower levels than gauge 4. The relative significant run-up level at gauge 5 again appeared to be independent of Ir_p.

6.3.3 Wave pressures

A comparison was made between pressures measured by the three transducers placed at the same elevation along the breakwater trunk (see Figure 6.40). No significant difference in the pressures could be discerned. Maximum impact events had magnitudes up to 3 H_s. The variation in impact pressures with elevation is illustrated in Figure 6.41 for transducers situated in the same column. The largest impacts were recorded on the transducer at SWL. Wave impacts on the units above and below SWL were significantly smaller.

The wave pressures recorded were also compared with those measured in the 2-D tests. These comparisons are shown in Figures 6.42 - 6.44. They illustrate that there is little significant difference in the magnitude of the largest impact events between the 2-D and 3-D tests. This suggests that the angle of wave attack does not affect the magnitude of the largest wave impacts. It should be noted, however, that none of the pressure transducers incorporated in the 3-D model used hypodermic tubes. Hence, the distribution of pressure on a single unit was not investigated in the 3-D tests. It is likely that angled wave attack will increase the magnitude of impact events on the side limbs, whilst decreasing impacts on the upper limbs.

6.3.4 Wave forces

The non-dimensionalised forces measured in the 3-D tests are shown in Figures 6.45 - 6.47. These graphs indicate that the up-slope drag force is smaller than

was observed in the 2-D tests. The largest up-slope drag force was measured on the unit on the roundhead directly facing the incident waves. Under angled attack, waves travel along the slope and the reduction in the up-slope drag force is accompanied by an increase in the transverse force. In fact, because the angle of wave attack is so acute, the transverse force is larger than the up-slope drag force on units on the trunk and at the back of the roundhead. Down-slope drag forces appeared to be independent of the position of the unit and wave conditions, and were similar to the forces measured in the 2-D tests.

Large in-slope lift forces were restricted to units on the trunk and at the front of the roundhead where waves break. For exposed units, in-slope lift forces were similar to those measured in the 2-D tests. Out of slope lift forces were small, particularly for units on the roundhead. This may occur because it is likely that there is only a very limited wave set-up inside the core at the roundhead.

7. CONCLUSIONS AND RECOMMENDATIONS

7.1 Conclusions

A series of laboratory and field studies have identified much new data on the hydraulic performance of rubble slopes armoured with hollow cube armour units. The results of these studies may be used by designers to dimension such a structure, or may contribute input data to further analysis of the stresses induced within armour units of the types studied.

7.1.1 Wave forces

Wave forces on Cobs or Sheds are very similar.

The forces out of the slope acting on a single Cob or Shed are seldom great enough to move the unit out of the armour layer. The historic mode of armour damage, ie extraction of up to 5% of the armour, is not therefore a relevant failure mode for this class of unit.

The largest forces are generally up-slope and in-slope due to wave slam. Down-slope forces were lowest for all wave conditions and transducer positions tested. Under angled wave attack the up-slope force is reduced, but the transverse force increases. There is no evidence that the resultant is any greater than the up-slope force under normal wave attack. Out of slope forces are less than for normal wave attack.

7.1.2 Wave pressure

Wave pressures on the units generally follow wave run-up levels, but some waves give impact pressure up to 3-5 higher. On any particular armour unit, such impacts may be quiet frequent when the water level is close (within about 1m) to the measurement unit. During field data collection on La Collette breakwater at Jersey, these impacts occurred at up to once in 20 to 60 seconds, corresponding to an impact event every 3-8 waves.

7.2 Recommendations for future work

7.2.1 Limitations of work to date

The main limitations to present design techniques arise because the loads transferred between armour units cannot be predicted with confidence. To date the loadings have been treated as applying to individual units. The transfer of loads between units has not been addressed in detail, yet data on this aspect will be required to refine the assumptions made. The development of a suitable model of load transfer within the armour array requires data on the processes of load transfer, particularly from armour to underlayer, and therefore on the response of the armour layer to any changes to the mound.

7.2.2 Proposals for future work

Field measurements of wave loads and reactions

It is proposed that a unit on an existing, or new structure if available, be replaced by a measurement unit. This will measure reaction loads transferred from adjoining units and from the underlayer. Wave pressures will be measured on each of the exposed faces of a unit and incident wave conditions will be determined directly, or indirectly.

Experimental work on full and small scale slopes may also be required to describe the factors influencing armour/underlayer friction. The field work will be supported by wave flume tests, particularly to derive transfer functions between wave pressures and the whole body forces.

Array model of load transfer

A numerical model of load transfer within the armour layer array, including to and from the underlayer should be developed. This area of work will complement the field work, as the array model requires input values from measurements at full scale, and the field measurements cannot be generalised without the array model.

Development of new units

The studies to date, together with observations of the performance in service, have demonstrated that there may be advantage in modifying the unit shape to increase its strength for certain loading cases. Further hydraulic model studies will be required to quantify the main performance parameters of any new units, to quantify wave forces and/or pressures acting on the new/revised unit, and thus to contrast their performance with that of present units.

8. ACKNOWLEDGEMENTS

The work reported here has been conducted principally by members of the Coastal Structures Section, assisted by others in the Maritime Engineering Department of Hydraulics Research. Considerable assistance in the development of the numerical models was given by Dr J Smallman and G Harding, and in analysis of the field data by Dr D Ryder.

This work formed part of the activities of the Single Layer Armour Research Club. Hydraulics Research are grateful for the support of members of the club, and particularly to A Bell, J Clifford, J Davis, J Read, R Richter/J Floyd, R Thomas, P Waldron, and A Wilkinson.

9. REFERENCES

1 Allsop N W H, "Concrete armour units for rubble mound breakwaters and sea walls; recent progress". Report SR 100, Hydraulics Research, Wallingford, March 1988.

2 Wilkinson A R & Allsop N W H, "Hollow block breakwater armour units". Proc conf Coastal Structures '83, ASCE, Arlington, Virginia, March 1983.

3 Dunster J A, Wilkinson A R & Allsop N W H, "Single layer armour units". Proc conf Breakwaters '88, ICE, Eastbourne, May 1988.

4 Port Sines Investigating Panel, "Failure of the breakwater at Port Sines, Portugal". ASCE, New York, 1982.

5 PIANC, "The stability of rubble mound breakwaters in deeper water". Report of a Working Group of PTC 2, Supplement to Bulletin 48, PIANC, Brussels, 1985.

6 Allsop N W H, Smallman J V & Stephens R V, "Development and application of a mathematical model of wave action on steep slopes". Proc 21st ICCE, Malaga, June 1988.

7 Smallman J V, "Developments in numerical modelling of waves". Proc Symp Developments in Coastal Engineering, University of Bristol, March 1991.

8 Goda, Y, "Random seas and design of maritime structures". University of Tokyo Press, 1985.

9 Beardsley A, Smallman J V & Stephens R V, "Development of a mathematical model of wave action on slopes - recent progress". Report IT 318, Hydraulics Research, Wallingford, July 1988, (Restricted).

10 Green A P E, "Further development of a mathematical model of wave action on slopes". Report IT 337, Hydraulics Research, Wallingford, March 1989, (Restricted).

11 Packwood A R & Peregrine D H, "Surf and run-up on beaches: models of viscous effects". Report no AM-81-07, School of Mathematics, University of Bristol, 1981.

12 Kobayashi N, Otta A K & Roy I, "Wave reflection and run-up on rough slopes". Jo W'way , Port, Coastal and Ocean Eng Div, ASCE, Vol 113, May 1987.

13 Thompson A C "Numerical model of breakwater wave flows". Proc 21st ICCE, Malaga, June 1988.

14 Allsop N W H, Hawkes P J, Jackson F A & Franco L "Wave run-up on steep slopes: model tests under random waves". Report SR 2, Hydraulics Research, Wallingford, August 1985.

15 Allsop N W H, "The SHED breakwater armour unit: model tests in random waves". Report EX 1124, Hydraulics Research, Wallingford, April 1983.

16 Harding G D, Herbert D M & Smallman J V, "WENDIS: the wave energy dissipation model". Report IT 352, Hydraulics Research, Wallingford, January 1990, (Restricted).

17 Hunt J.N. 'Amortitissement par viscosité de la houle sur un fond incliné dans un canal de largeur finié ('Viscous damping of waves over an inclined bed in a channel of finite width'). La Houille Blanche December 1952.

18 Bretschneider C.L. and Reid R.O. 'Modification of wave height due to bottom friction, percolation and refraction. Beach Erosion Board Technical Memorandum No 45. October 1954.

19 Weggel, J.R. 'Maximum breaker height'. ASCE. J. Waterways, Harbours and Coastal Div. No WW4, Vol 98, pp 529-548, 1972.

20 Van der Meer, J W, "Extreme shallow water wave conditions". Report No H198, Delft Hydraulics, The Netherlands, January 1990.

21 Seelig, W N and Ahrens, J P, "Estimating nearshore conditions for irregular waves". CERC, Technical Paper No 80-3, 1980.

22 Wilkinson A R, "St Helier." Consulting Engineer, October 1978.

23 Stephens R V & Davis J P, "Preliminary field work and instrument trials". Report IT311, Hydraulics Research, Wallingford, July 1988, (Restricted).

24 Stephens R V, "Field work on La Collette breakwater, Jersey, January to May 1988". Report IT327, Hydraulics Research, Wallingford, March 1989, (Restricted).

25 Ryder D K, Herbert D M, & Allsop N W H, "Further measurements of wave pressures on La Collette breakwater, September 1989 to June 1990". Report IT354, Hydraulics Research, Wallingford, March 1990, (Restricted).

26 Herbert D M & Hare G R, "Physical model testing of a COB armoured structure". Report IT344, Hydraulics Research, Wallingford, January 1990, (Restricted).

27 Jensen, O J & Klinting, P. "Evaluation of scale effects in hydraulic models by analysis of laminar and turbulent flows" Coastal Engineering, pp 319-329, 1983.

28 Gilbert, G & Thompson, D M. "Reflections in random waves, the frequency response function method" Report IT 173, Hydraulics Research, Wallingford, March 1978.

29 Kajima, R. "Estimation of an Incident Wave Spectrum under the Influence of Reflection" Coastal Engineering in Japan, Vol 12, 1969.

30 Allsop NWH & Hettiarachchi SSL "Reflections from coastal structures" Proc 21st ICCE, Malaga, June 1988 (also available as Hydraulics Research published paper 17.

31 Jones, R J & Herbert, D M. "Physical model testing of a Shed armoured structure'. Report IT 361 (Restricted), Hydraulics Research, Wallingford, March 1991.

32 Fuhrboter, A. 'Model and Prototype Tests for Wave Impact and Run-up on a Uniform Slope of 1:4'. Proc Water Wave Research, Hanover, May 1985.

33 'Slopes of Loose Materials'. Delft Hydraulics, Report M1983, Part 3, 1988.

TABLE.

Table 5.1: Run-up levels on La Collette, second deployment

Date	U10 m/s	Dirn °N	Offshore H_s m	Offshore T_m s	Run-up R_{us} m	Run-up T_m s	Ir_m	R_{us}/H_s
11/1/88	12	190	1.56	5.3	1.4	5.9	4.0	0.90
12/1/88	19	160	2.41	4.6	2.0	6.8	2.2	0.83
13/1/88	7	180	1.67	9.5	1.8	9.8	6.7	1.08
14/1/88	10	170	1.75	8.2	2.0	9.4	5.5	1.14
01/2/88	24	240	4.53	8.6	2.1	9.1	2.2	0.46
02/2/88	23	260	3.87	7.5	2.7	7.8	2.3	0.70
10/2/88	28	280	3.01	7.5	2.1	7.8	2.9	0.70
08/3/88	7	010	0.39	7.1	0.8	4.6	21.3	2.05
15/3/88	22	260	2.85	6.2	2.2	5.9	2.5	0.77
16/3/88	22	290	3.17	8.2	2.5	8.1	3.0	0.79
17/3/88	6	170	0.69	9.1	1.1	6.2	15.5	1.59
18/3/88	2	280	3.23	9.5	1.2	6.8	3.5	0.37
19/3/88	13	190	0.66	9.0	1.1	6.6	16.0	1.67

FIGURES.

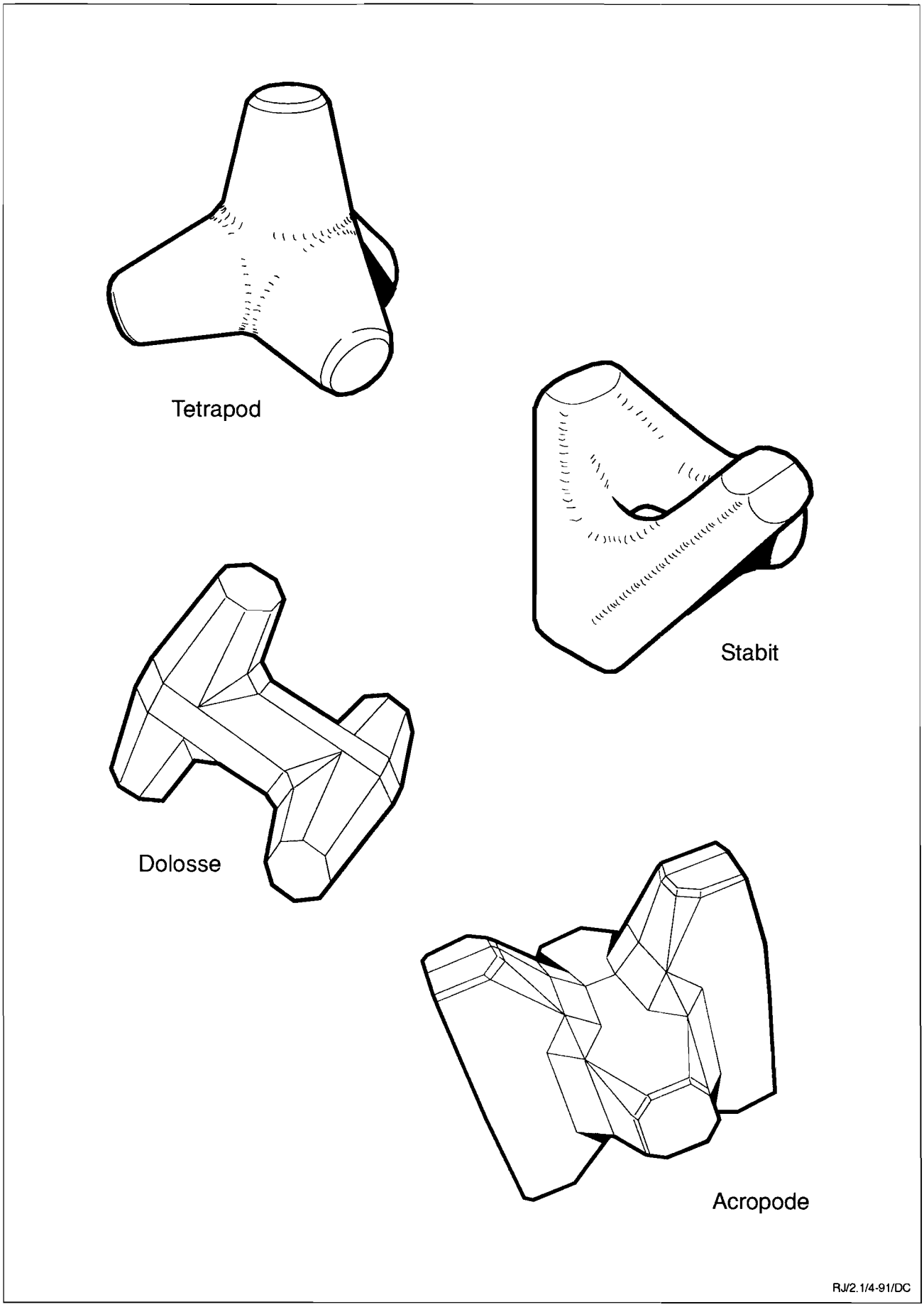

Fig 2.1 Tetrapod, Stabit, Dolosse and Acropode armour units

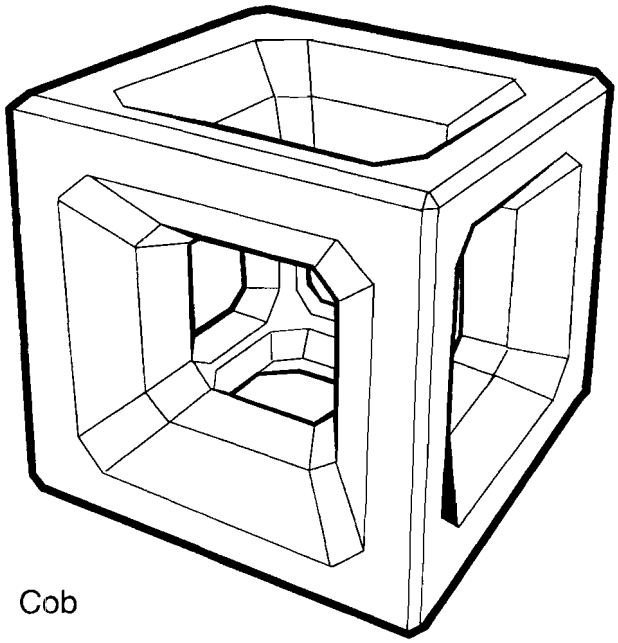

Cob

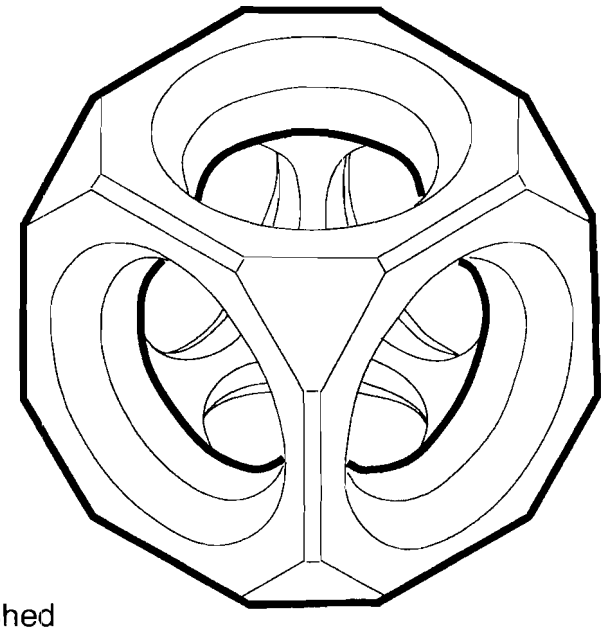

Shed

RJ/2.2/4-91/DC

Fig 2.2 Cob and Shed units

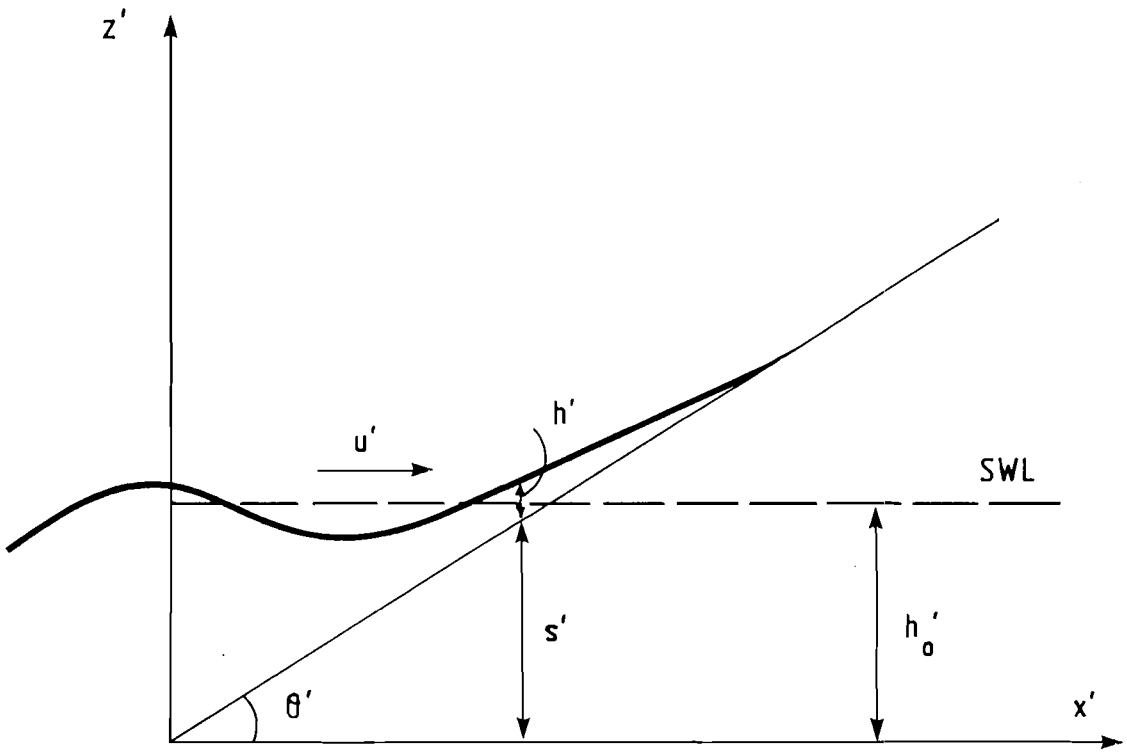

Incident wave amplitude a' , period T'

Fig.4.1 Mathematical model definitions, SLACWAVE.

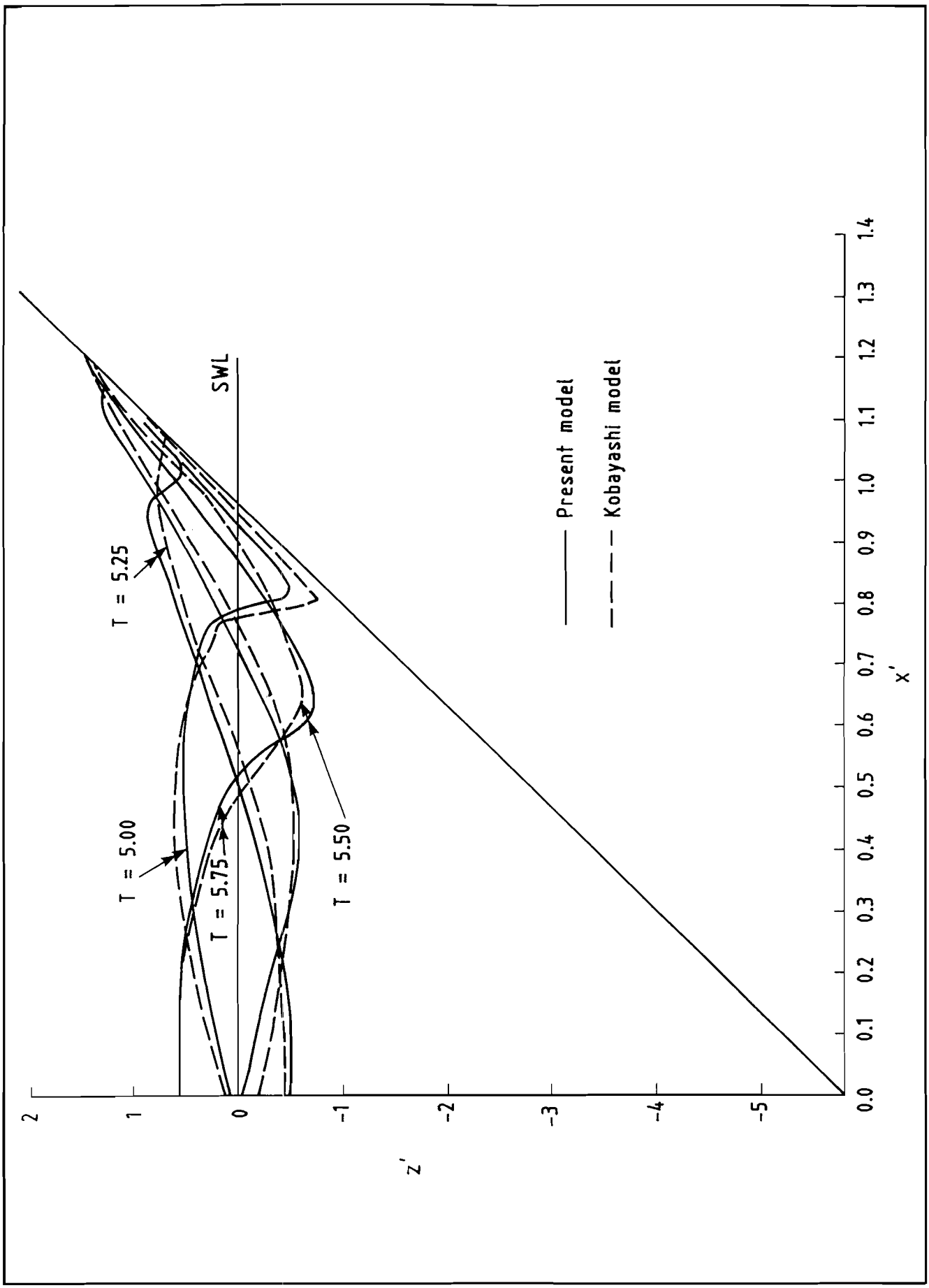

Fig 4.2 Comparison of model elevations with those of Kobayashi et al (Ref 12)

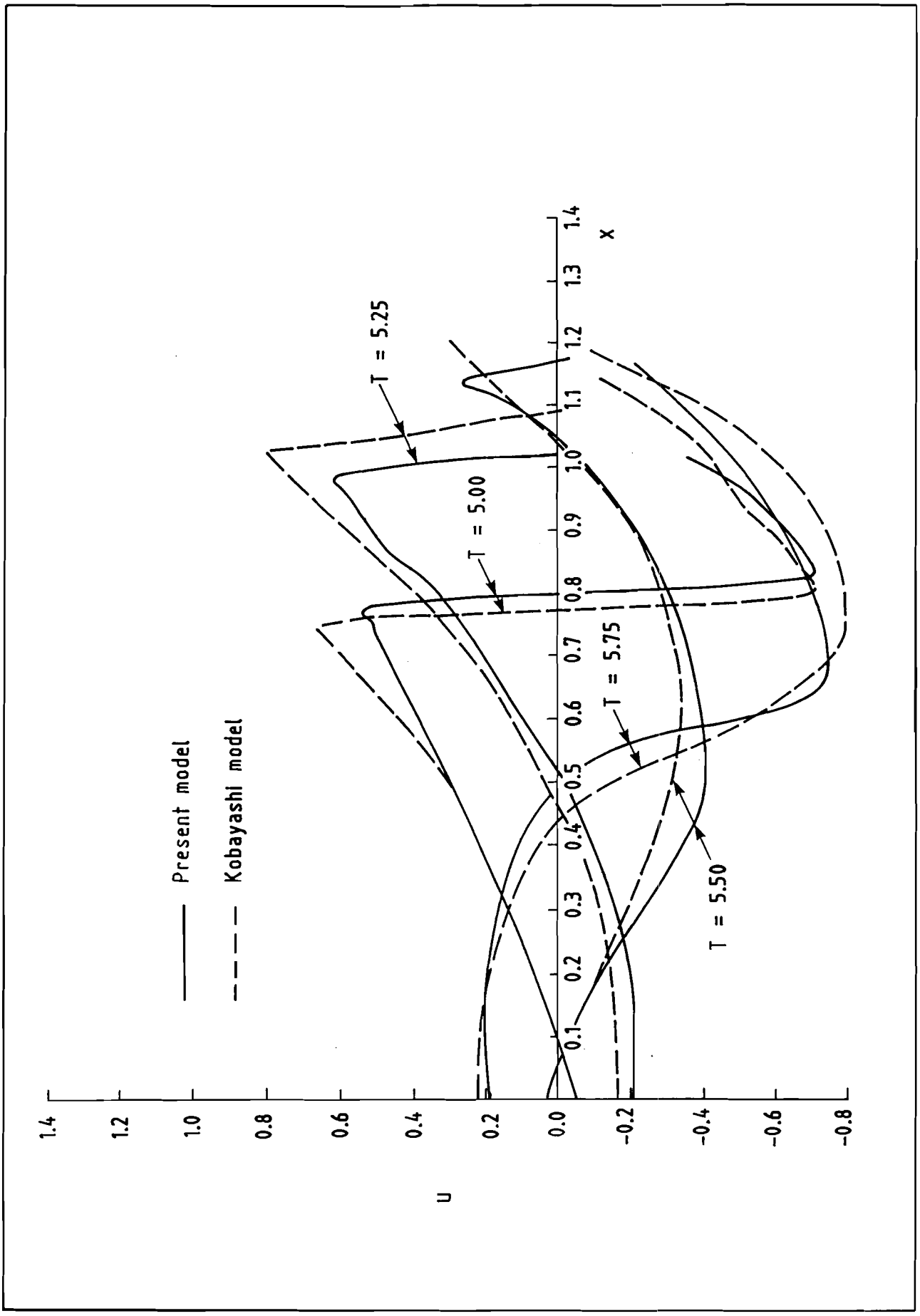

Fig. 4.3 Comparison of model velocities with those of Kobayashi et al (Ref 12).

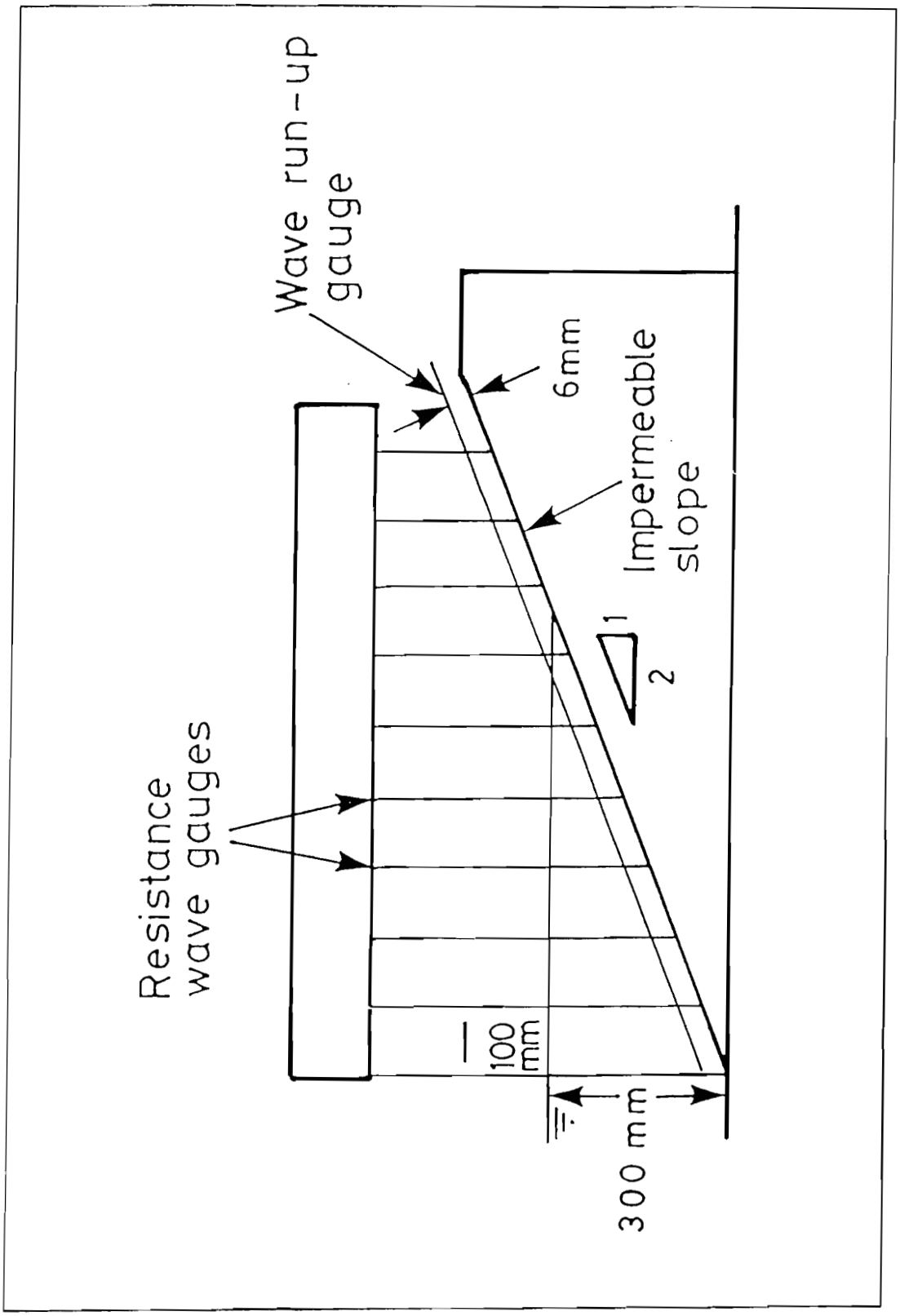

Fig 4.4 Layout for physical model tests, calibration stage 2.

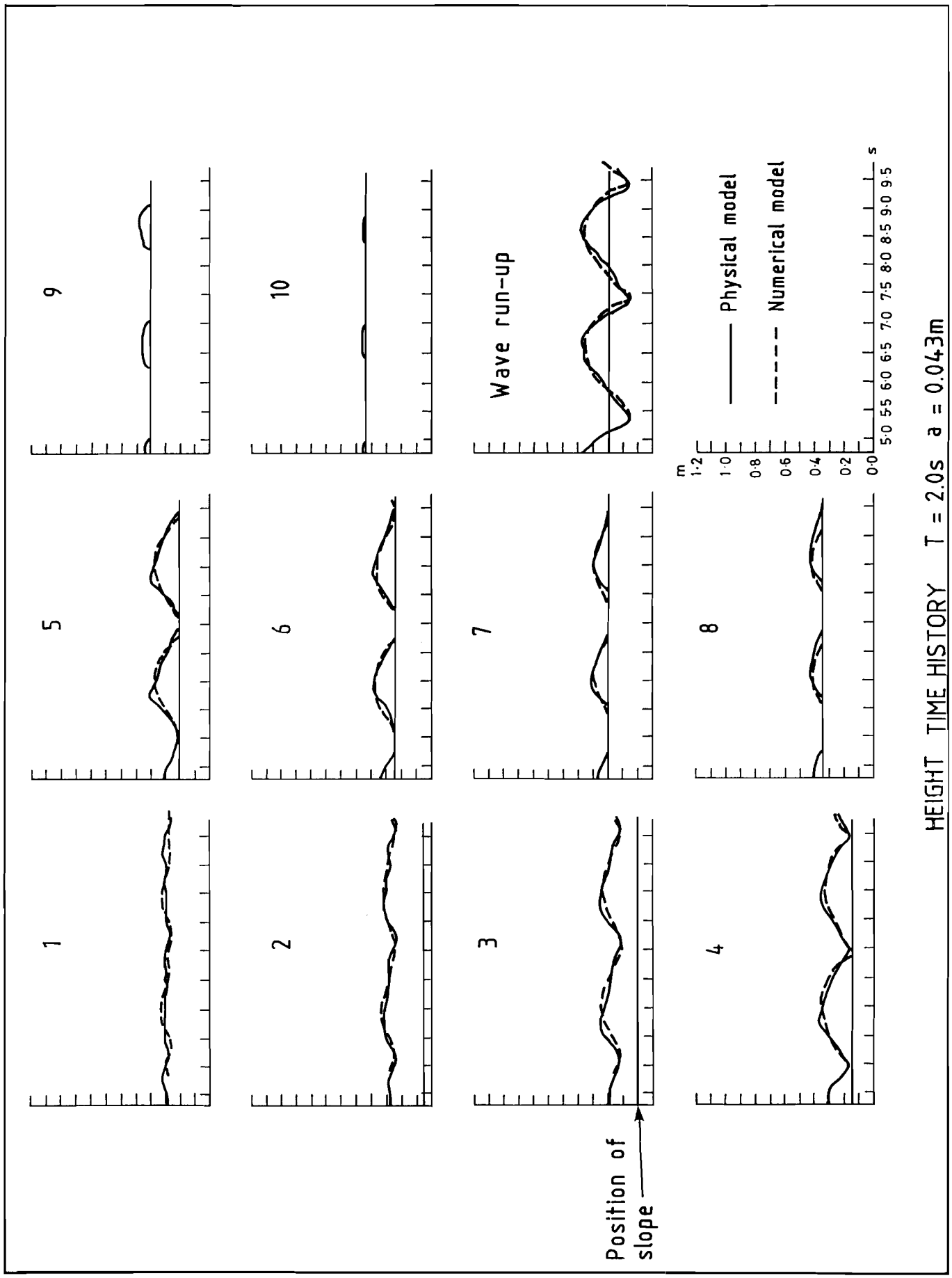

Fig 4.5 Comparison of elevations for physical and numerical models

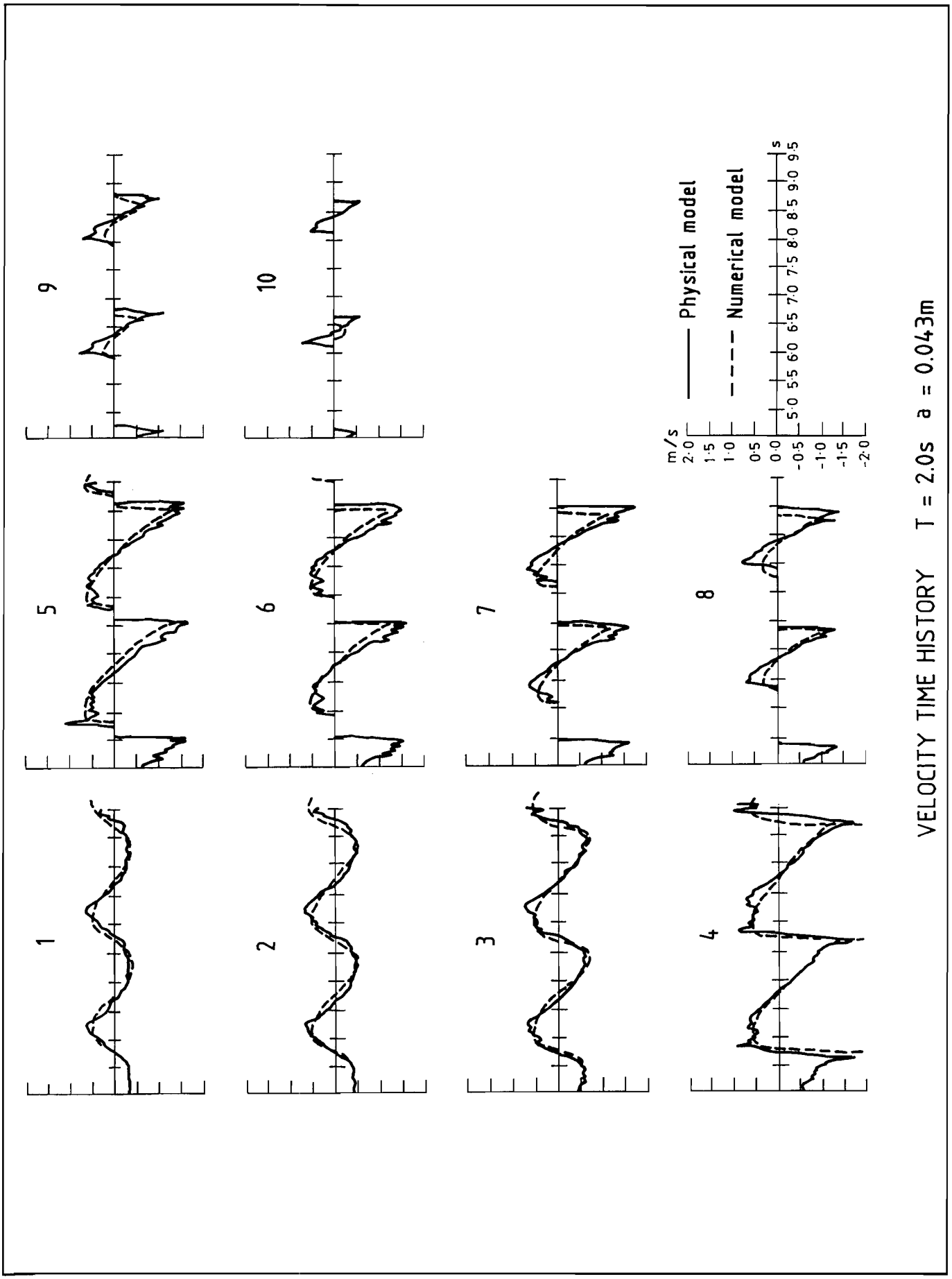

Fig. 4.6 Comparison of velocities for physical and numerical models

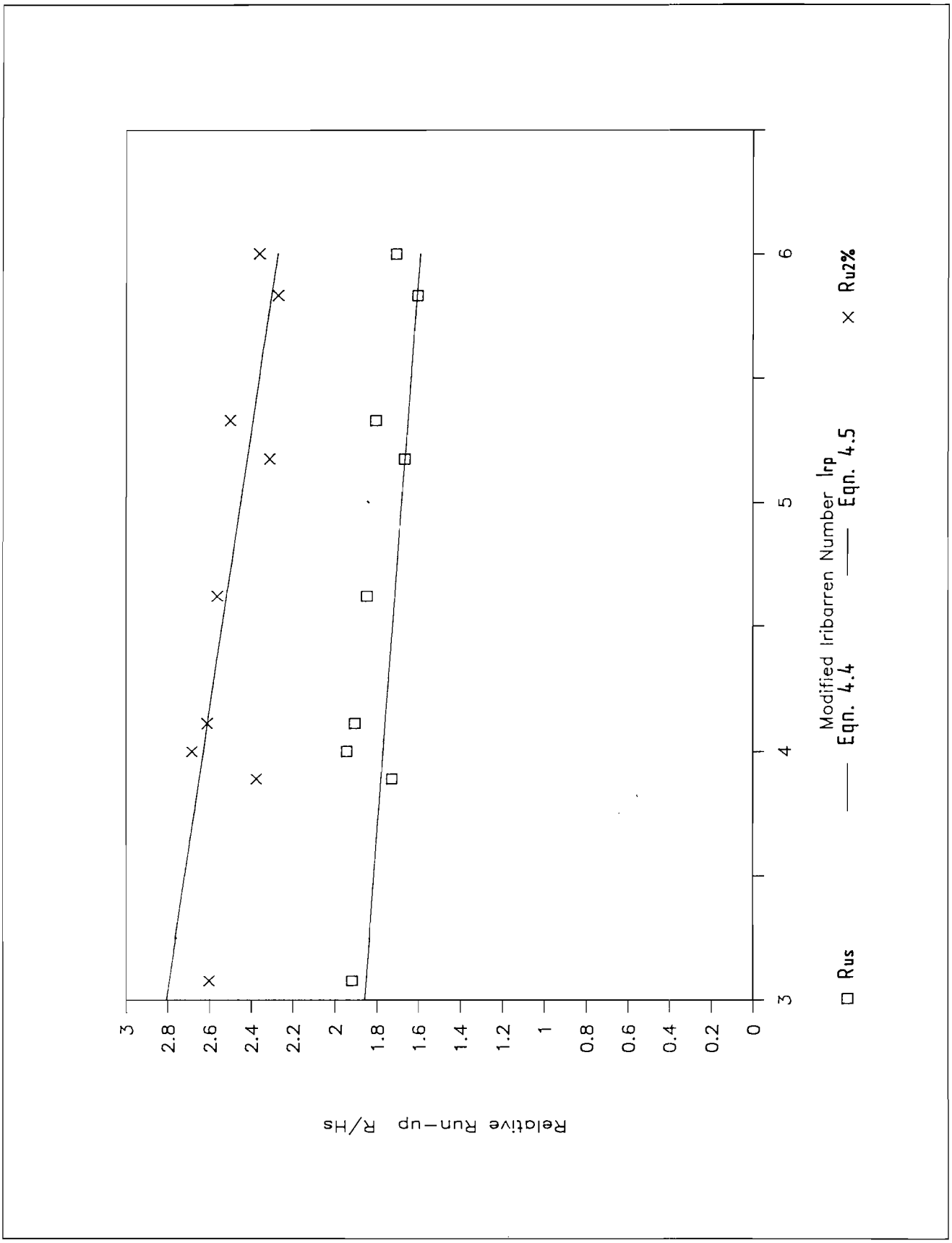

Fig 4.7 Comparisons of relative run-up levels calculated by SLACWAVE and by empirical equations (Ref 14)

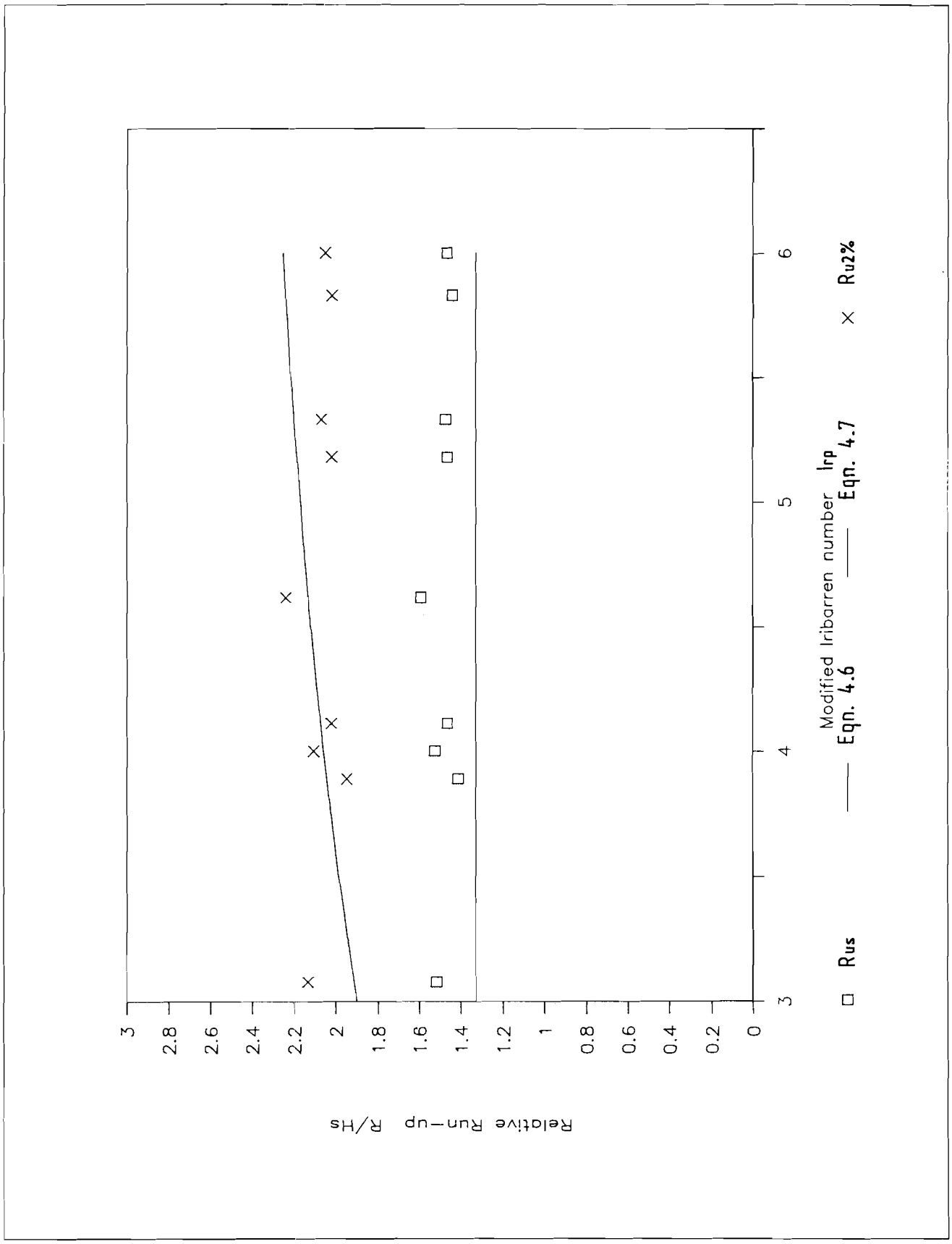

Fig 4.8 Comparisons of relative run-up levels on armoured slopes calculated by SLACWAVE and by empirical equations (Ref 15)

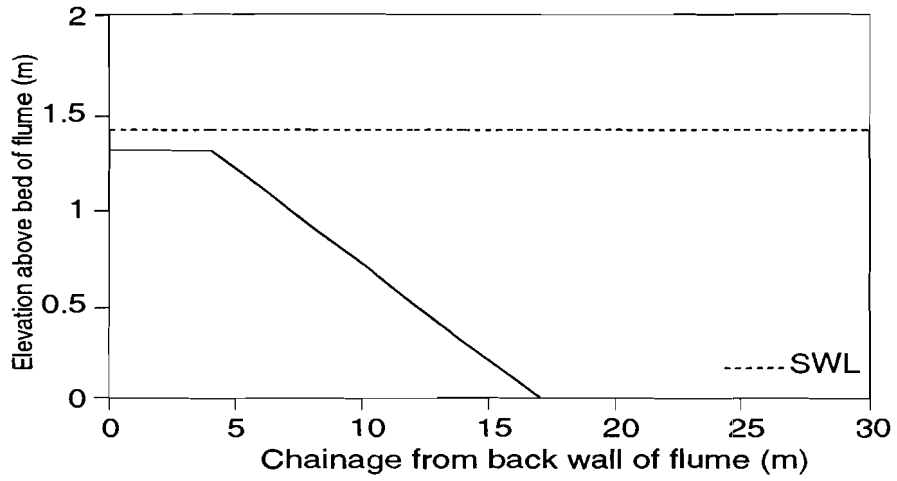

Bathymetry 1

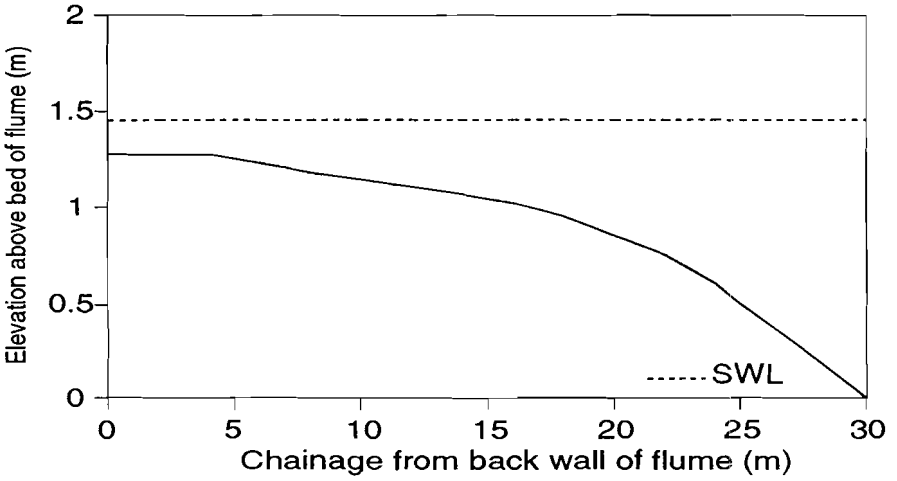

Bathymetry 2

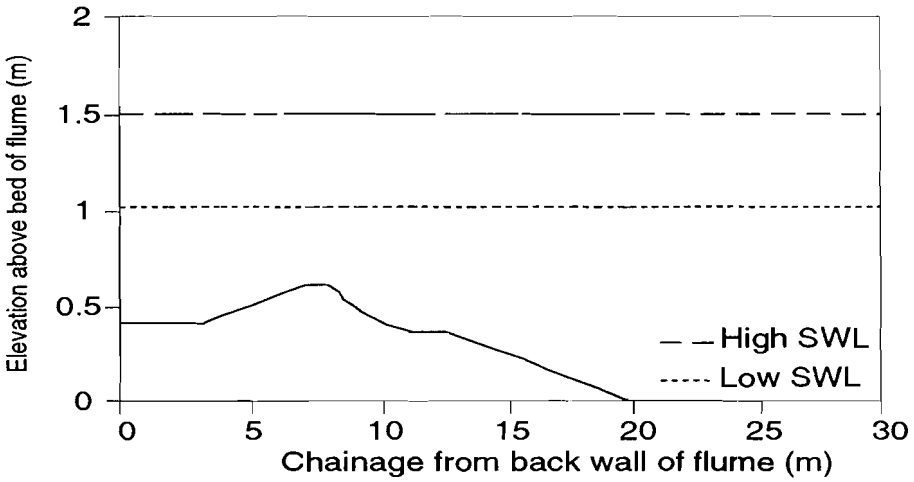

Bathymetry 3

RJ/4.9/4-91/DC

Fig 4.9 Bathymetries used to test WENDIS

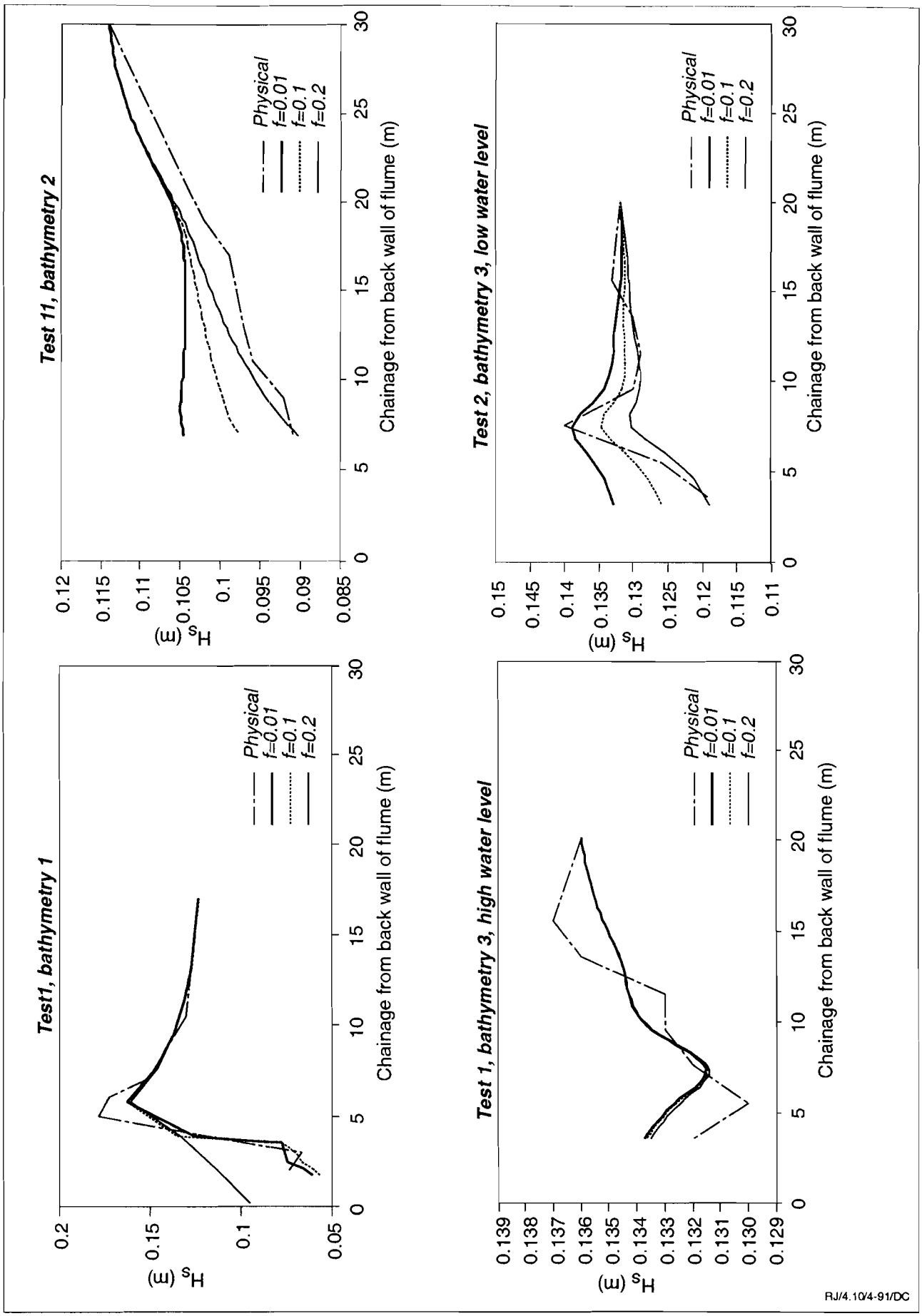

Fig 4.10 Calibration of friction factor in WENDIS, B_C=0.75

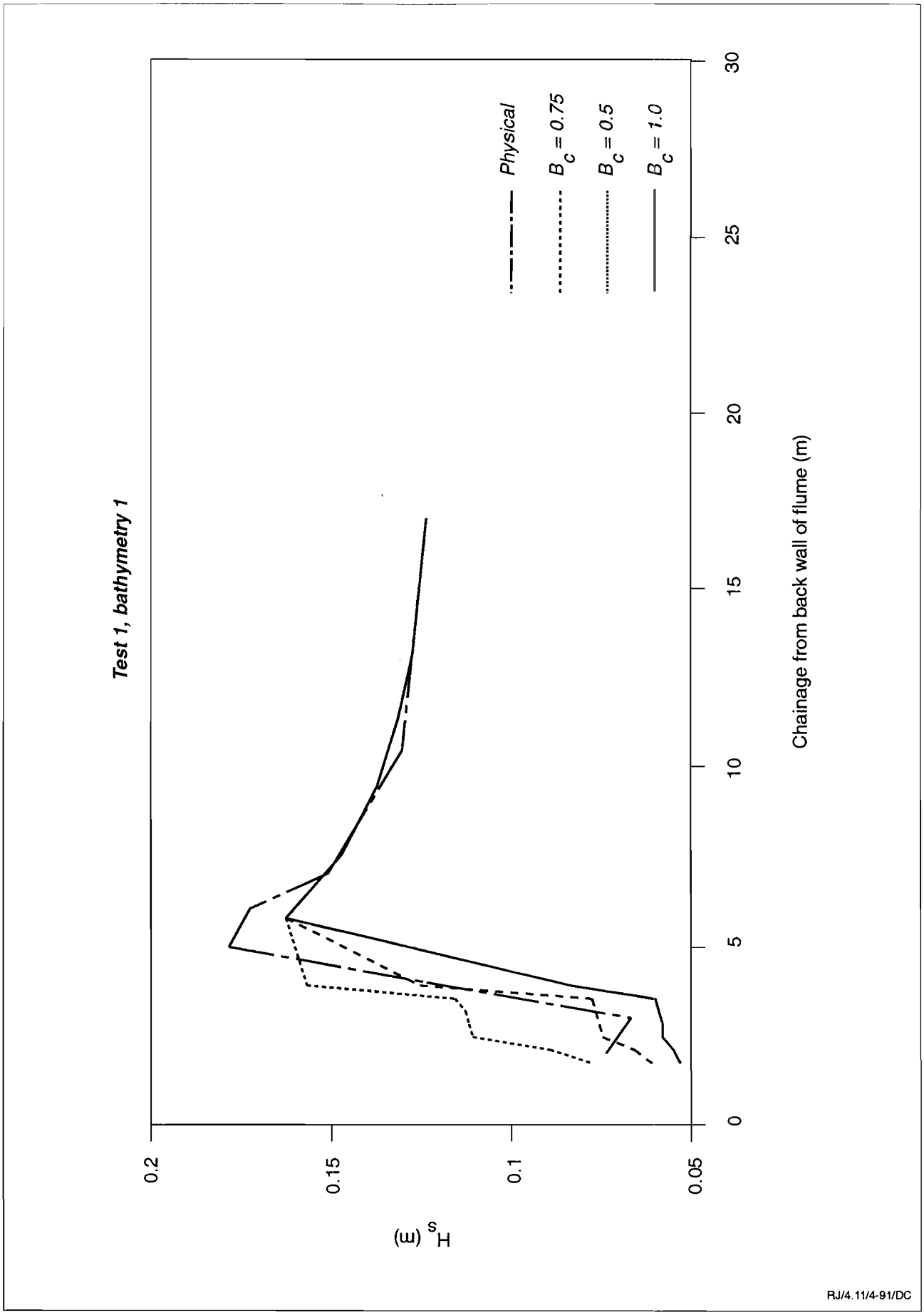

Fig 4.11 Calibration of breaking coefficient in WENDIS, f=0.01

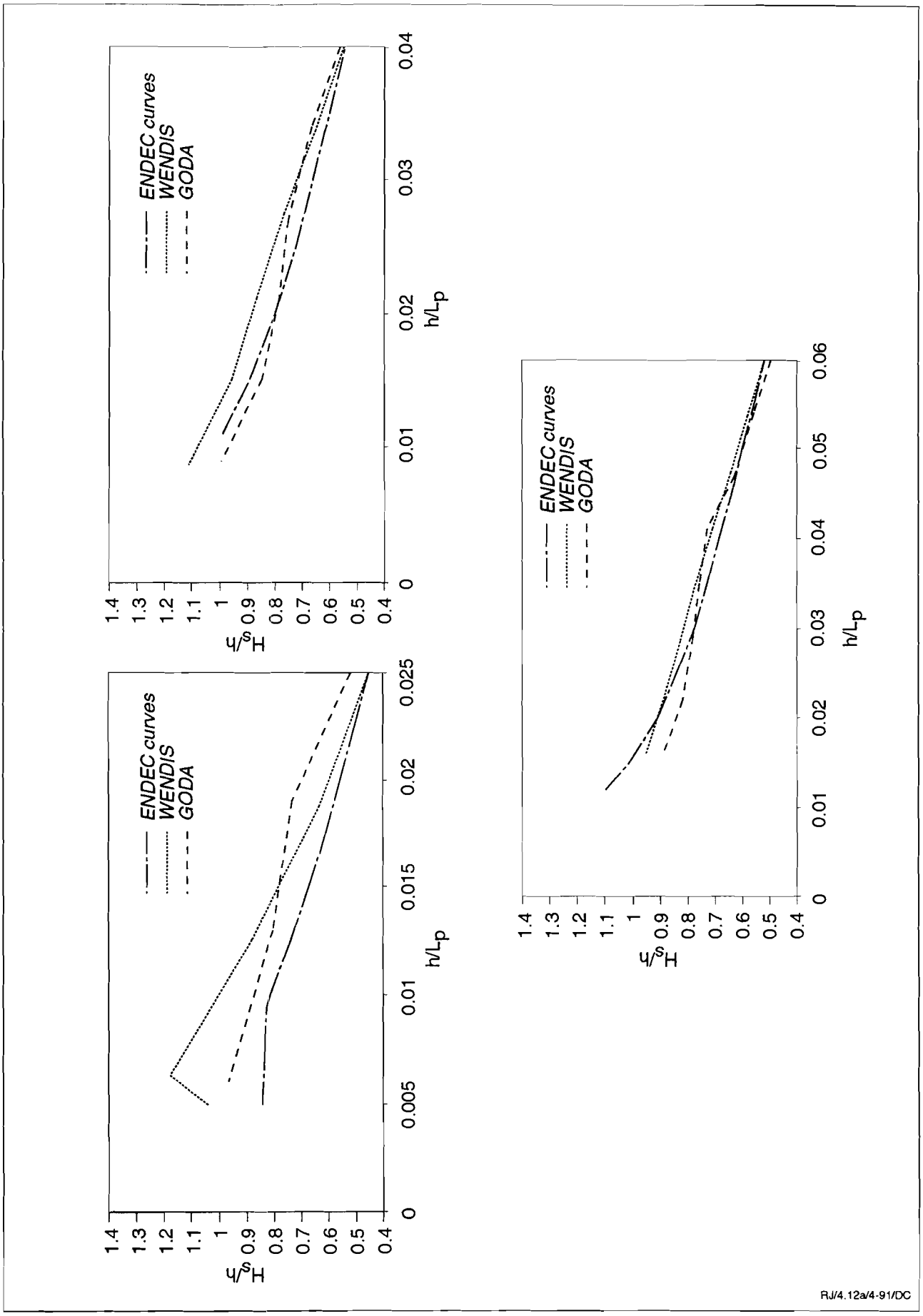

Fig 4.12a Inshore wave height comparisons, m=1/20

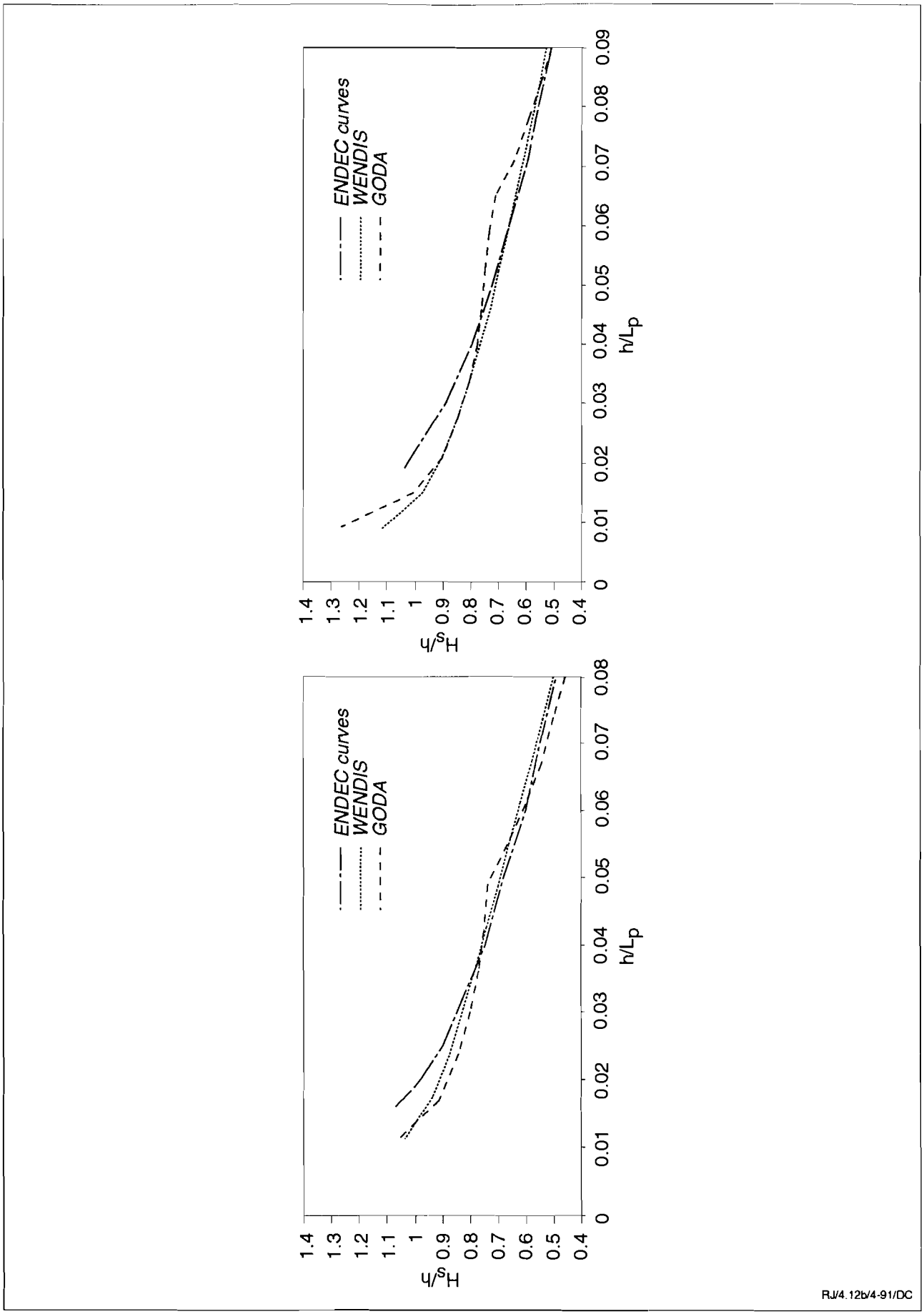

Fig 4.12b Inshore wave height comparisons, m=1/20

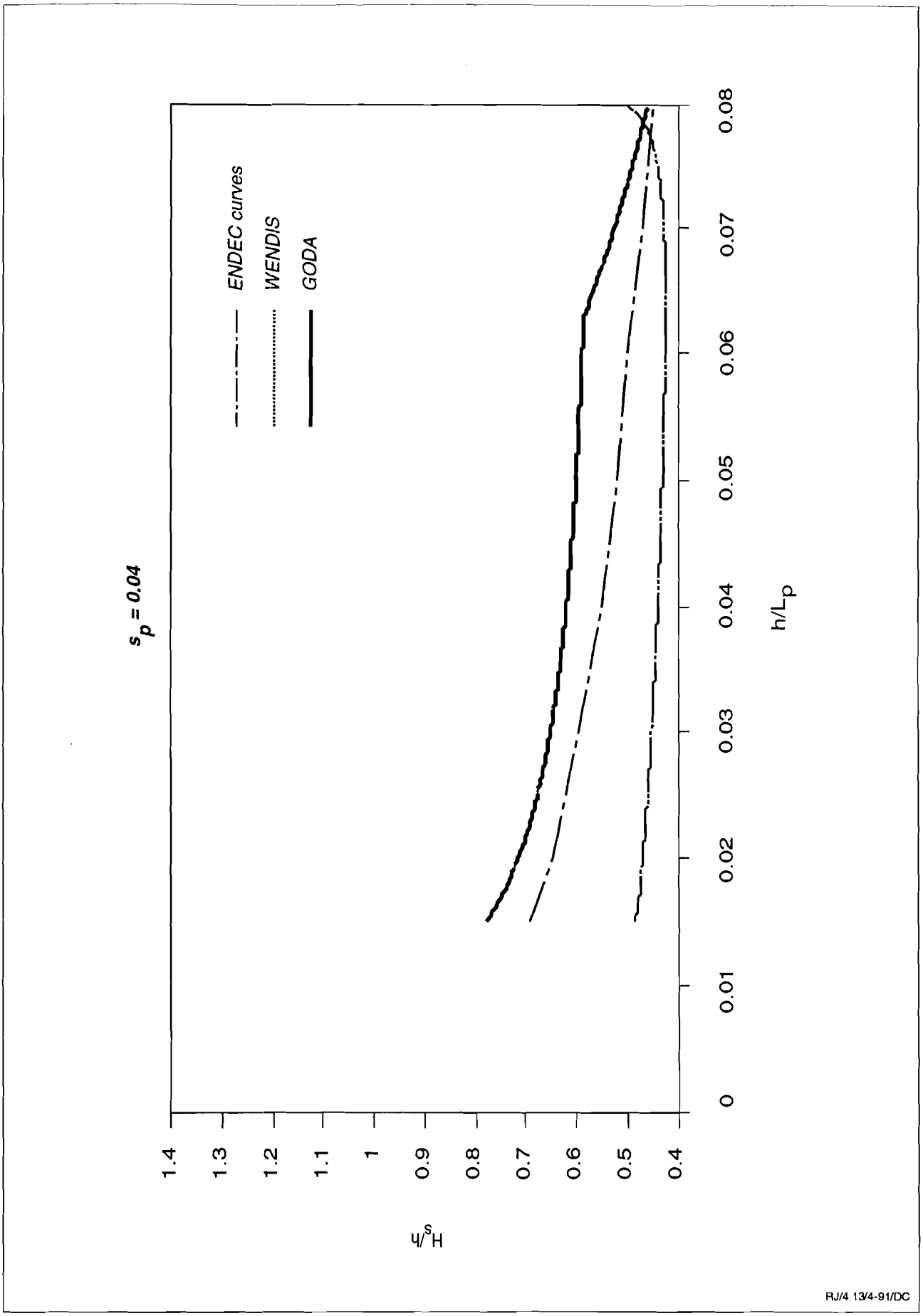

Fig 4.13 Inshore wave height comparisons, m=1/500

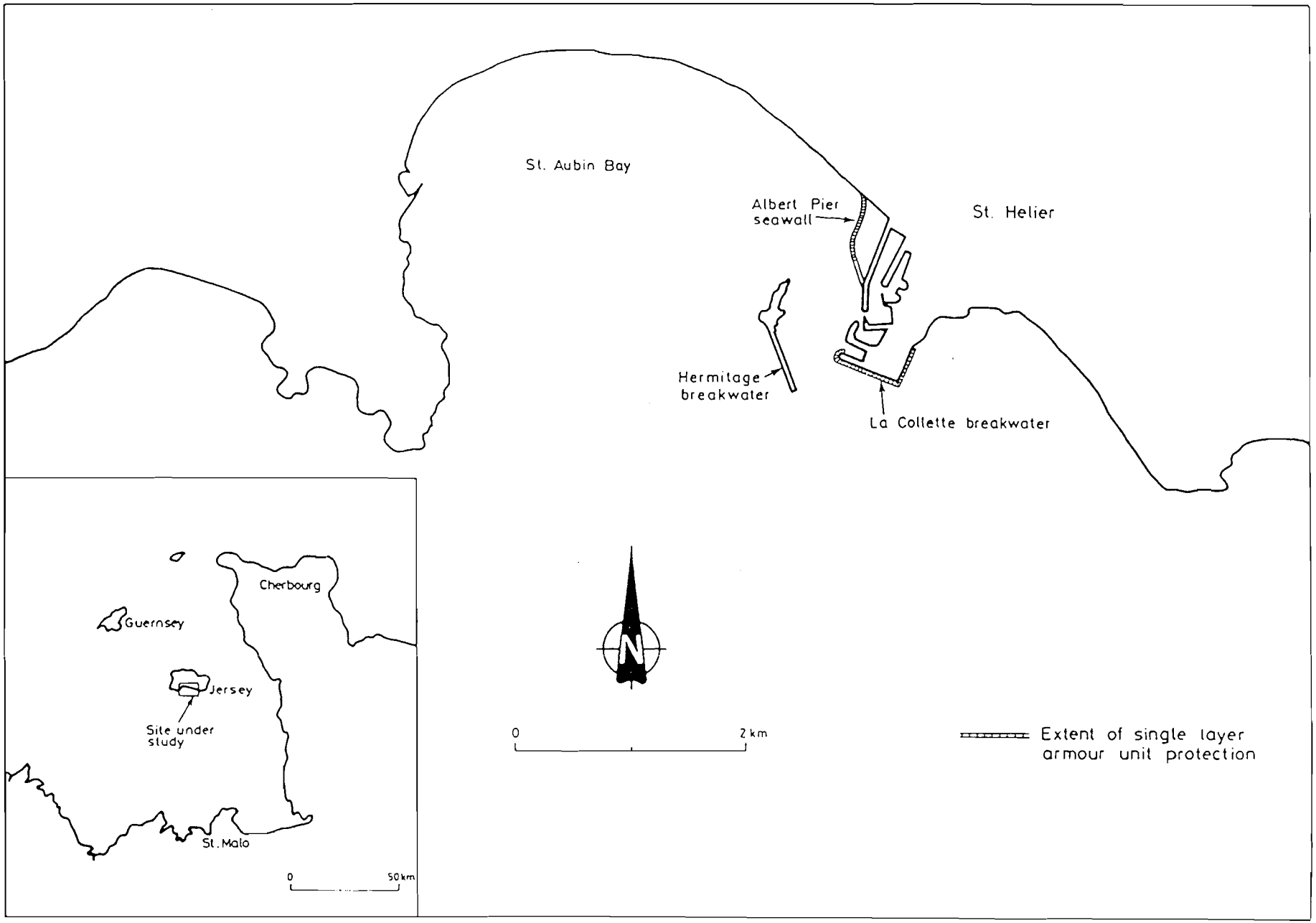

Fig 5.1 Location map, La Collette

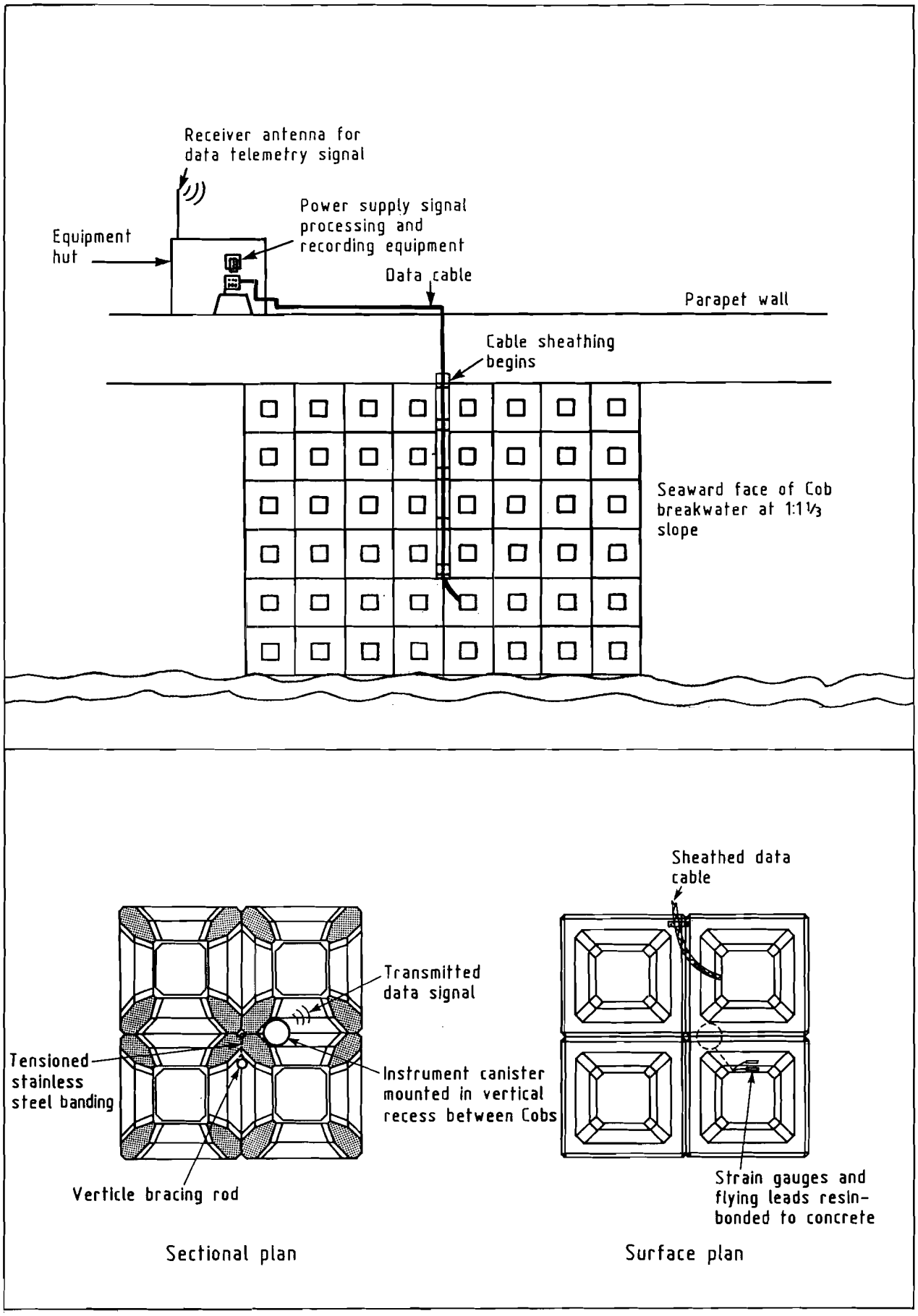

Fig 5.2 Instrumentation layout.

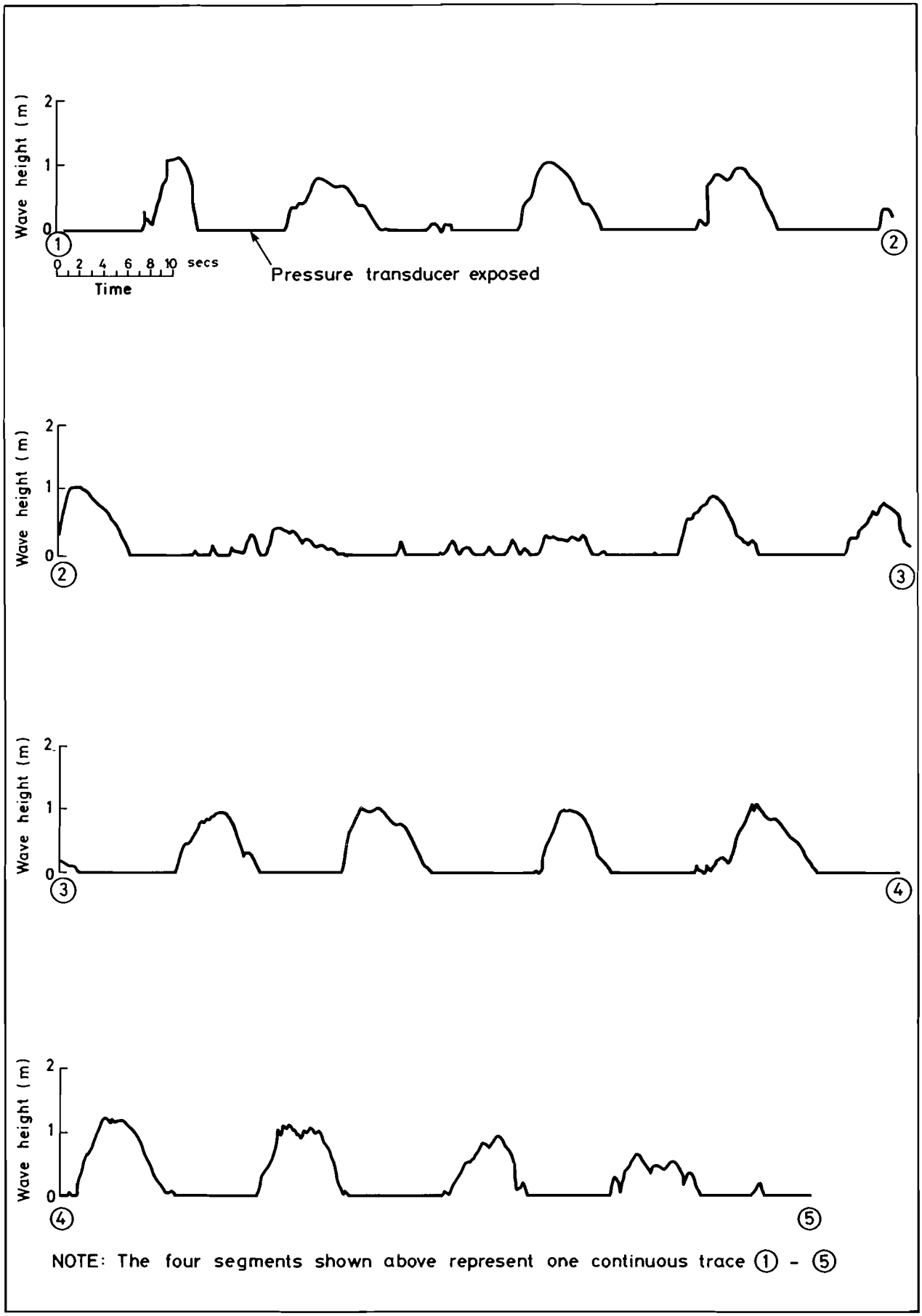

Fig 5.3 Sample pressure record, 1st deployment.

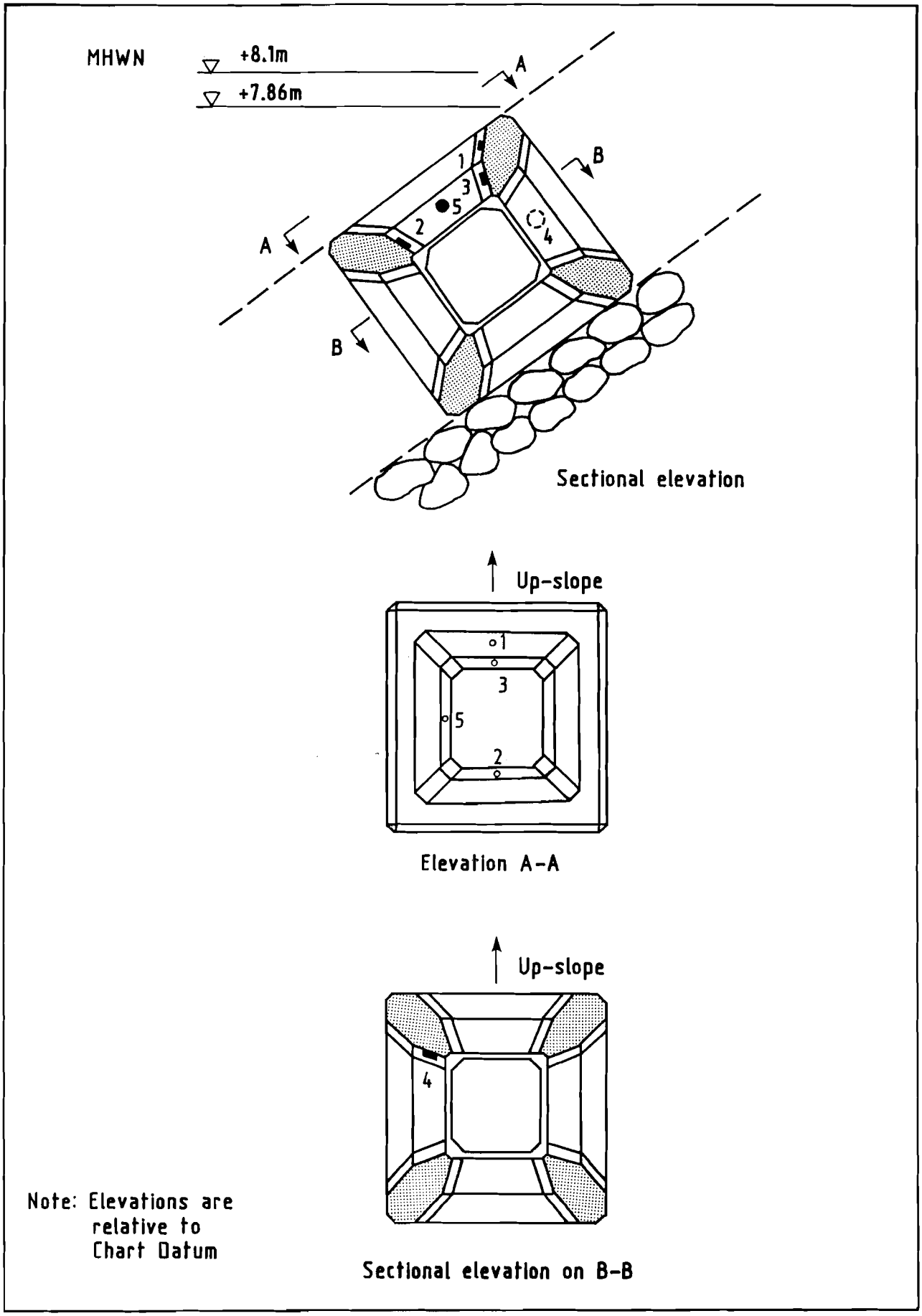

Fig 5.4 Location of pressure transducers

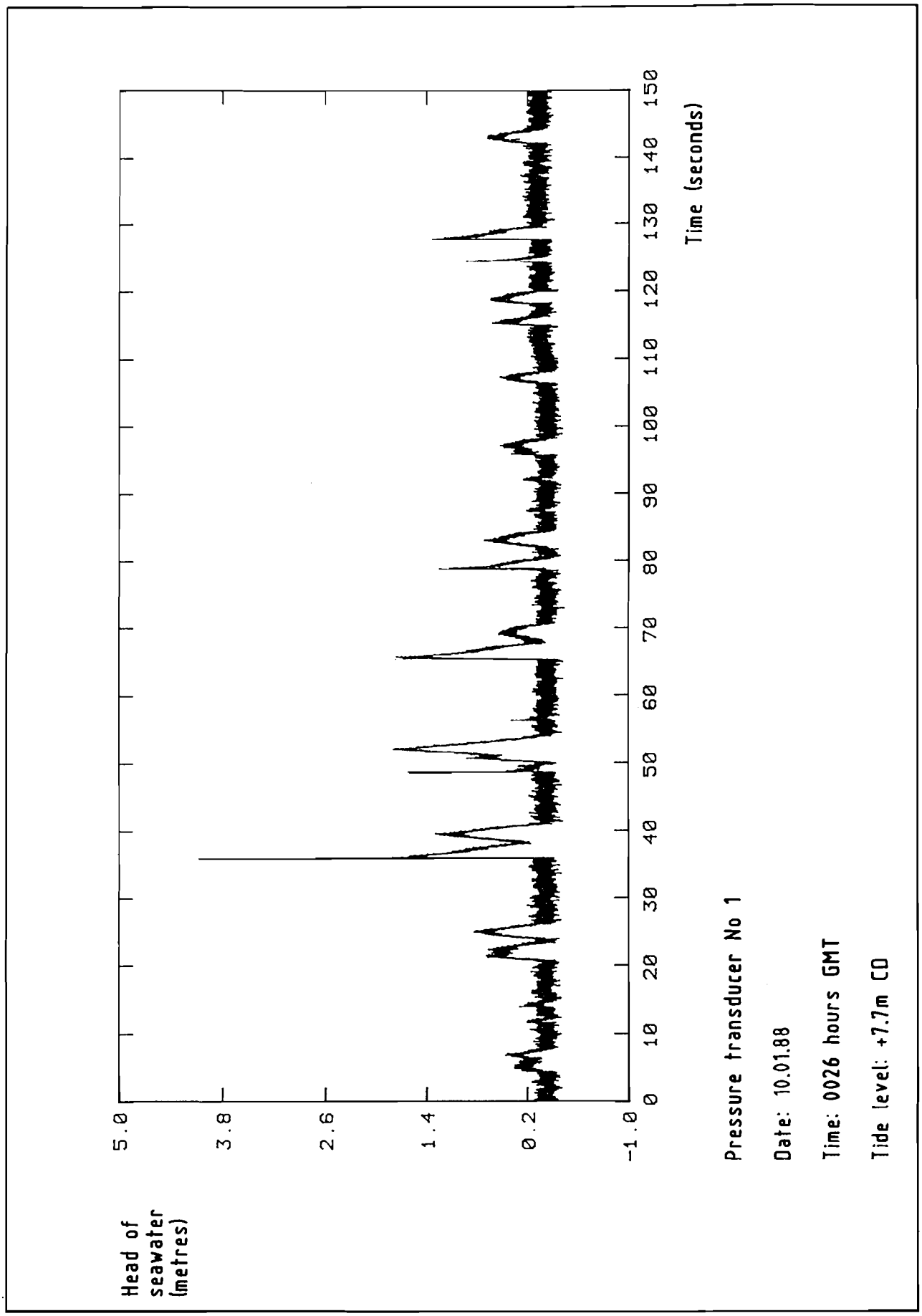

Fig 5.5 Sample pressure record, 2nd deployment.

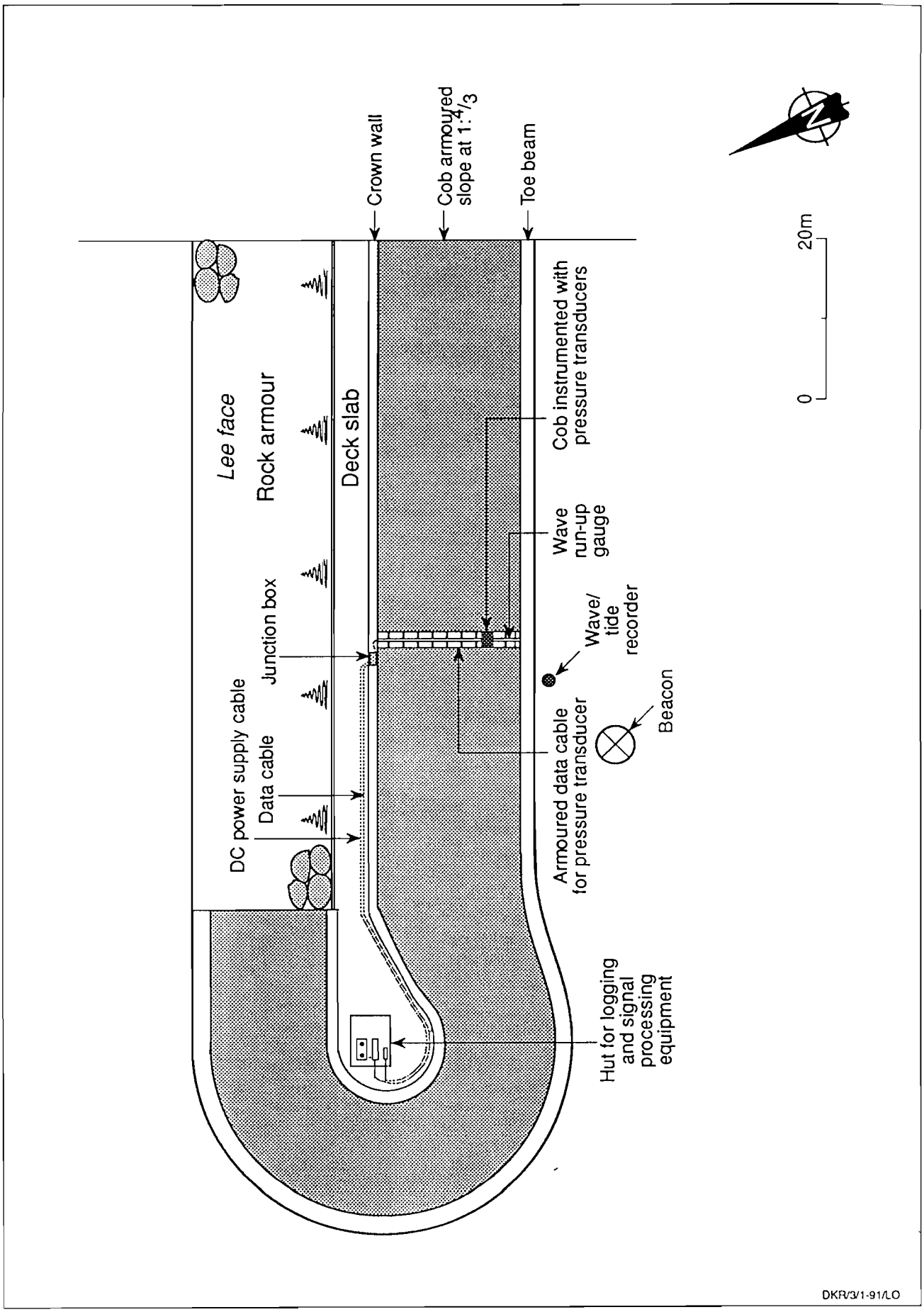

Fig 5.6 La Collette breakwater showing instrumentation details

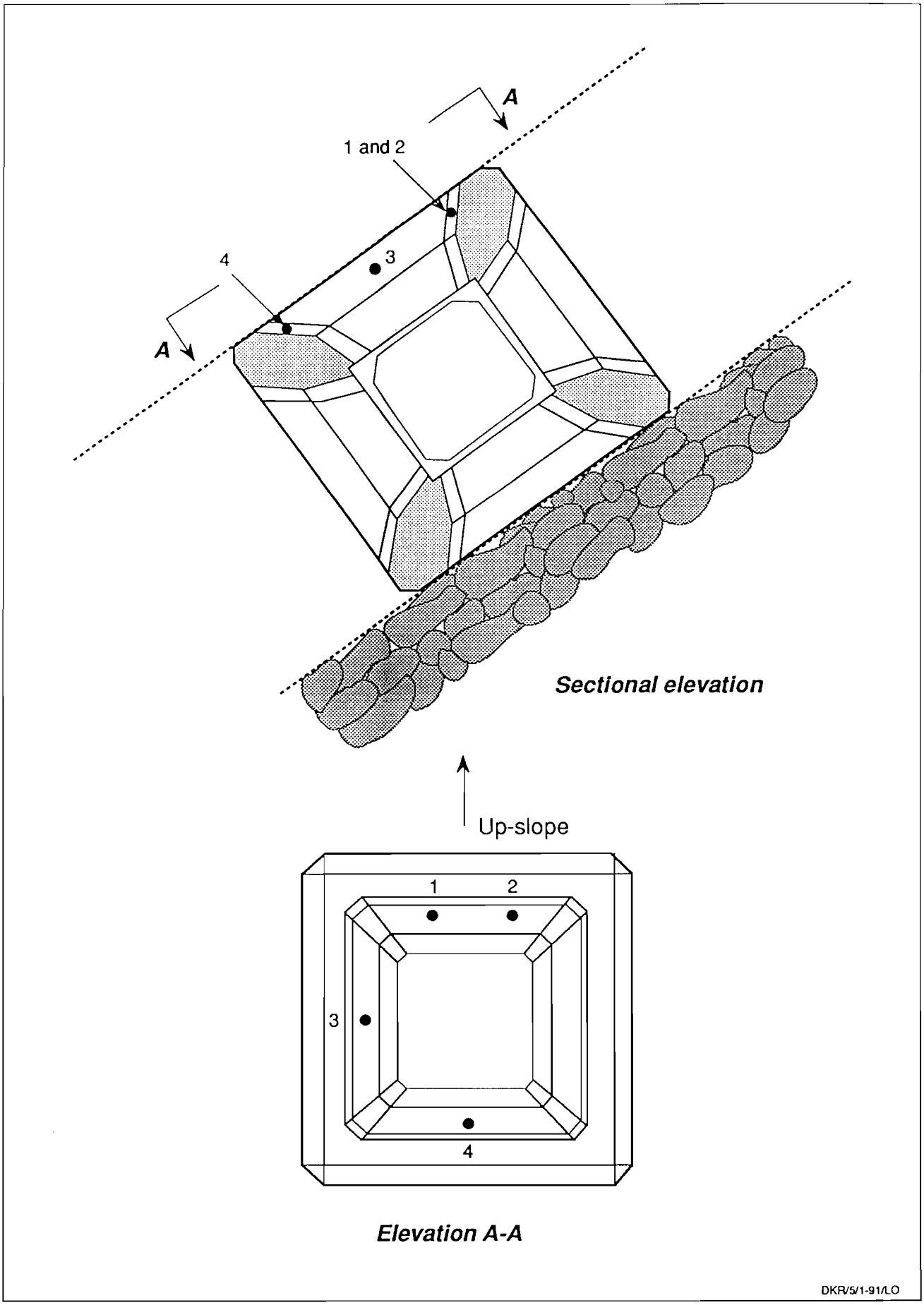

Fig 5.7 Location of pressure transducers during 3rd deployment

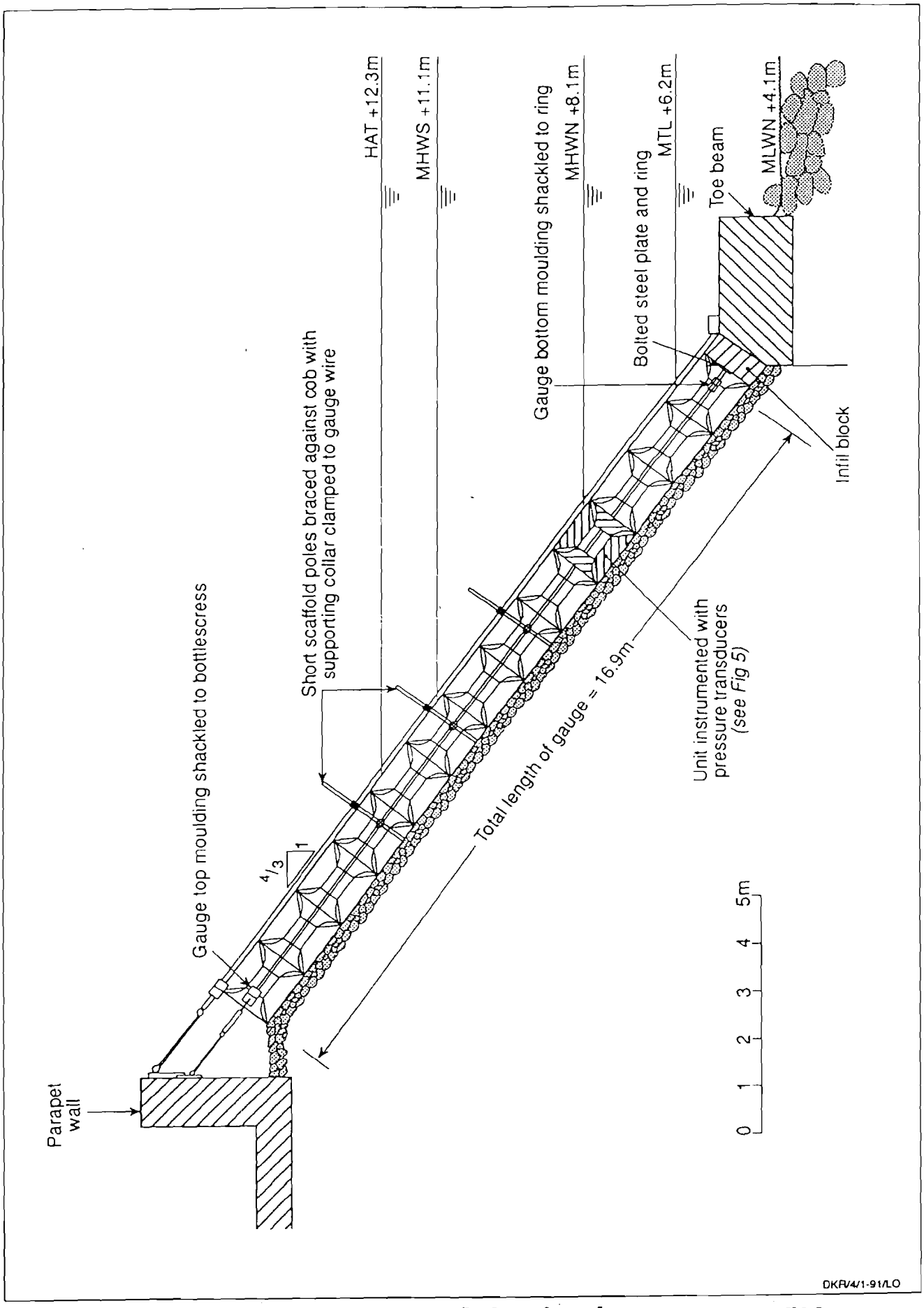

Fig 5.8 Section through column of Cobs showing run-up gauges

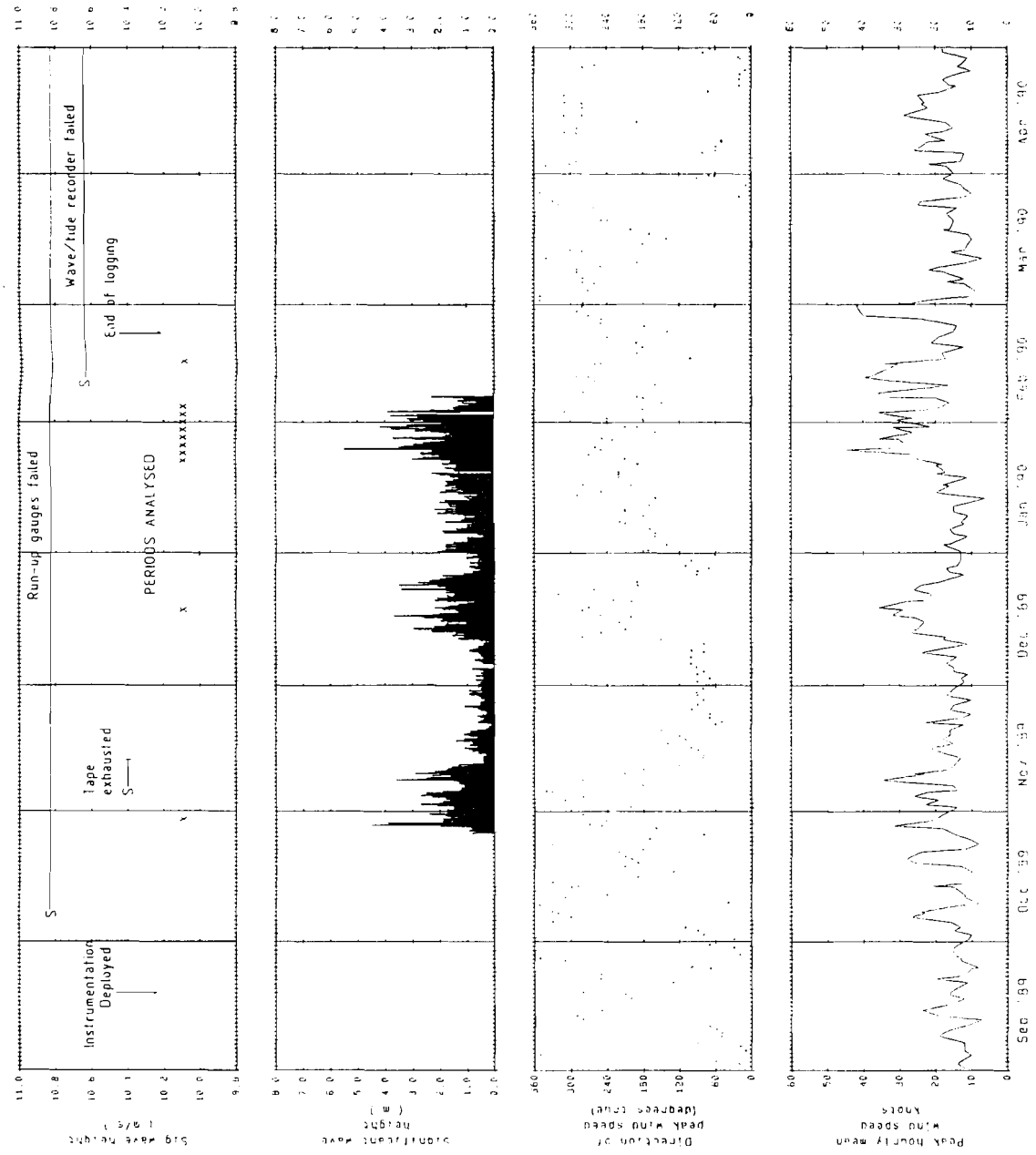

Fig 5.9 Wind and waves during 3rd deployment

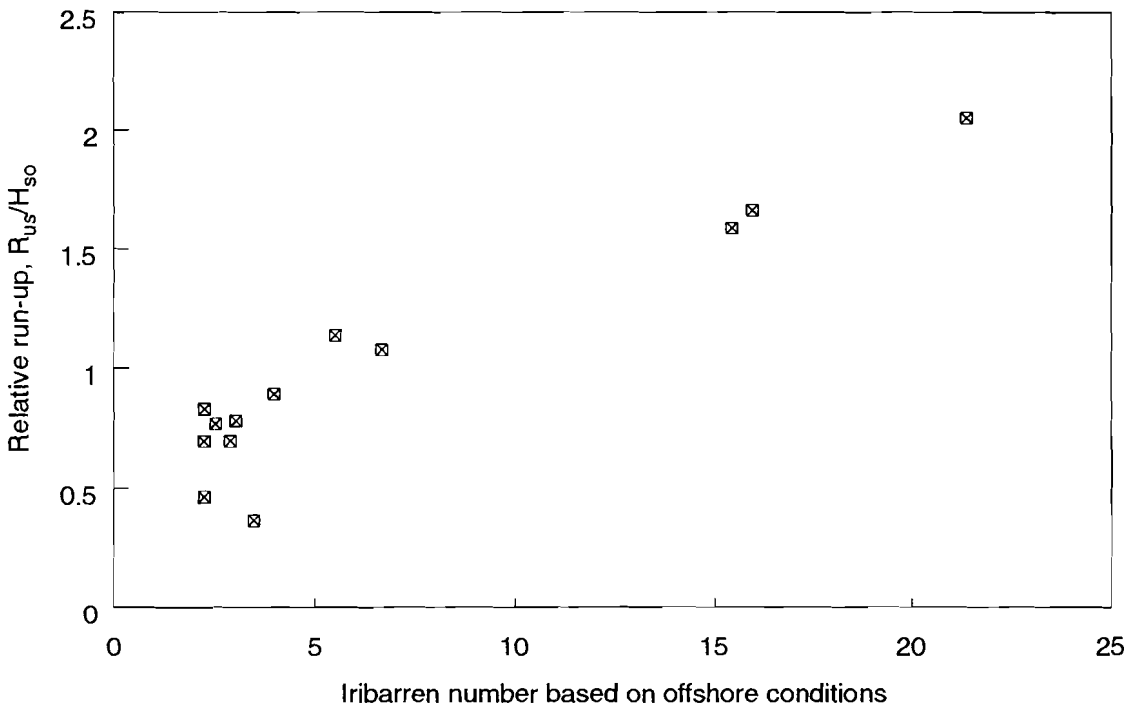

RJ/5.10/4-91/DC

Fig 5.10 Run-up on La-Collette, 2nd deployment

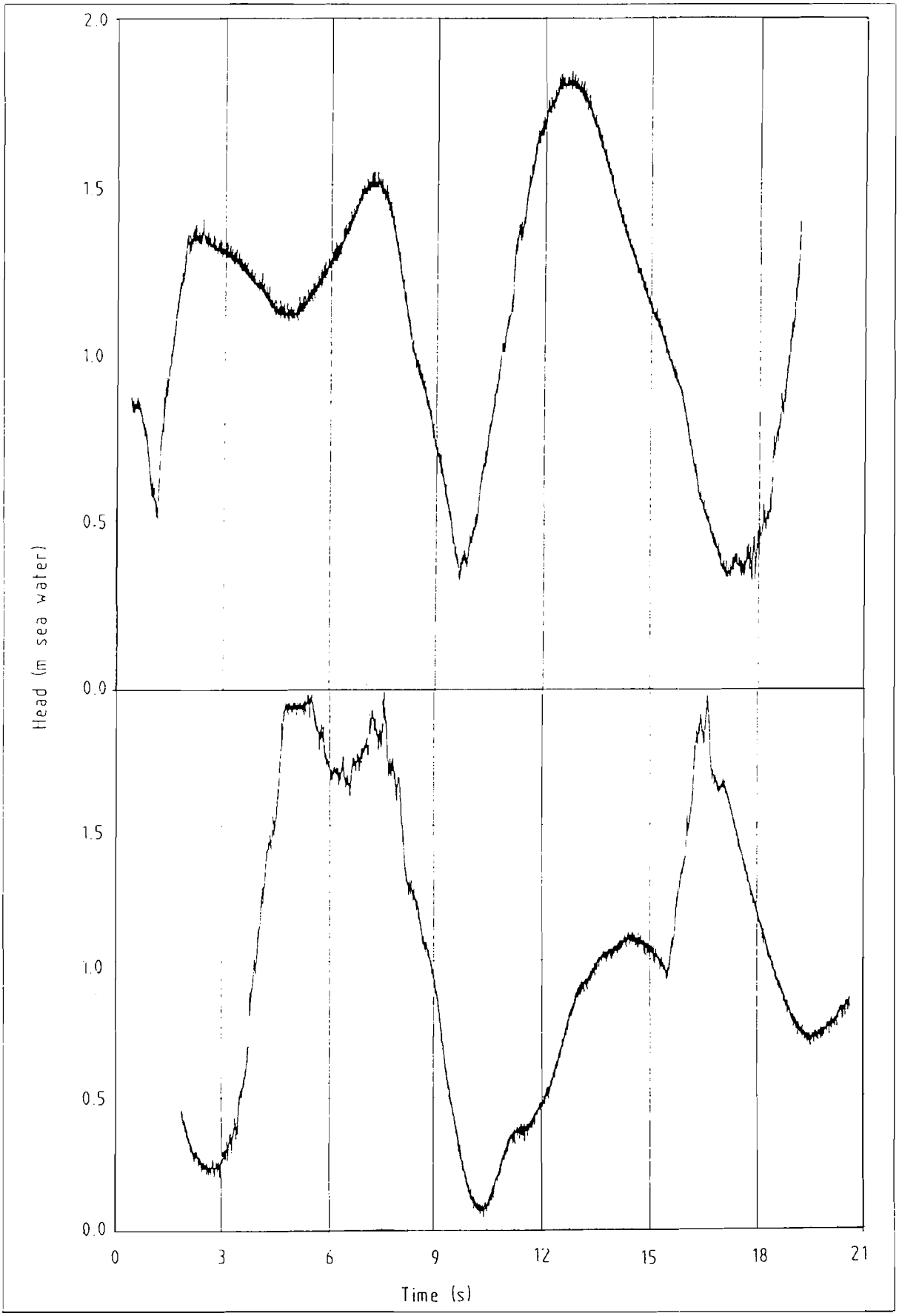

Fig 5.11 Typical raw pressure record (500 Hz)

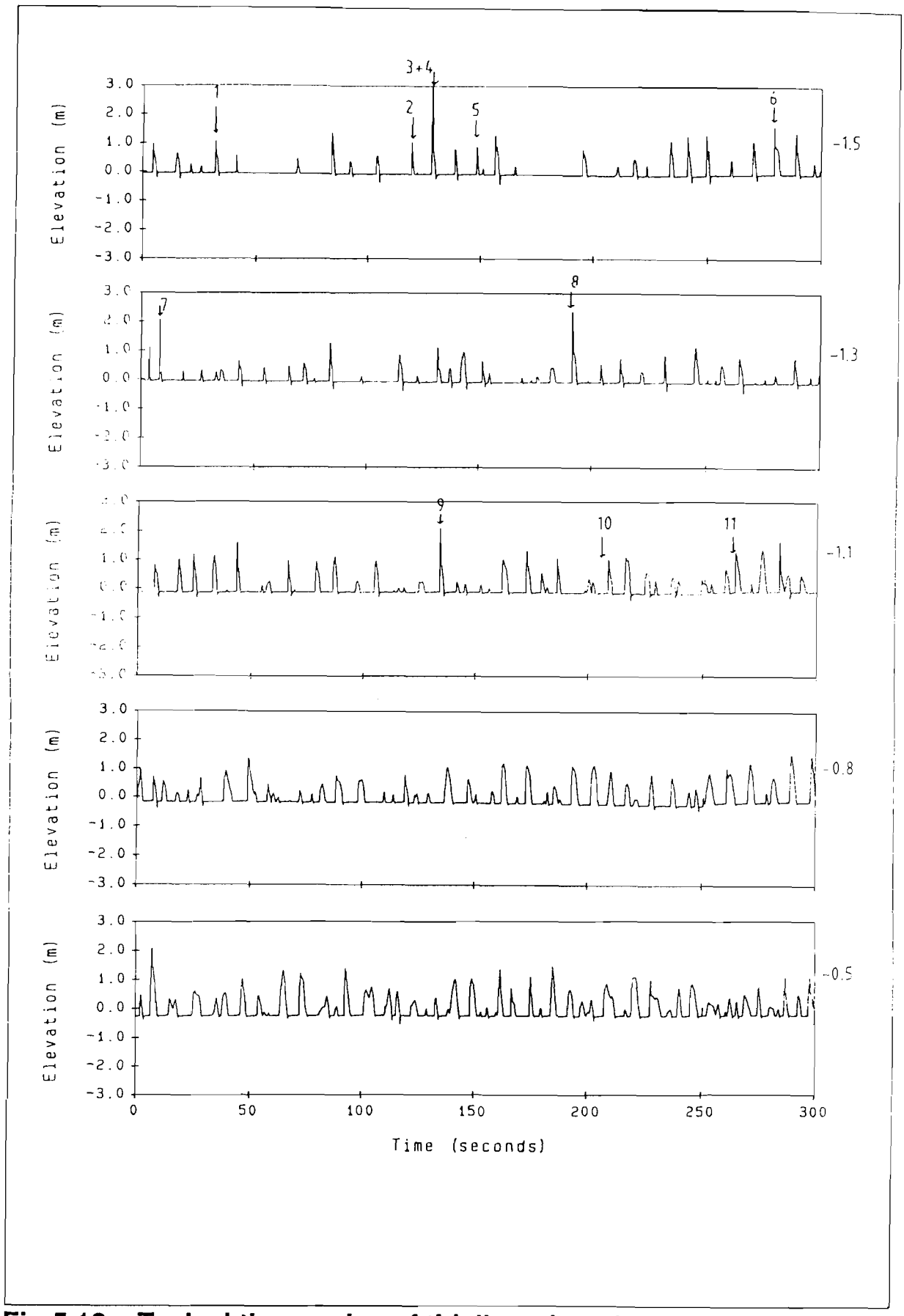

Fig 5.12a Typical time series of tidally reduced pressures during rising tide on 28/01/91 - Sensor 1

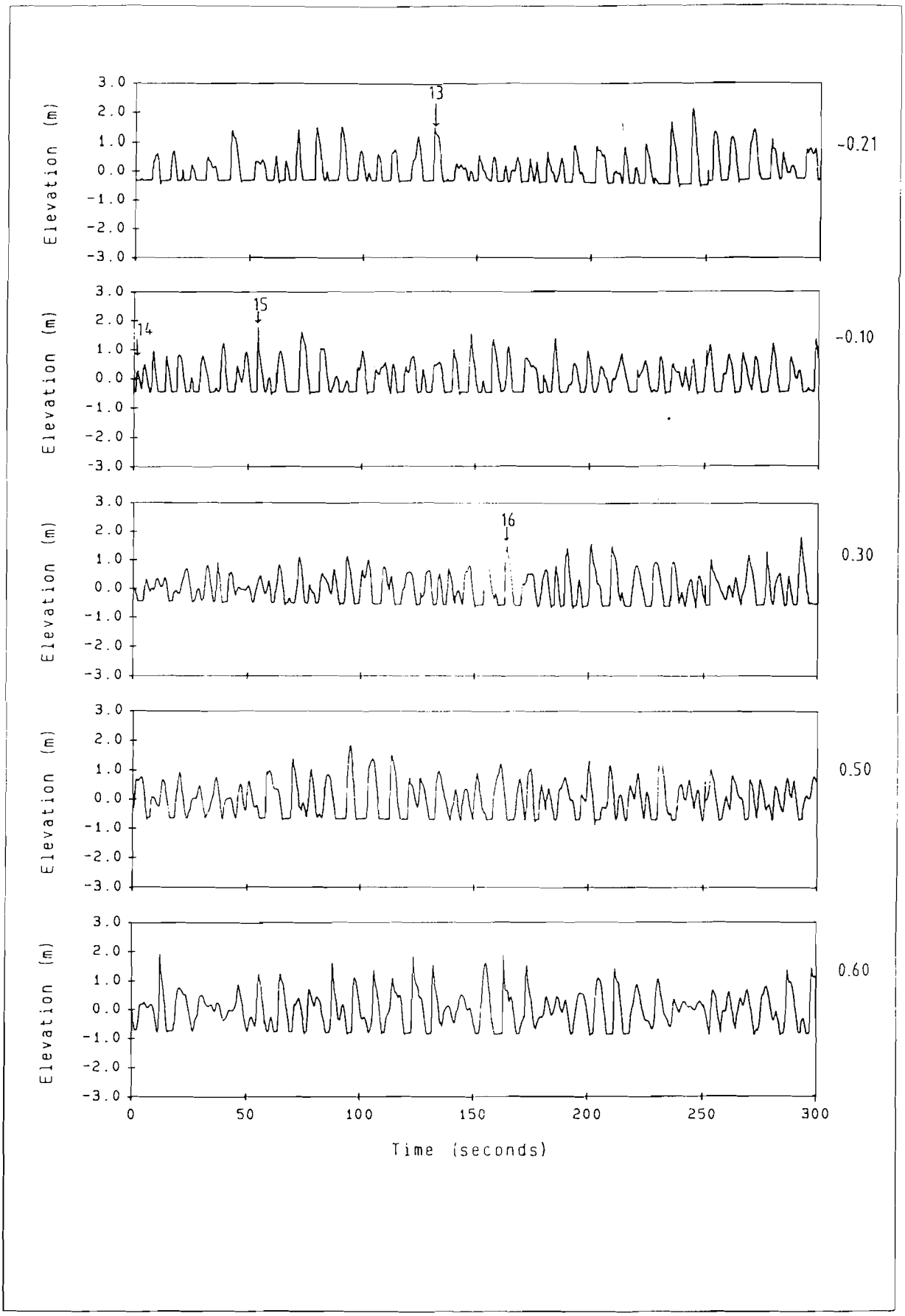

Fig 5.12b Typical time series of tidally reduced pressures during rising tide on 28/01/91 - Sensor 1

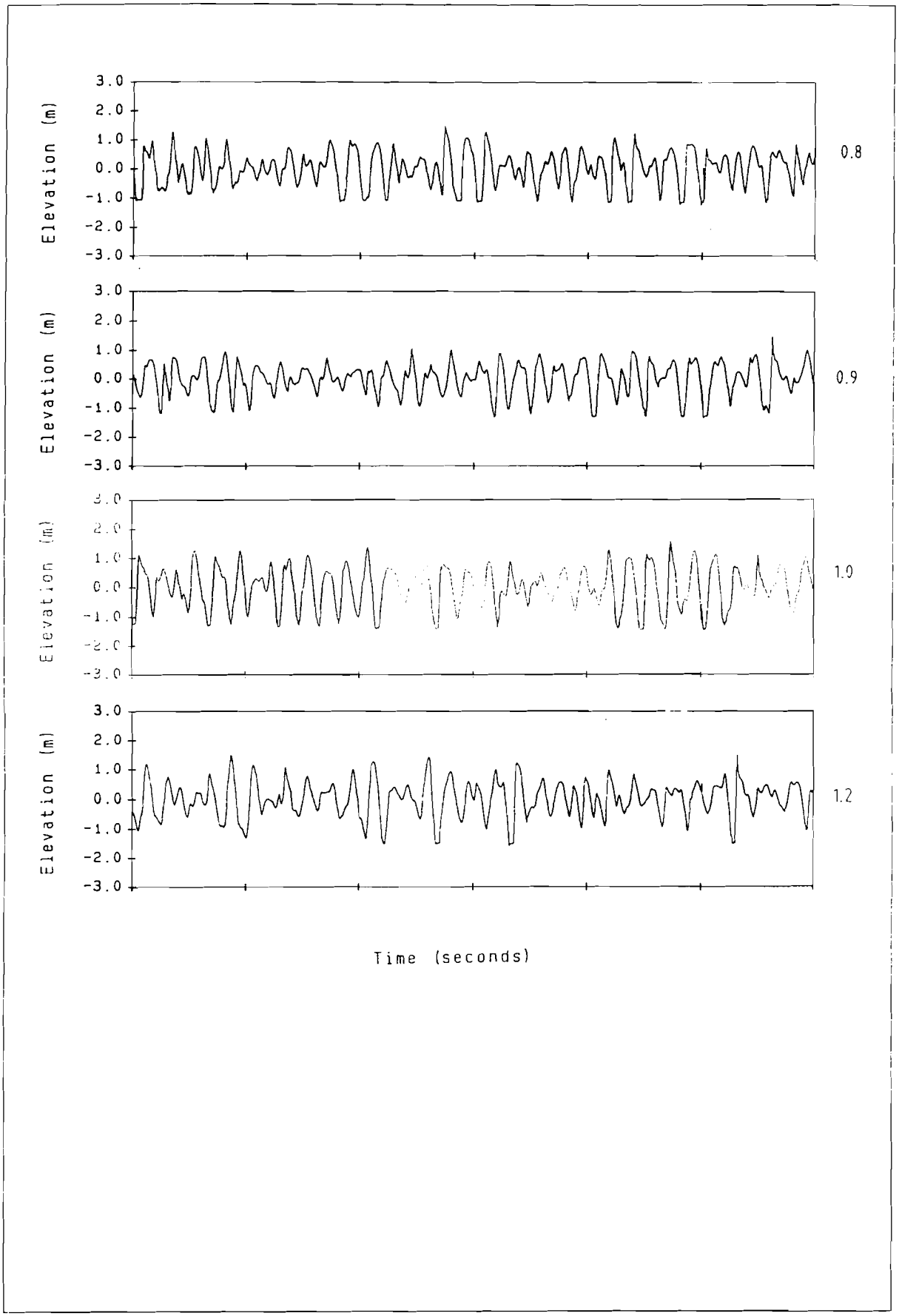

Fig 5.12c Typical time series of tidally reduced pressures during rising tide on 28/01/91 - Sensor 1

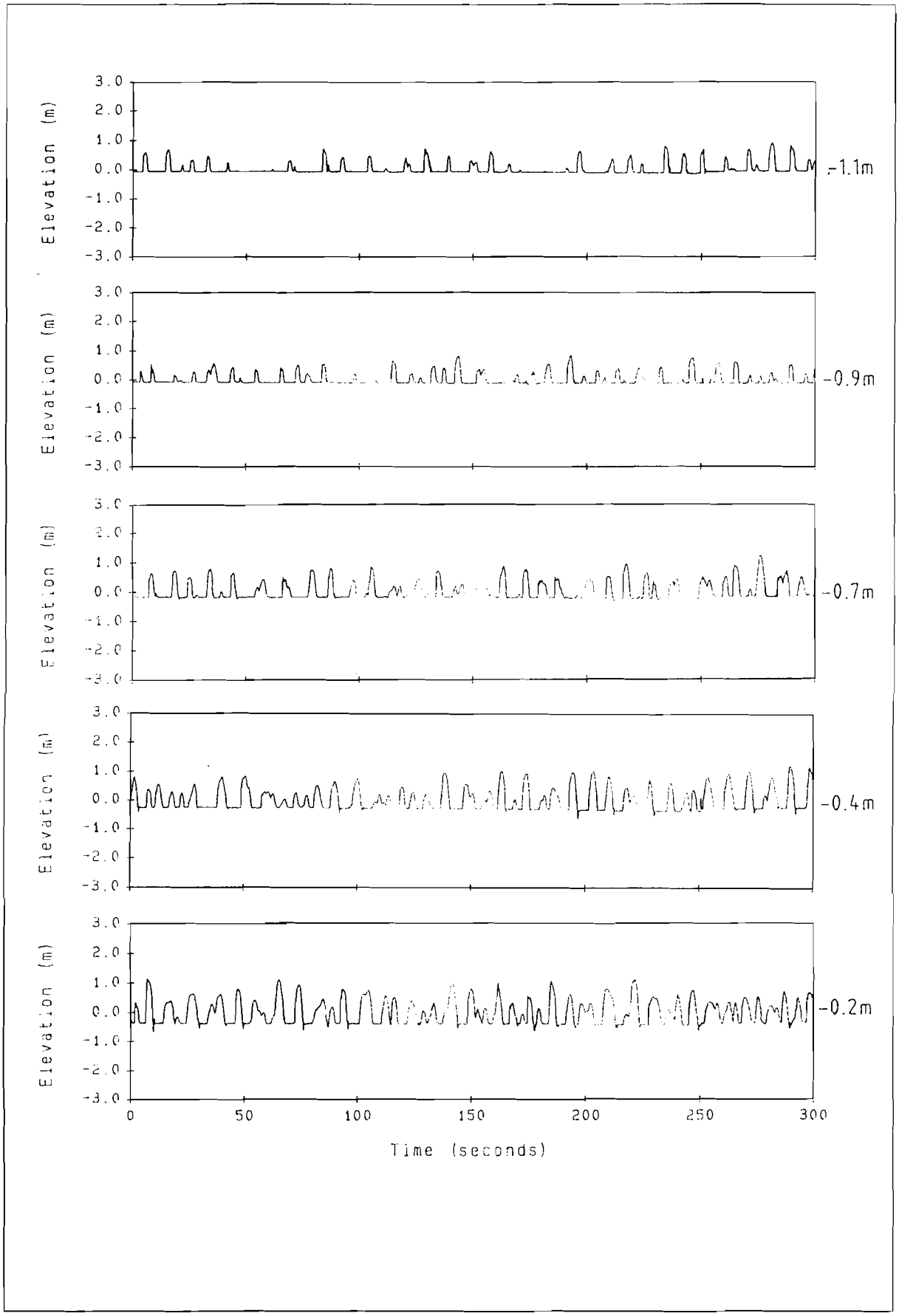

Fig 5.13a Typical time series of tidally reduced pressures during rising tide on 28/01/91 - Sensor 4

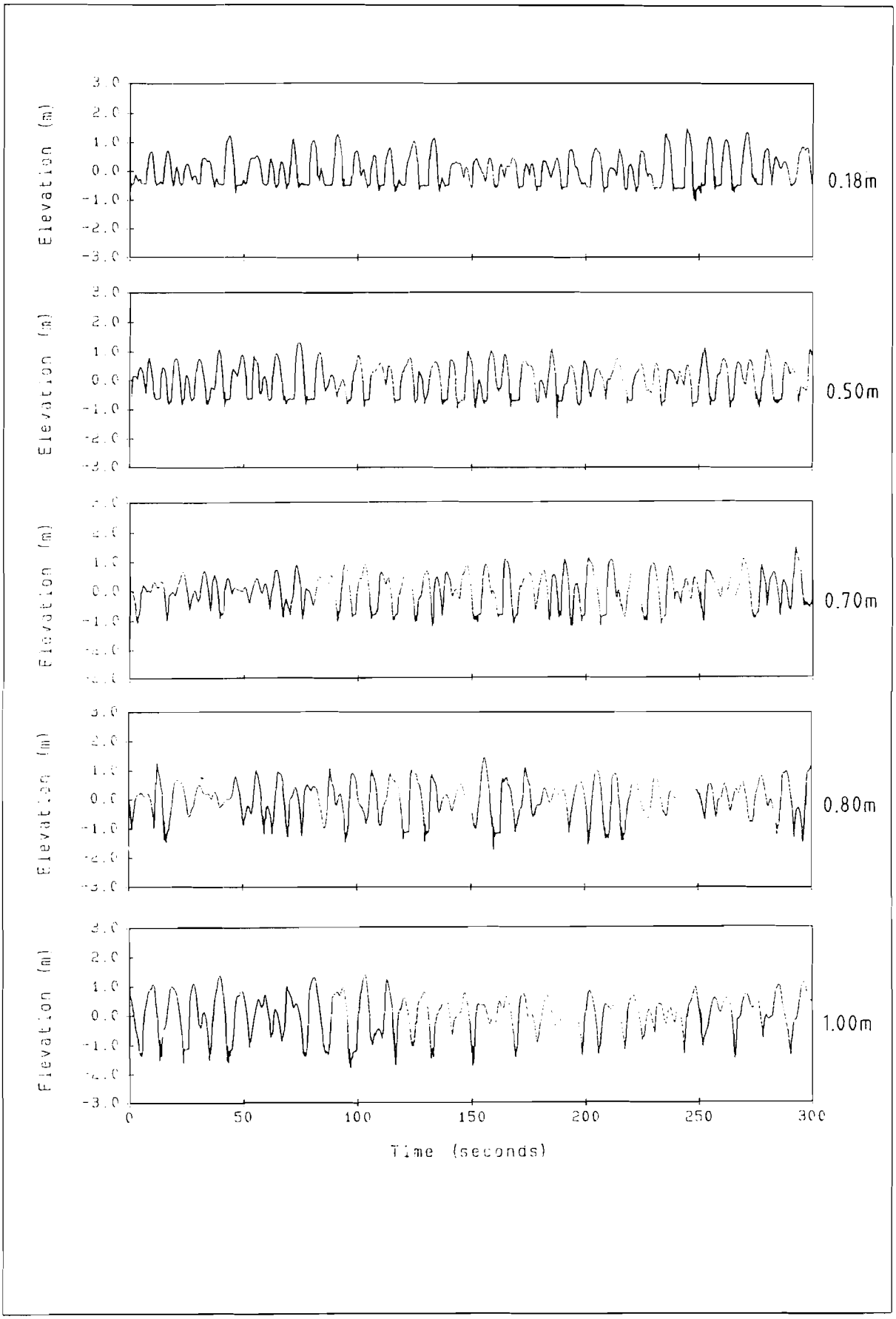

Fig 5.13b Typical time series of tidally reduced pressures during rising tide on 28/01/91 - Sensor 4

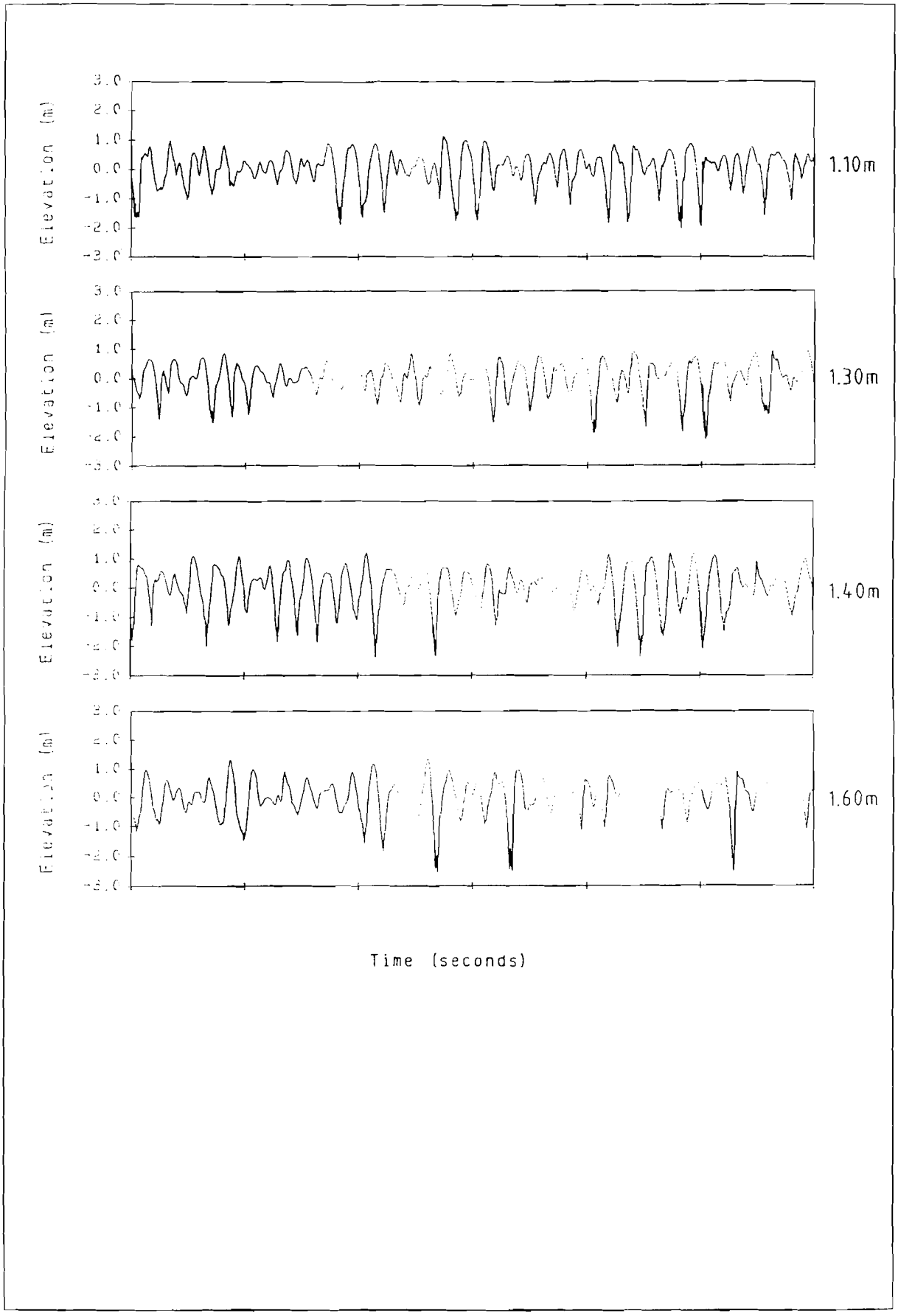

Fig 5.13c Typical time series of tidally reduced pressures during rising tide on 28/01/91 - Sensor 4

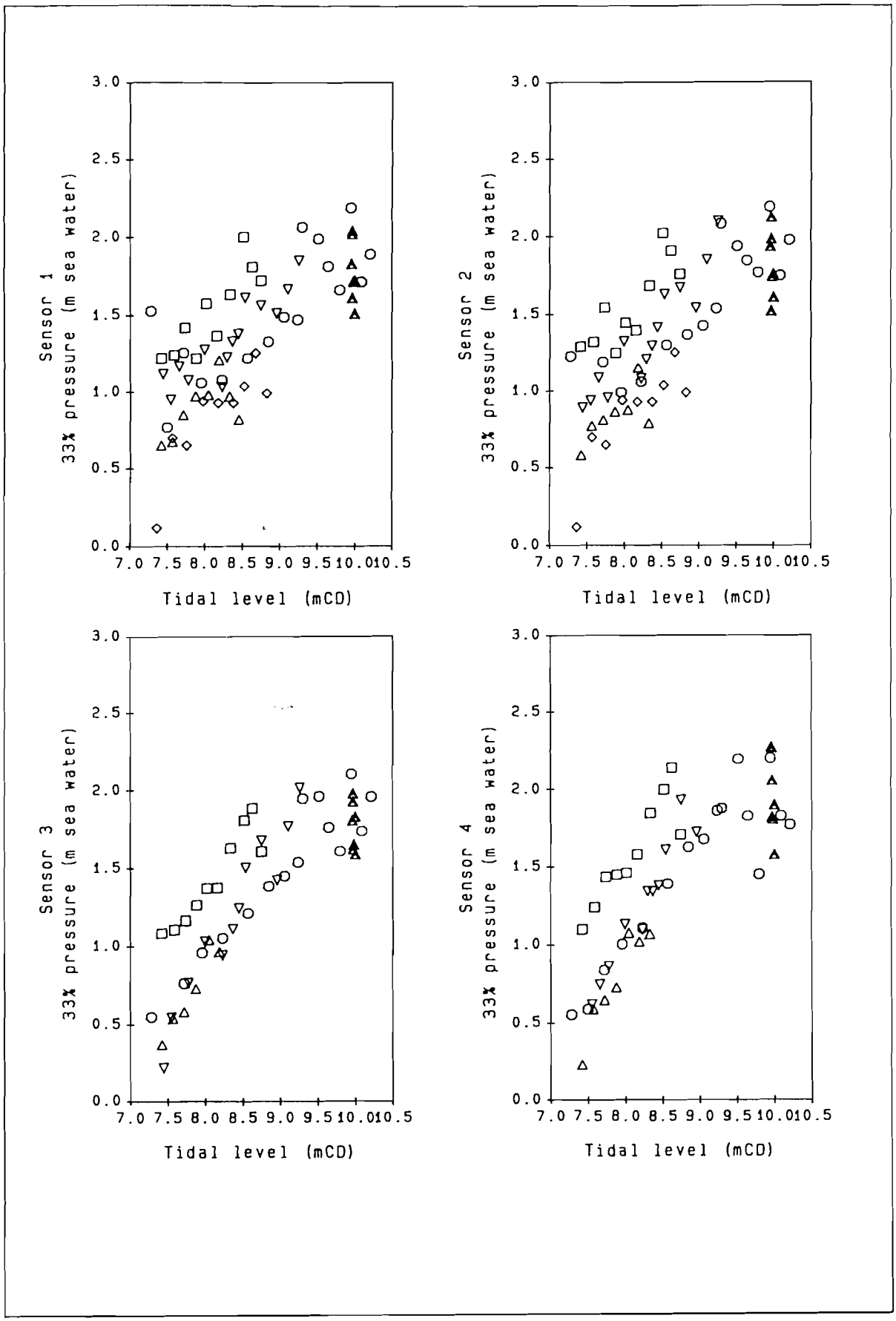

Fig 5.14 Significant pressures versus tidal elevation

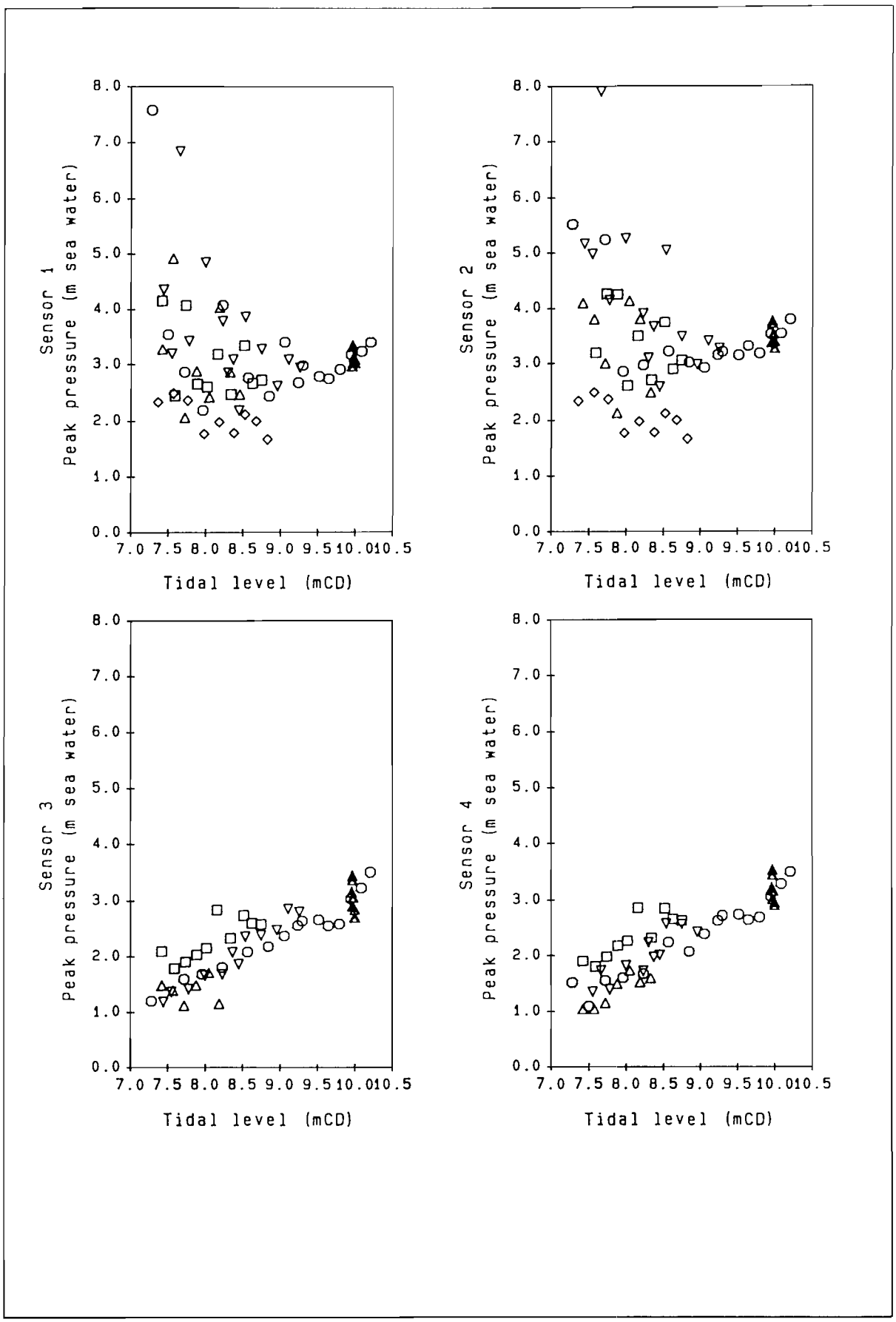

Fig 5.15 Peak pressures versus tidal elevation

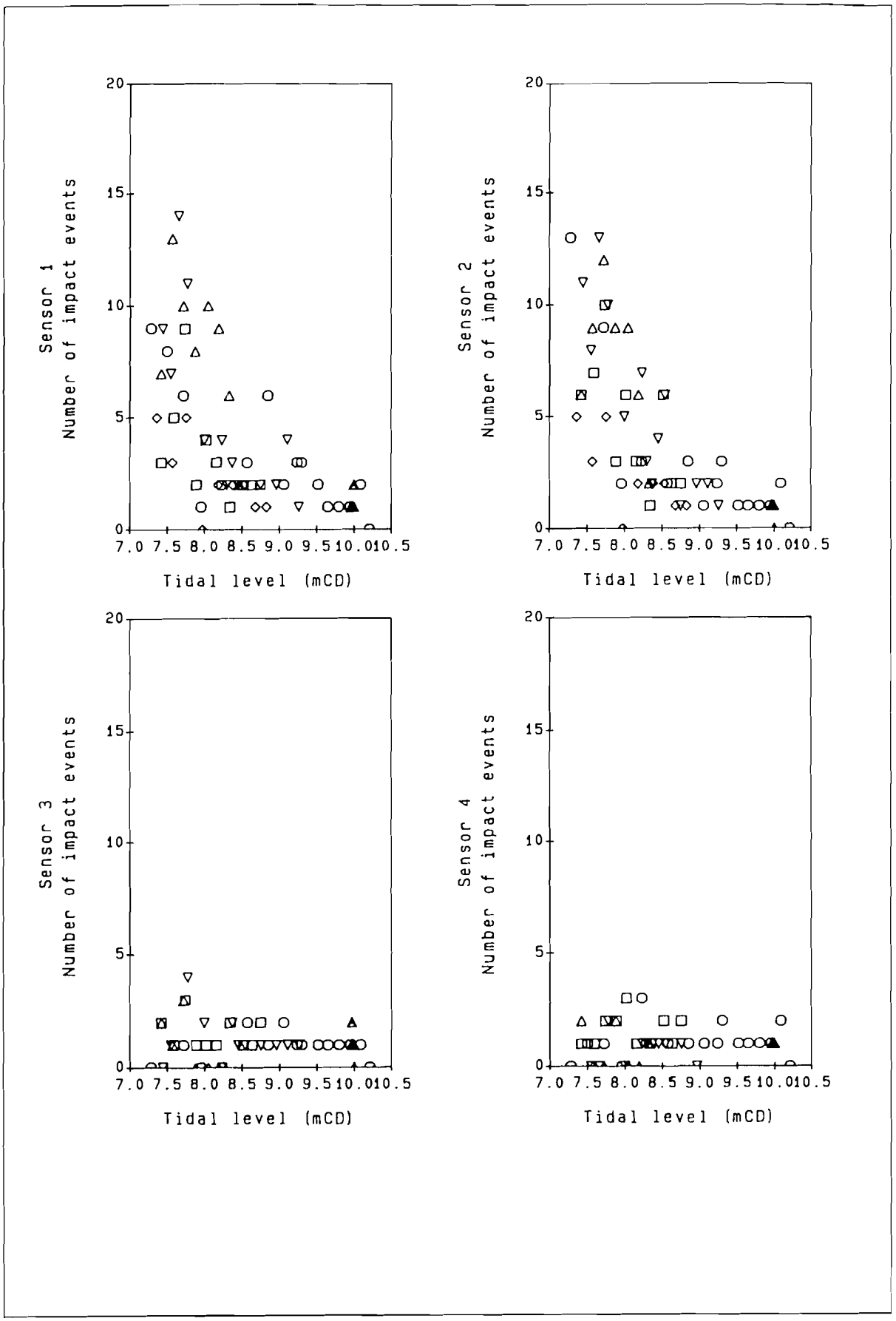

Fig 5.16 Number of impact events during 5 minute period versus tidal elevation

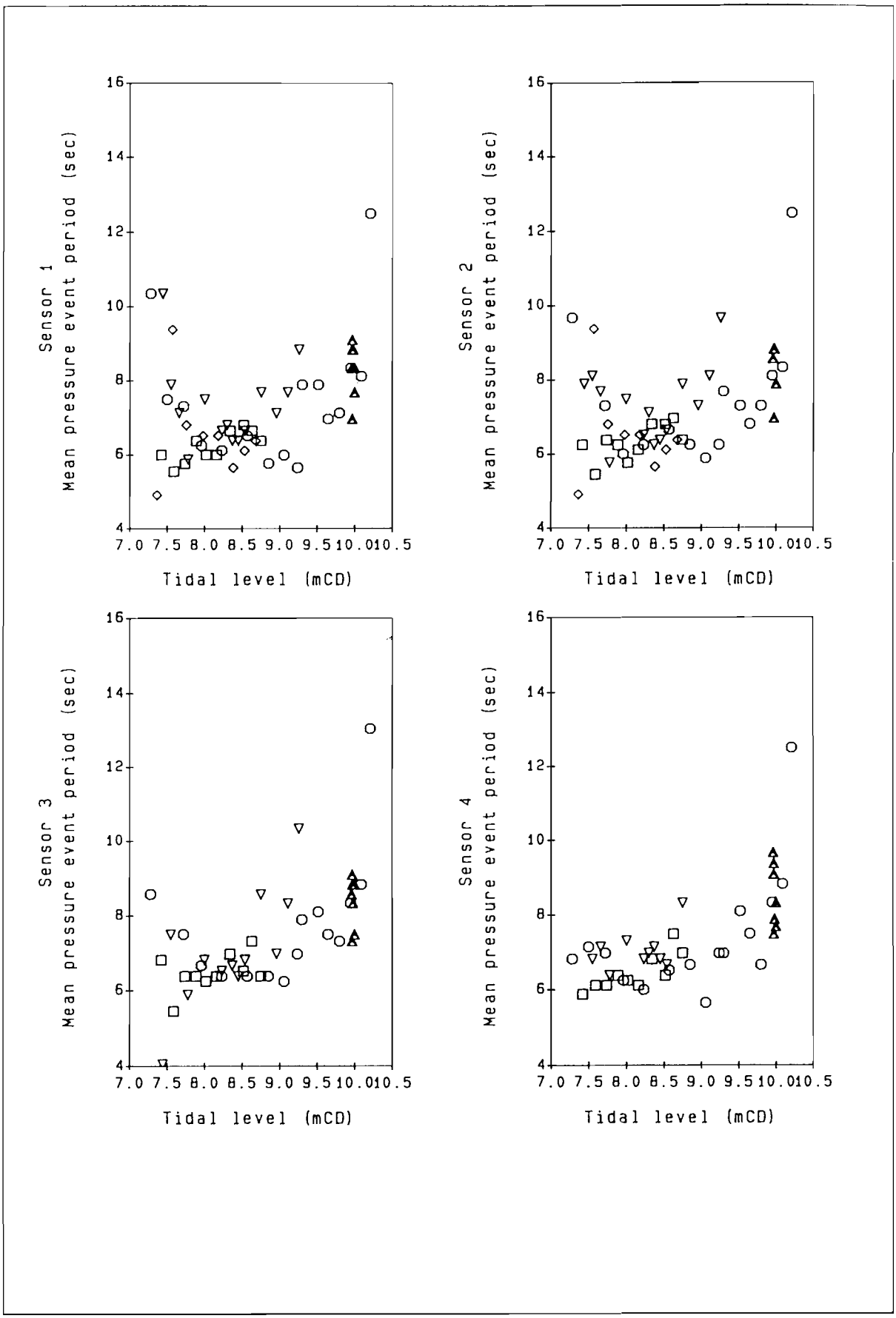

Fig 5.17 Mean period of pressure events versus tidal elevation

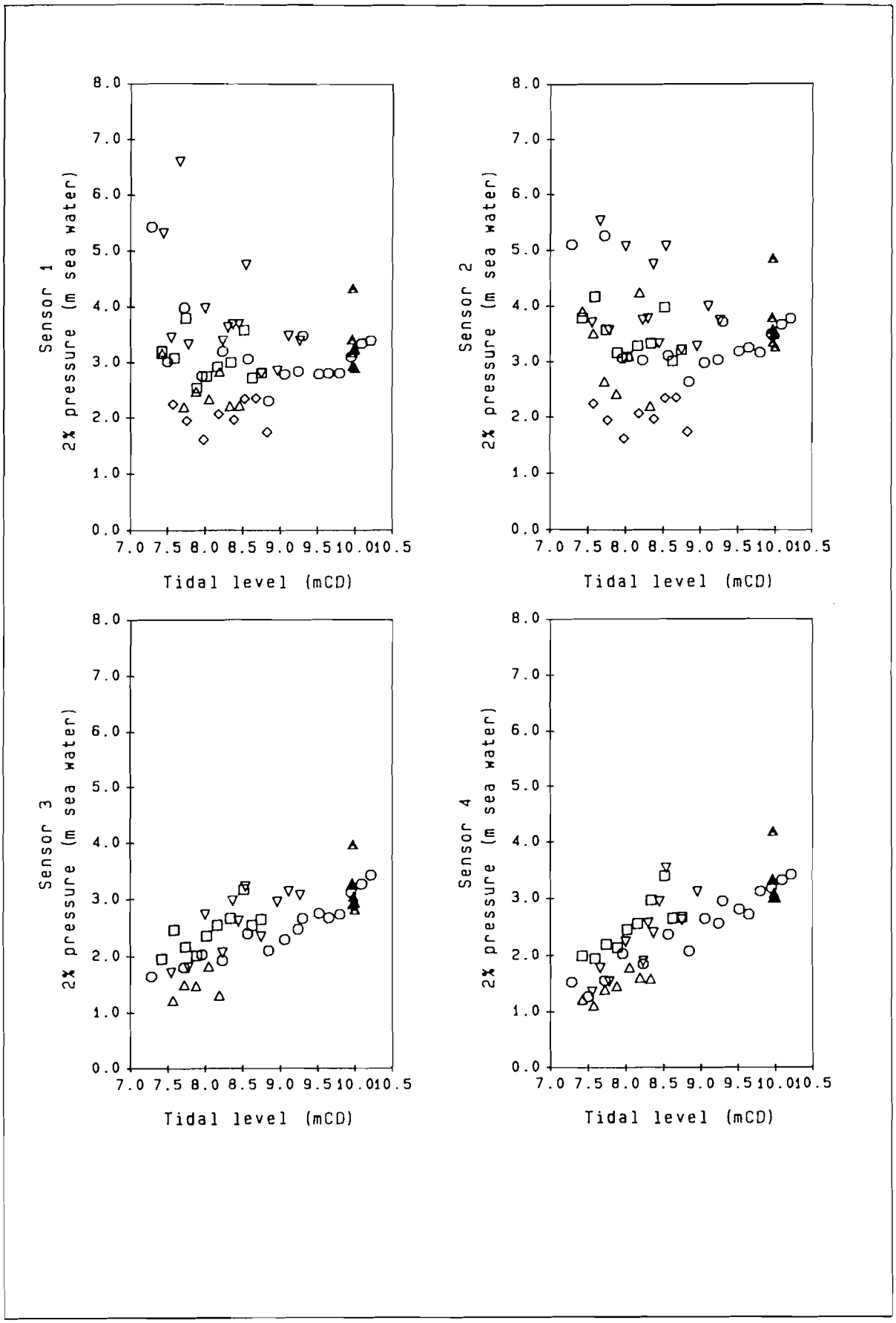

Fig 5.18 2 percentile exceedence pressures versus tidal elevation

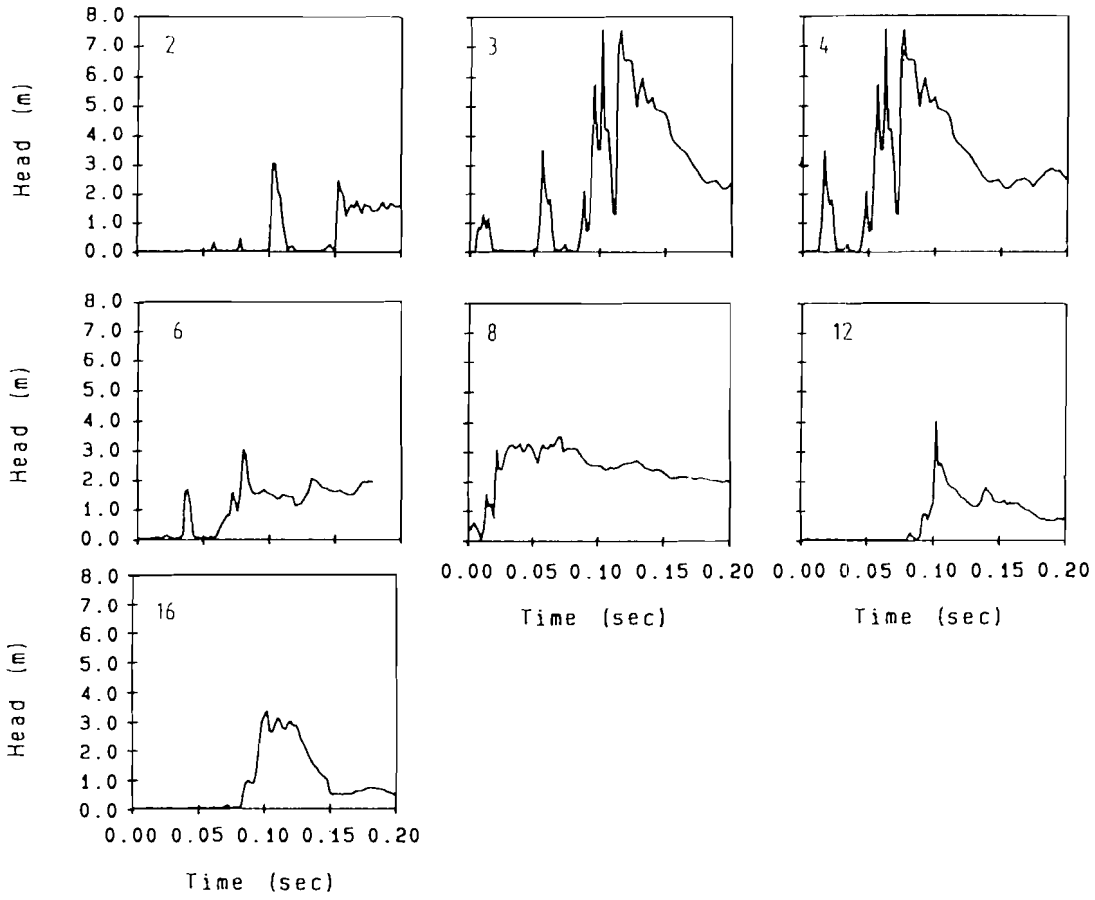

Fig 5.19a Major impact events on 28/01/91 - Sensor 1

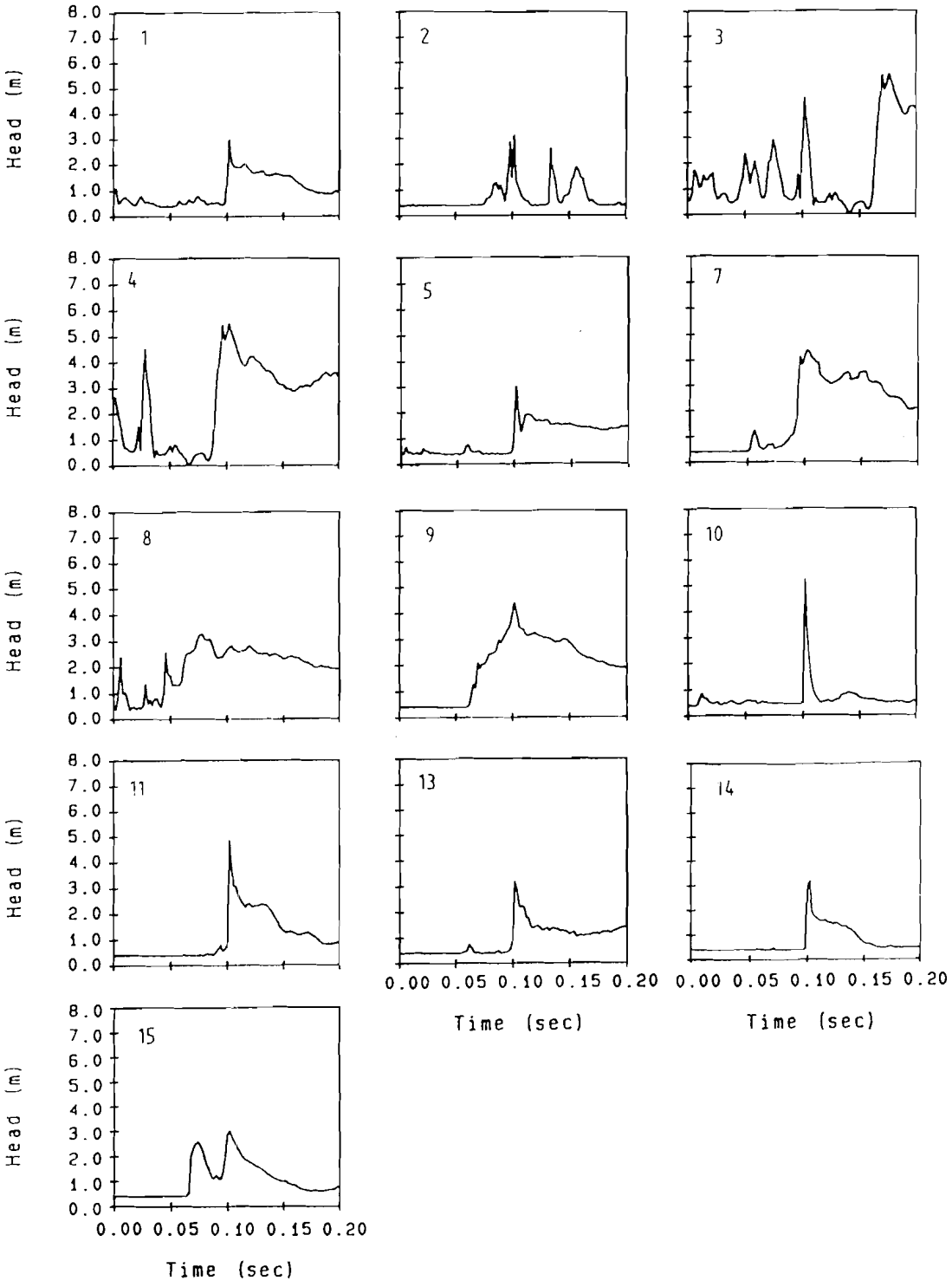

Fig 5.19b Major impact events on 28/01/91 - Sensor 2

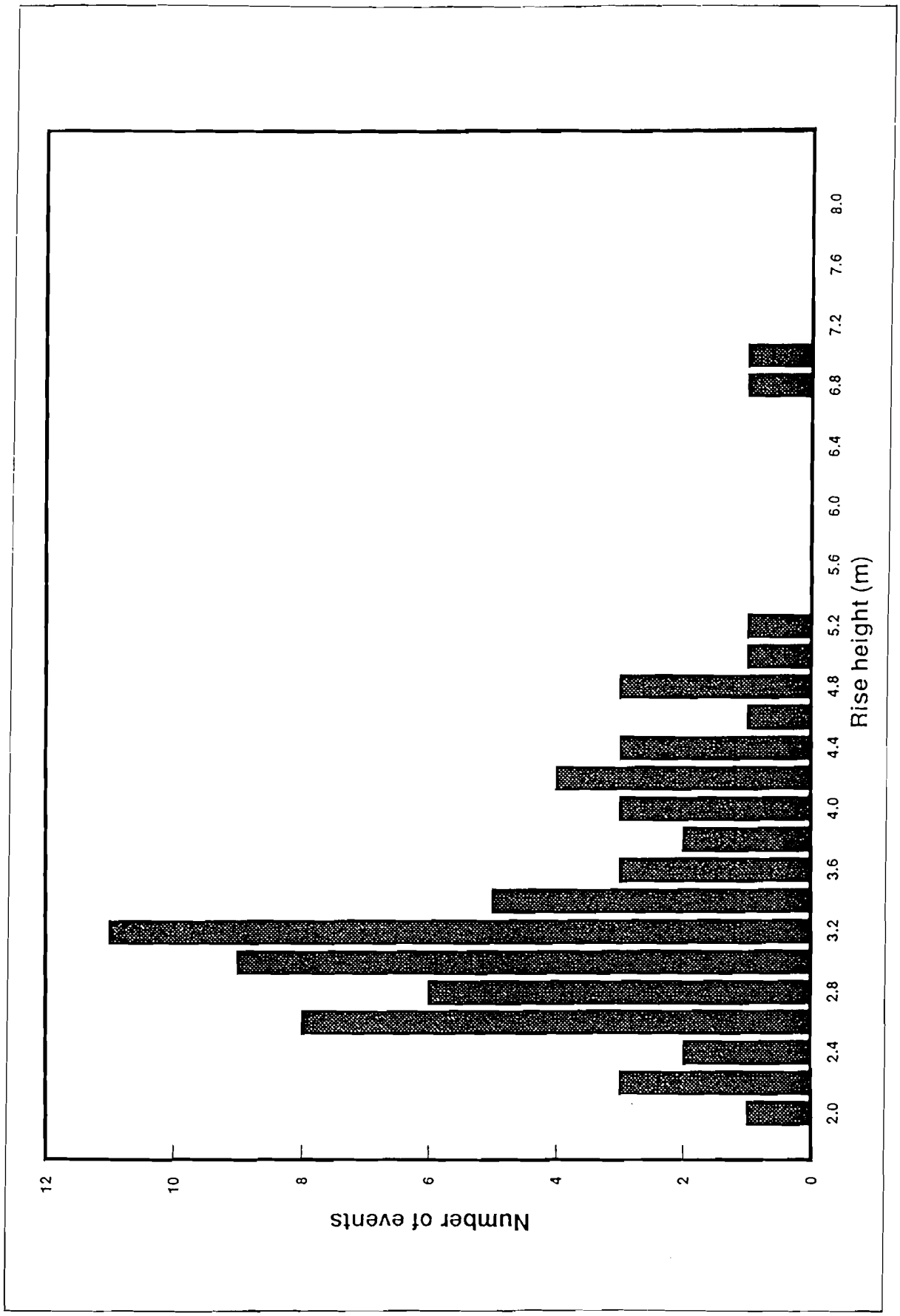

Fig 5.20 Major impact events identified.

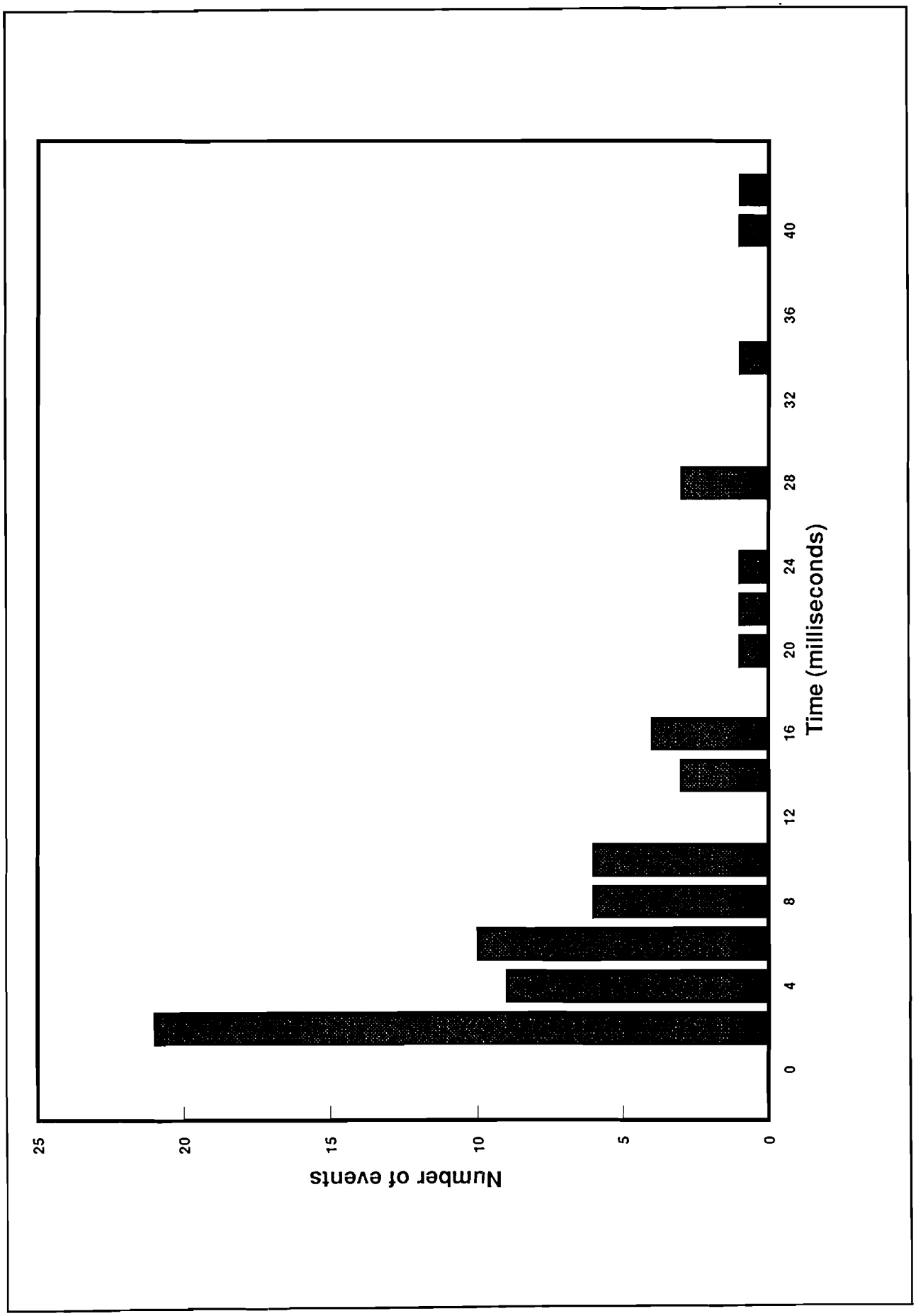

Fig 5.21 Distribution of major pressure event rise times.

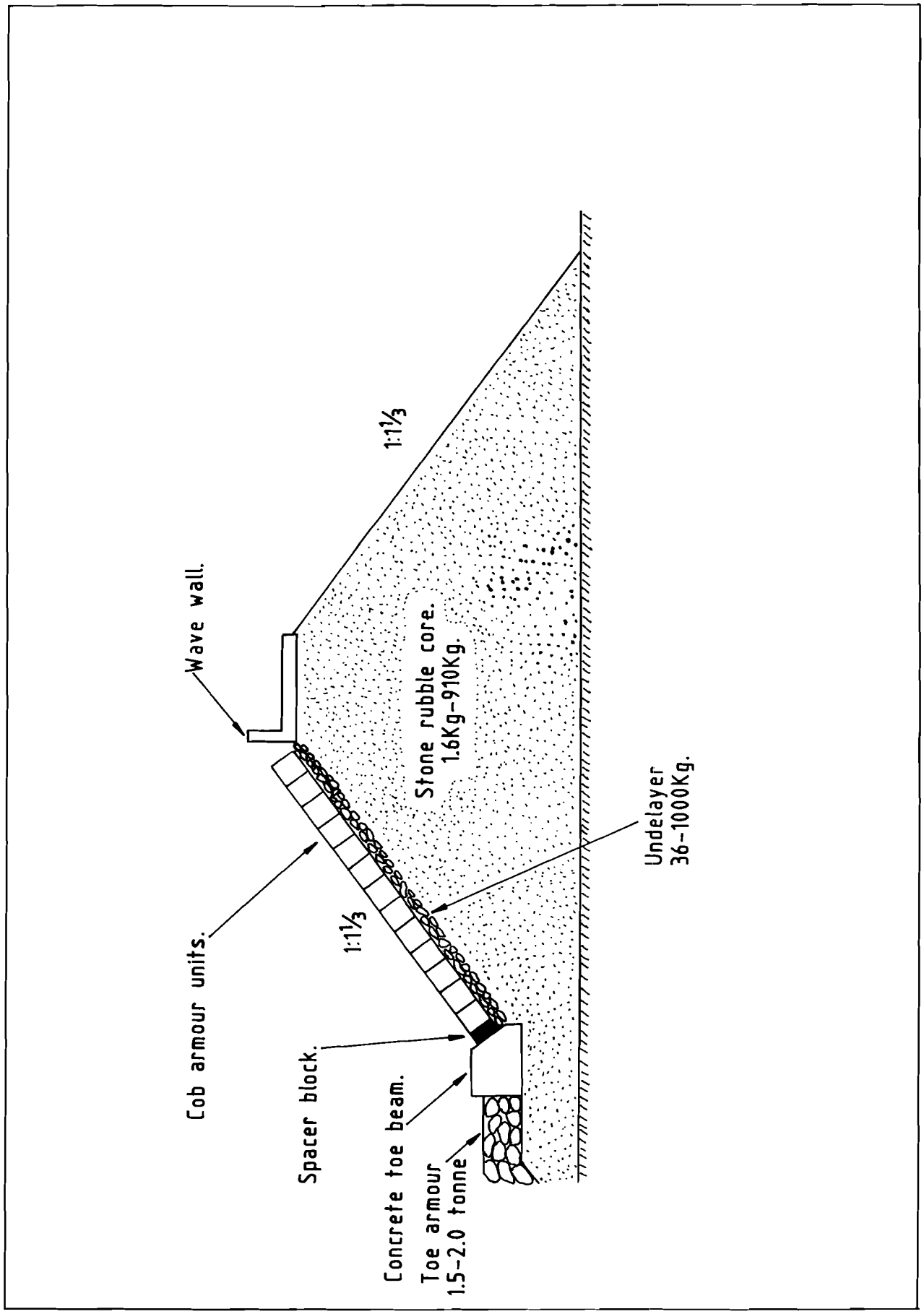

Fig 6.1 La Collette breakwater, Section 1.

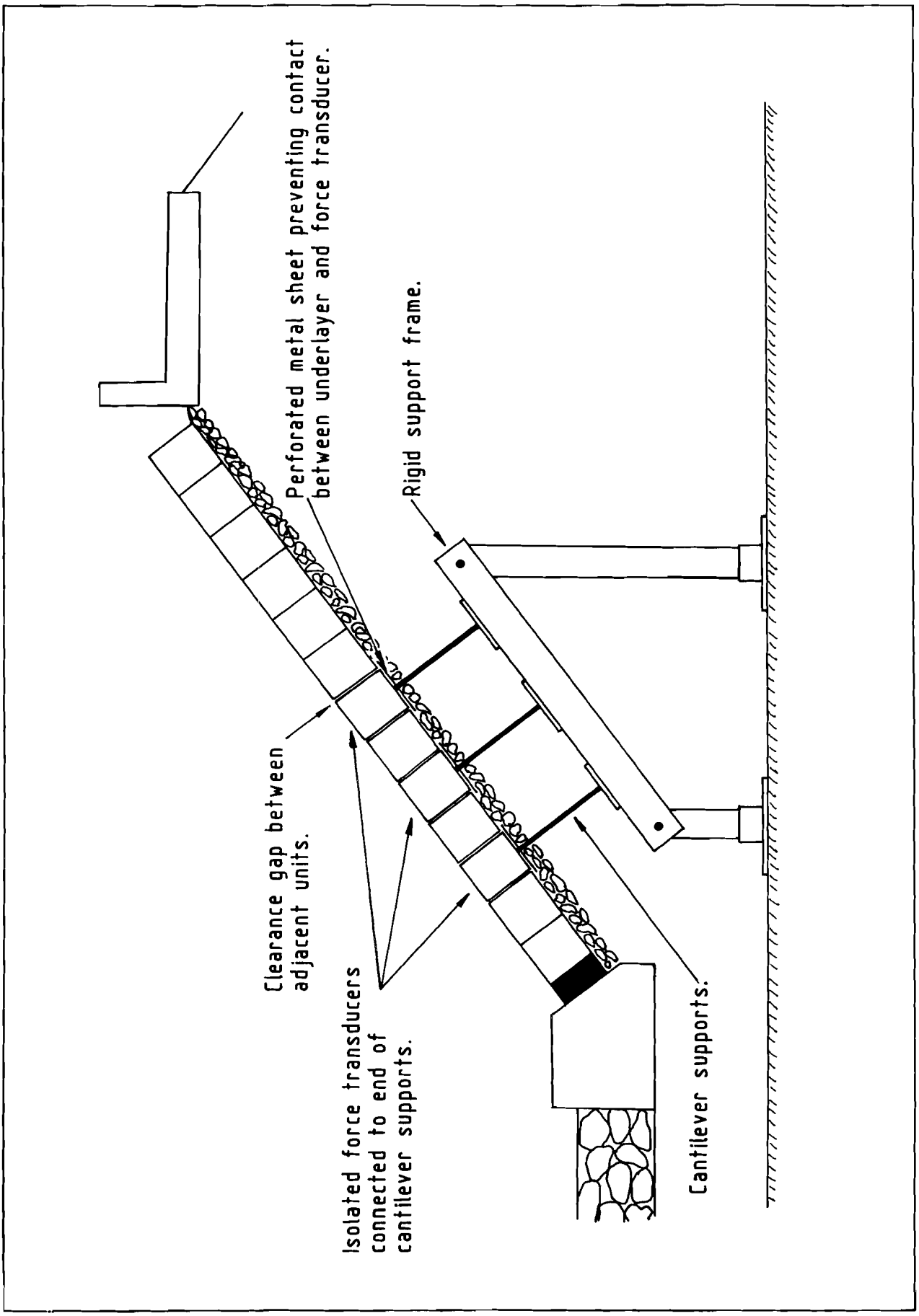

Fig 6.2 Positioning of the force tranducers, Section 1.

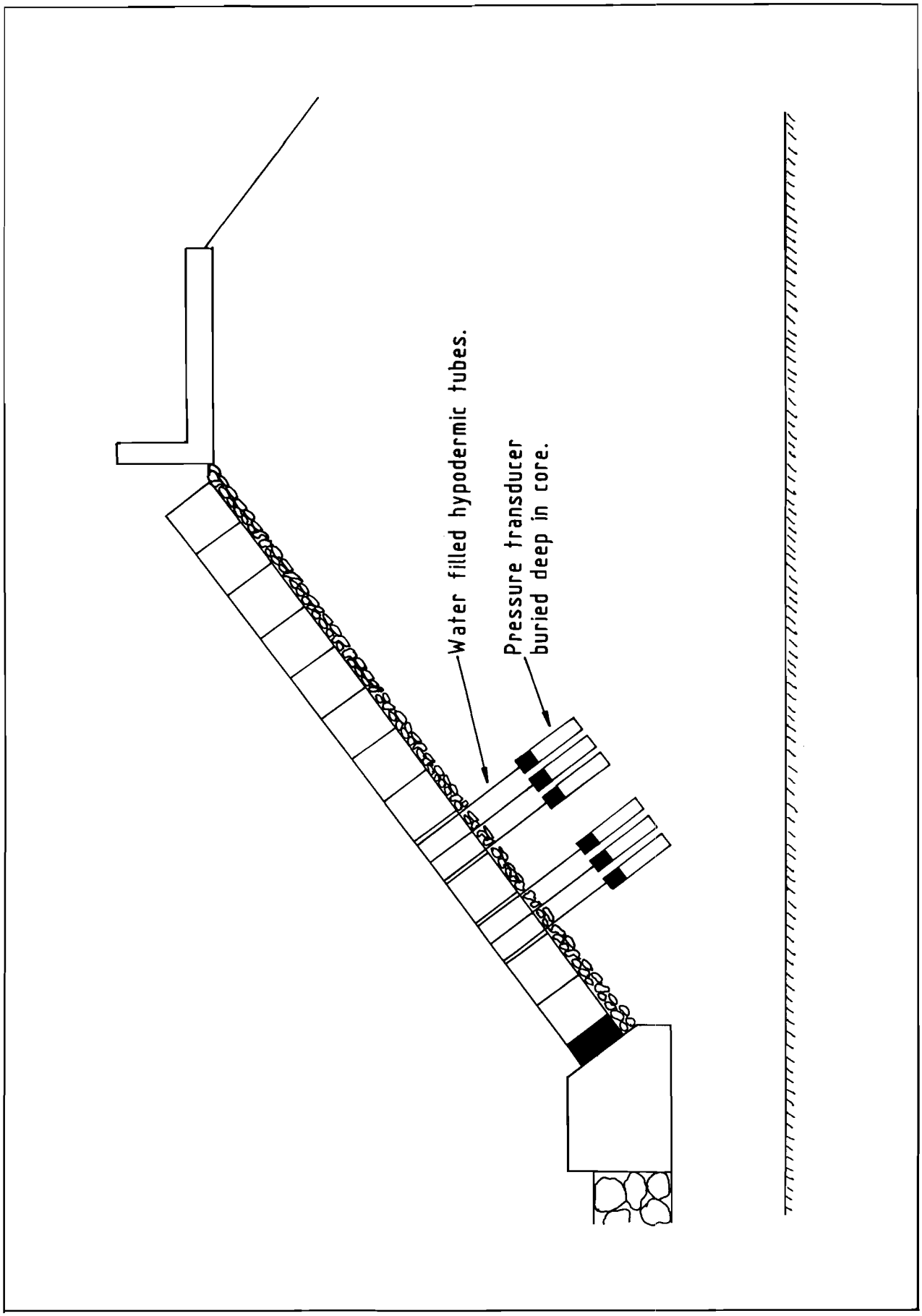

Fig 6.3 Positioning of the pressure transducers, Section 1.

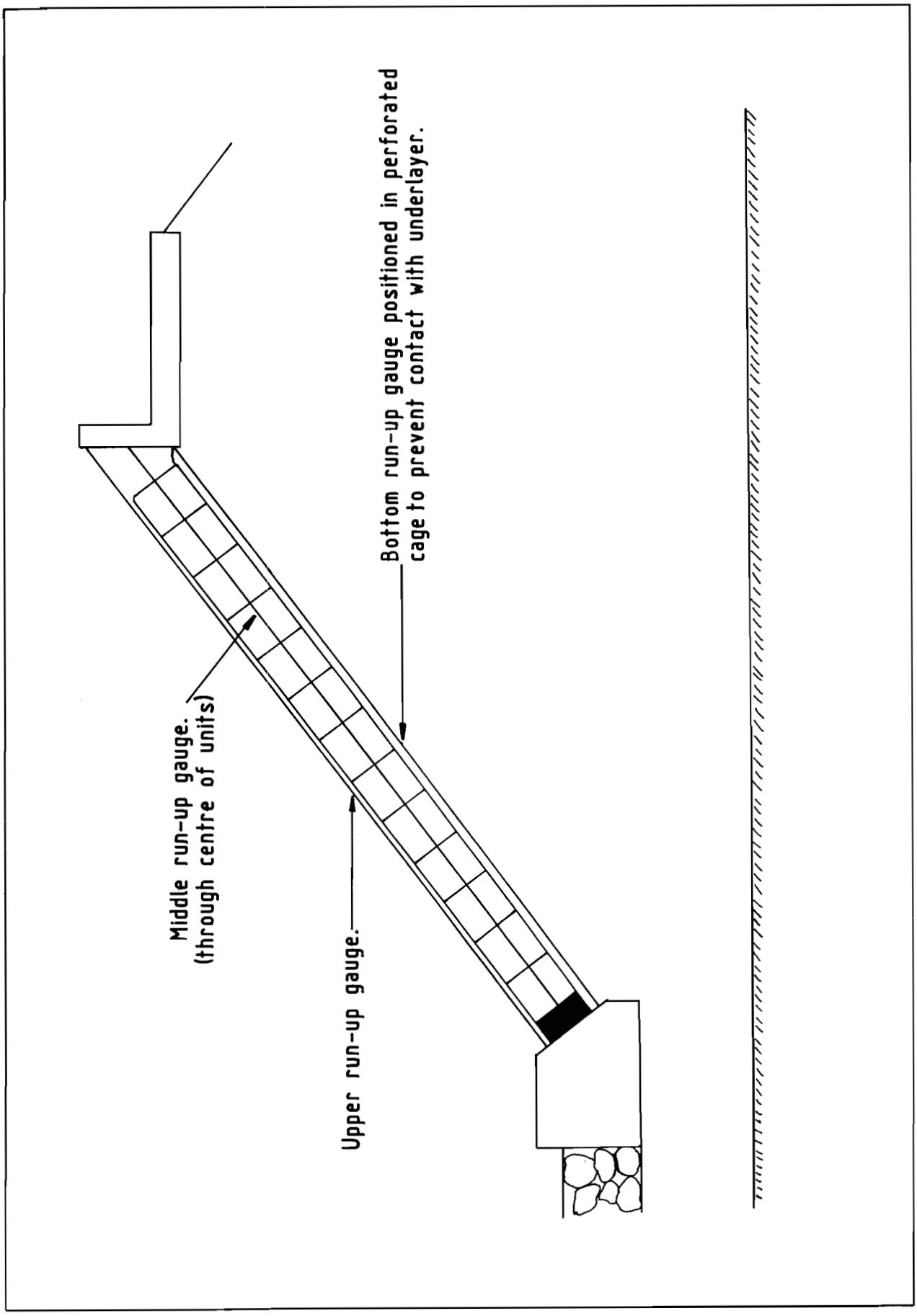

Fig 6.4 Positioning of the run-up gauges, Section 1.

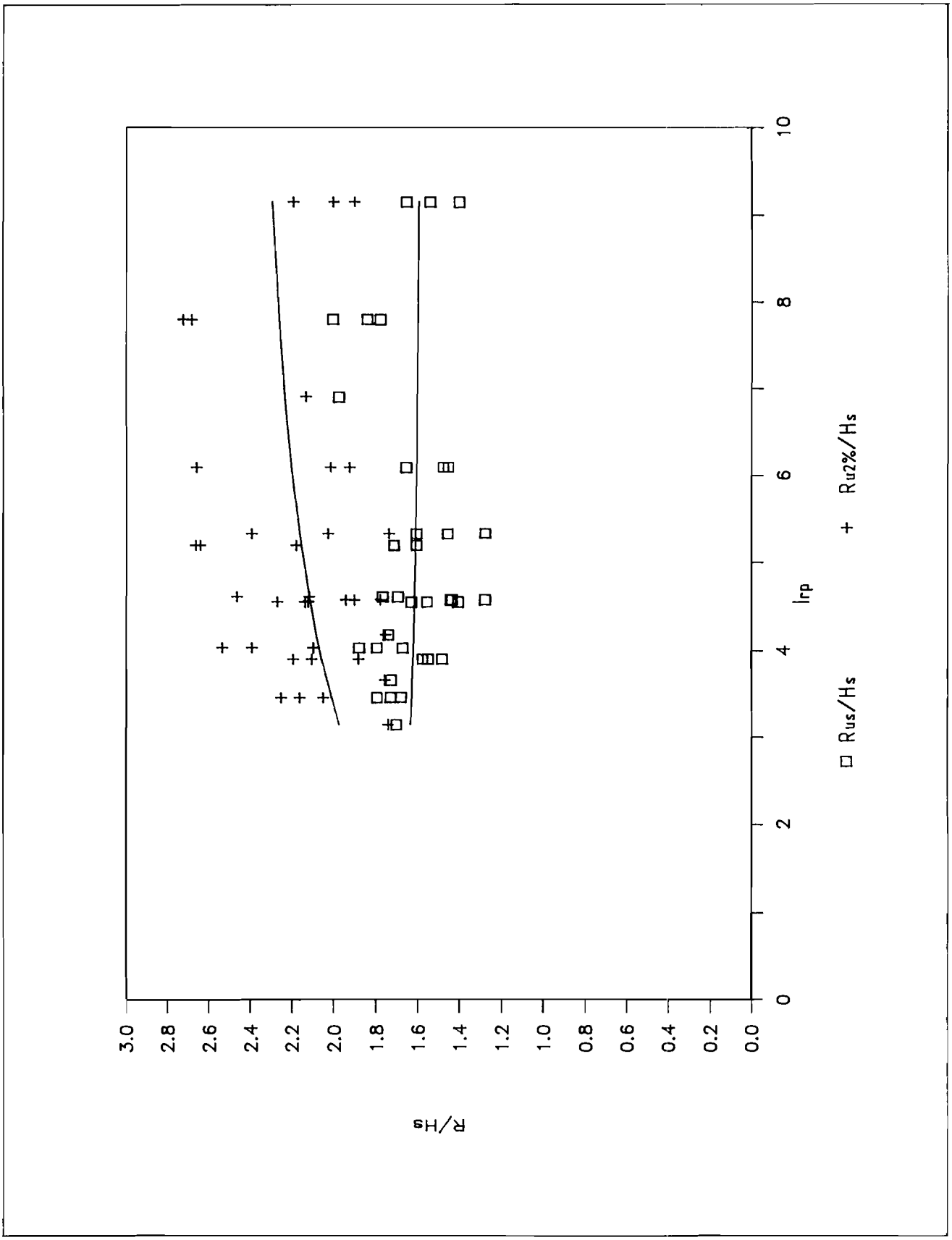

Fig 6.5 Run—up data, upper gauge, section 1

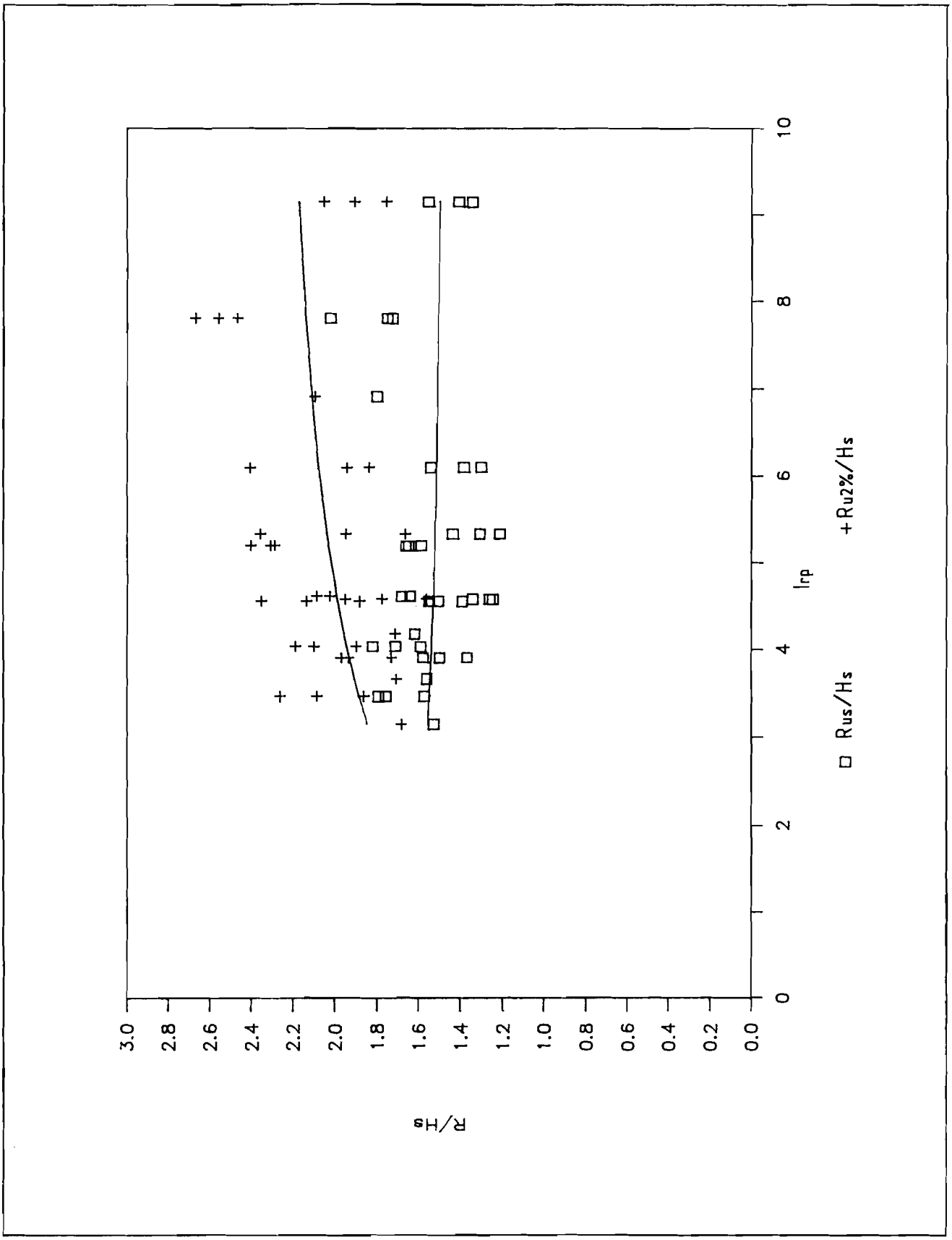

Fig 6.6 Run—up data, middle gauge, section 1

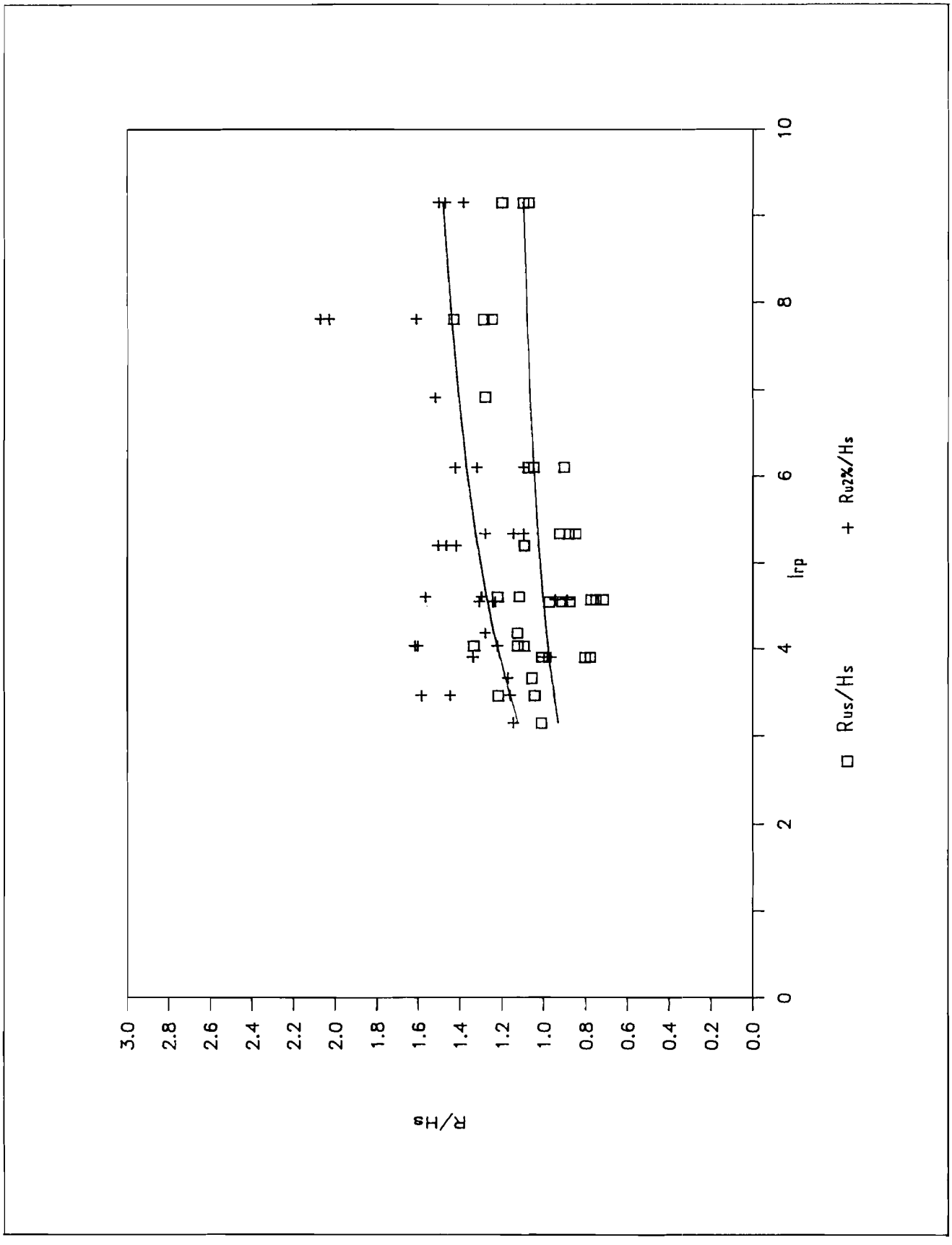

Fig 6.7 Run—up data, bottom gauge, section 1.

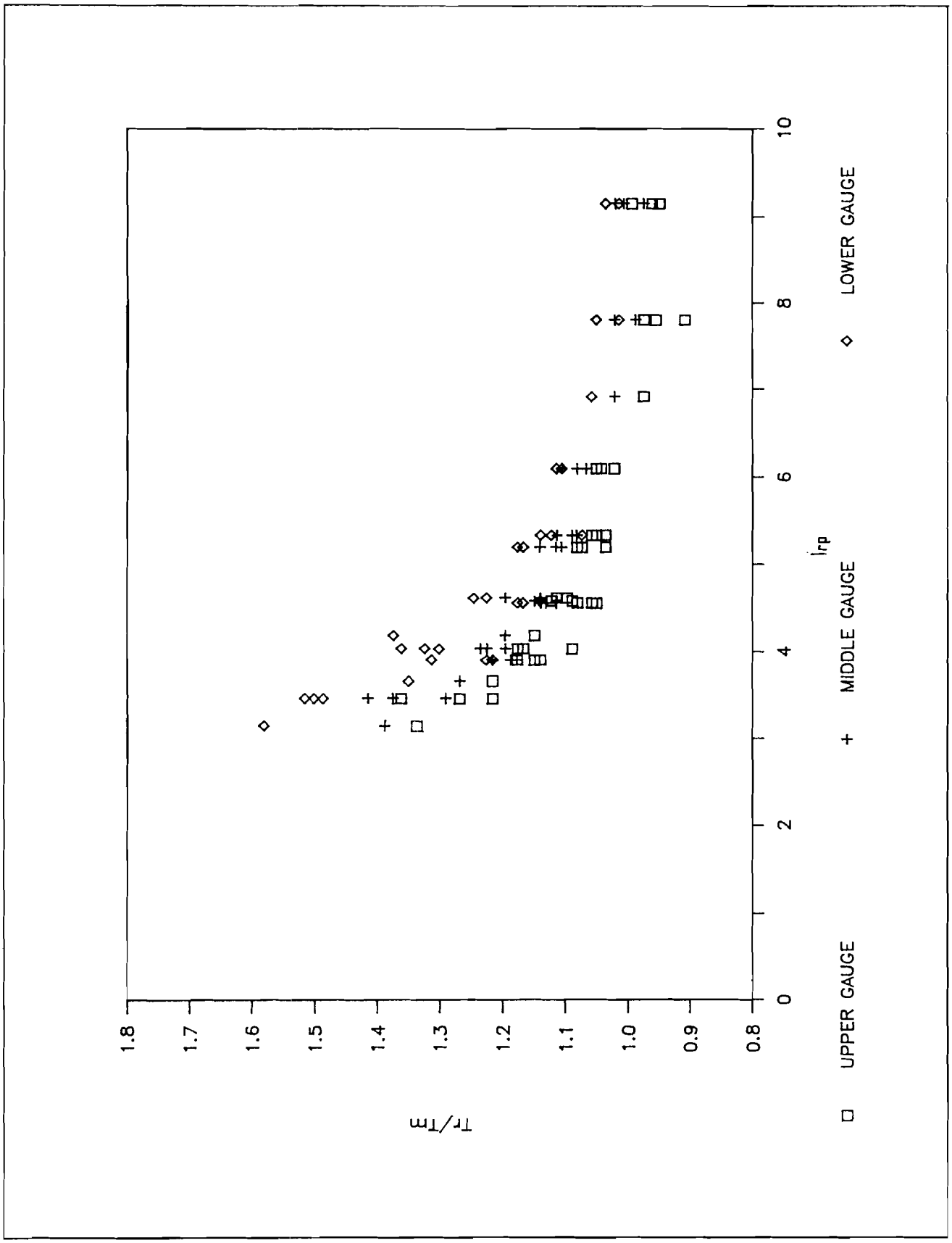

Fig 6.8 Run—up period data, section 1.

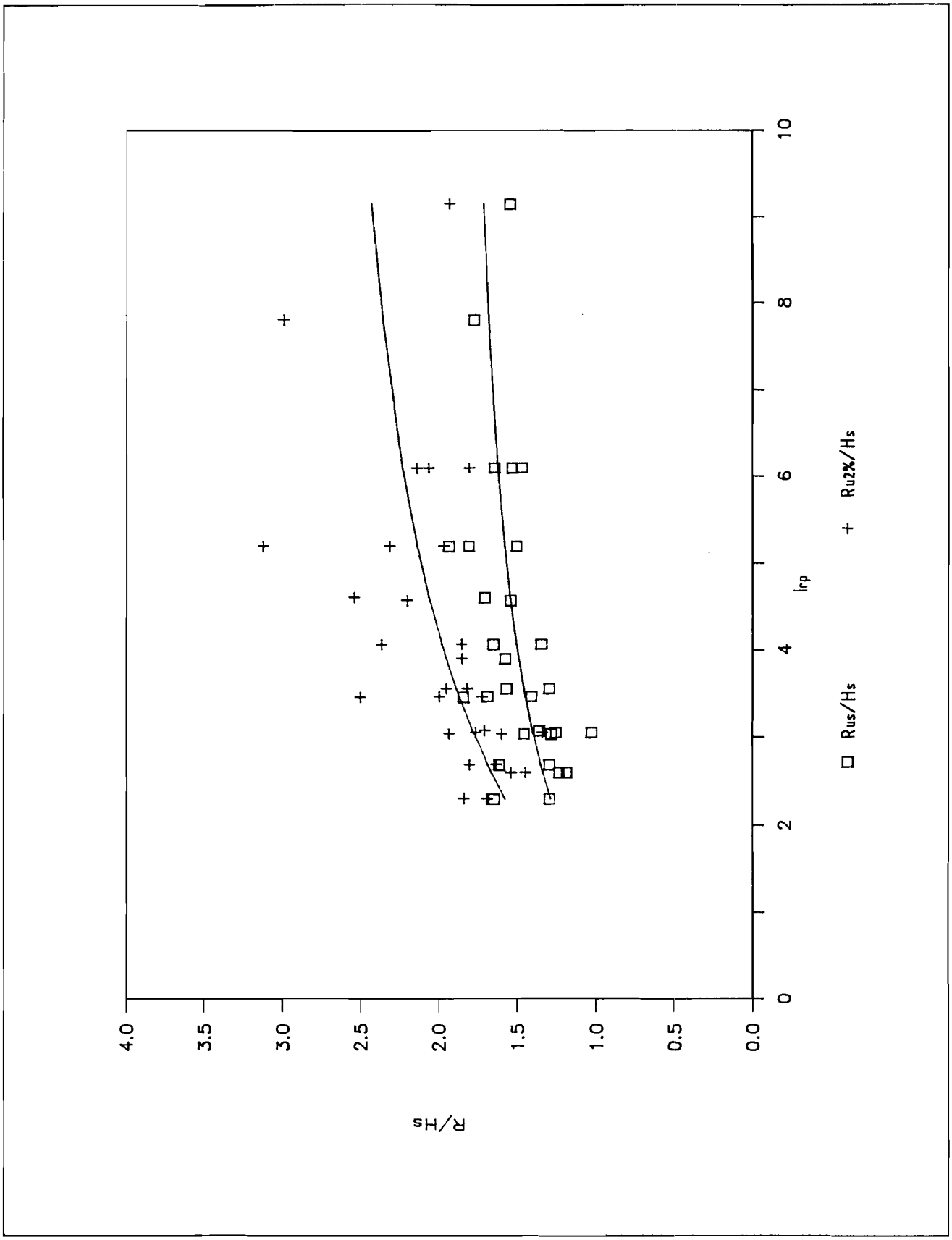

Fig 6.9 Run—up data, upper gauge, sections 2 and 3

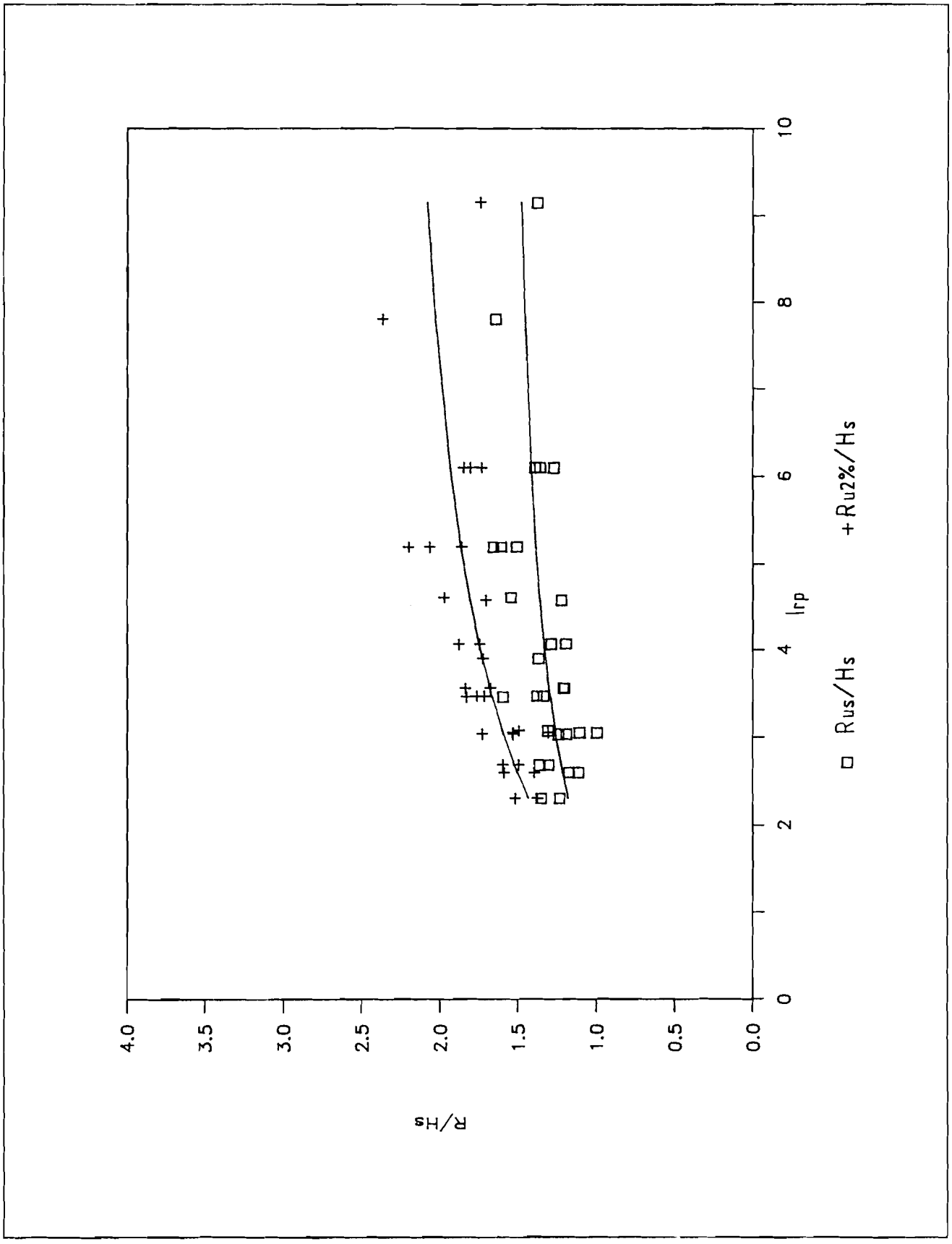

Fig 6.10 Run—up data, middle gauge, sections 2 and 3.

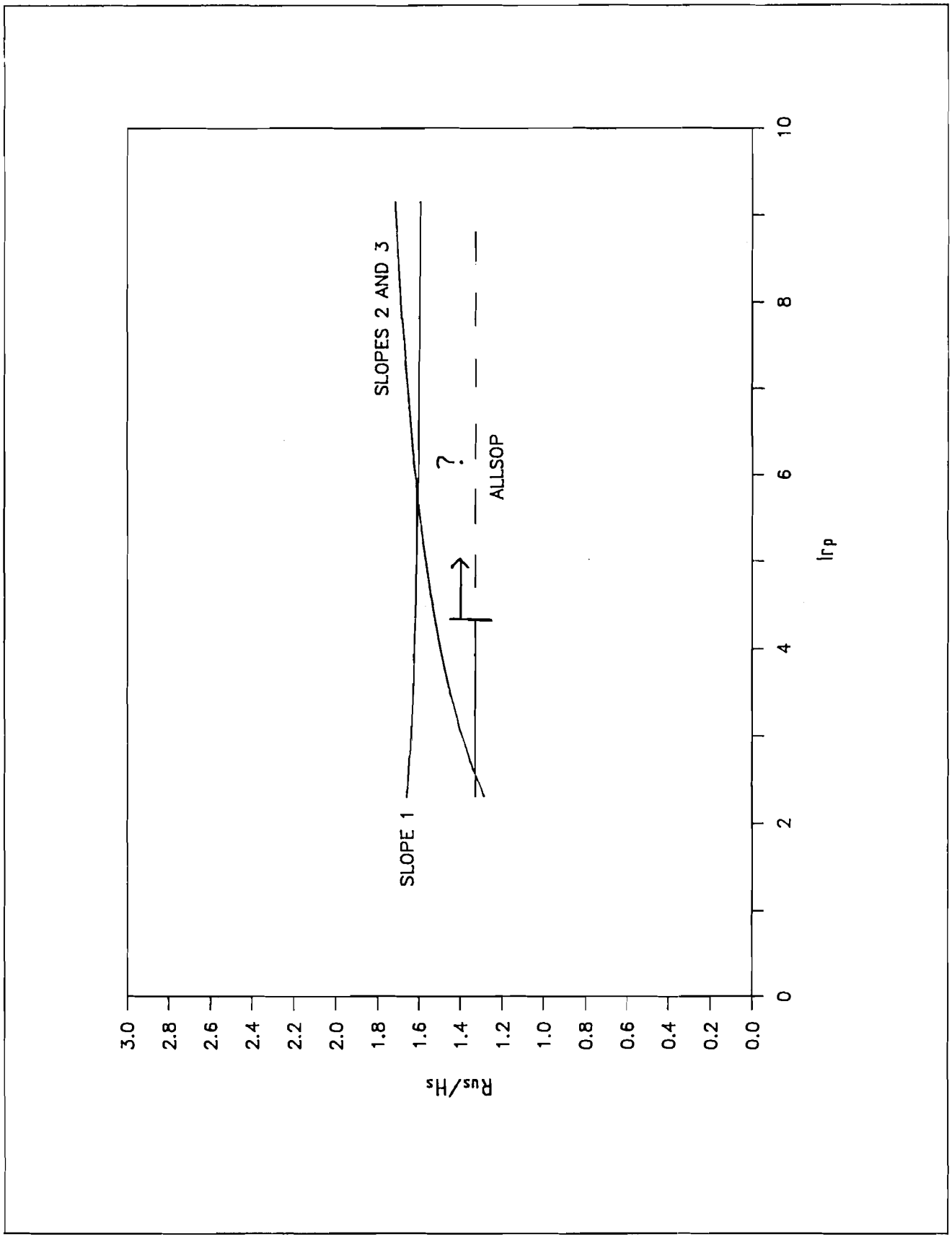

Fig 6.11 A comparison of significant run-up data

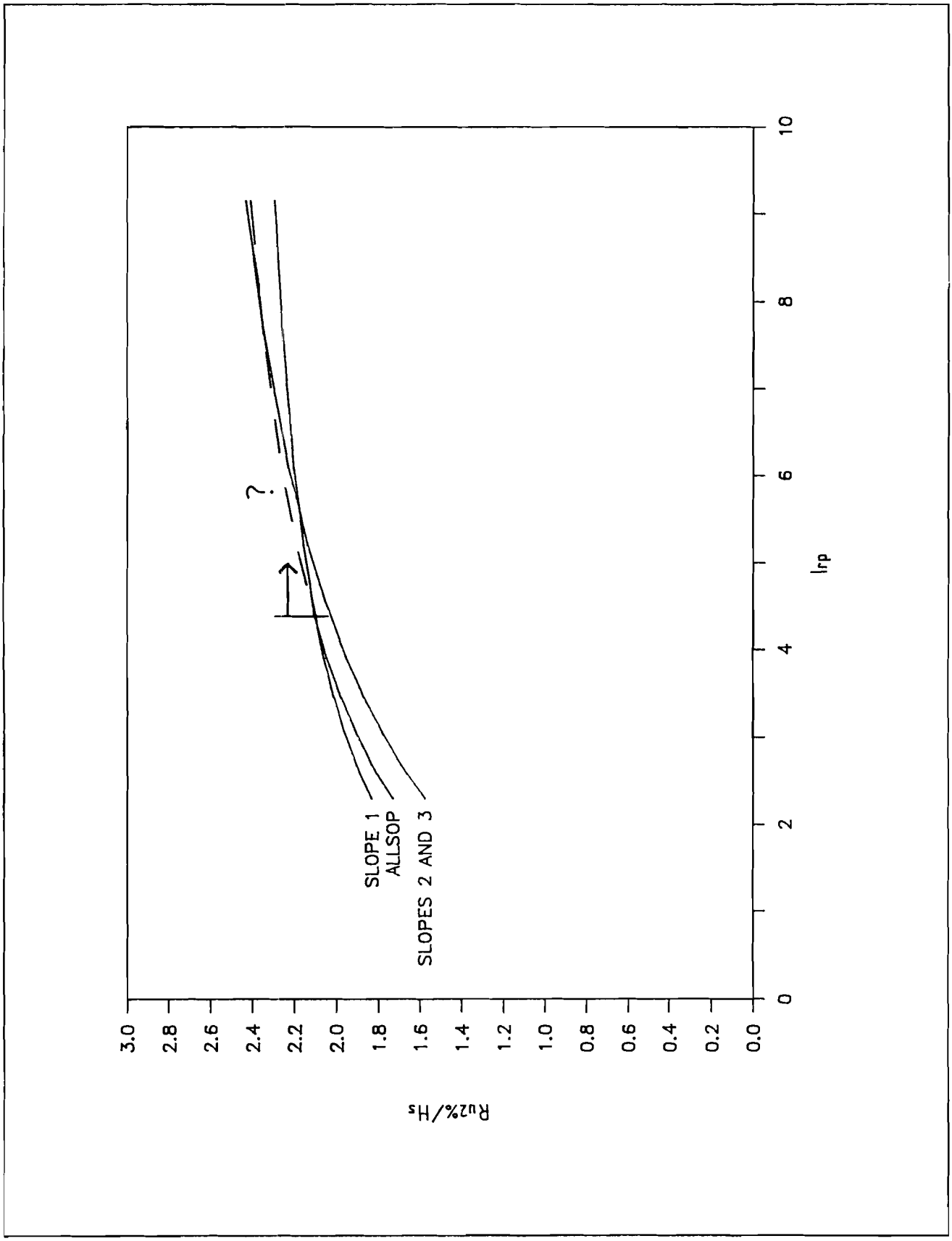

Fig 6.12 A comparison of 2% run-up data

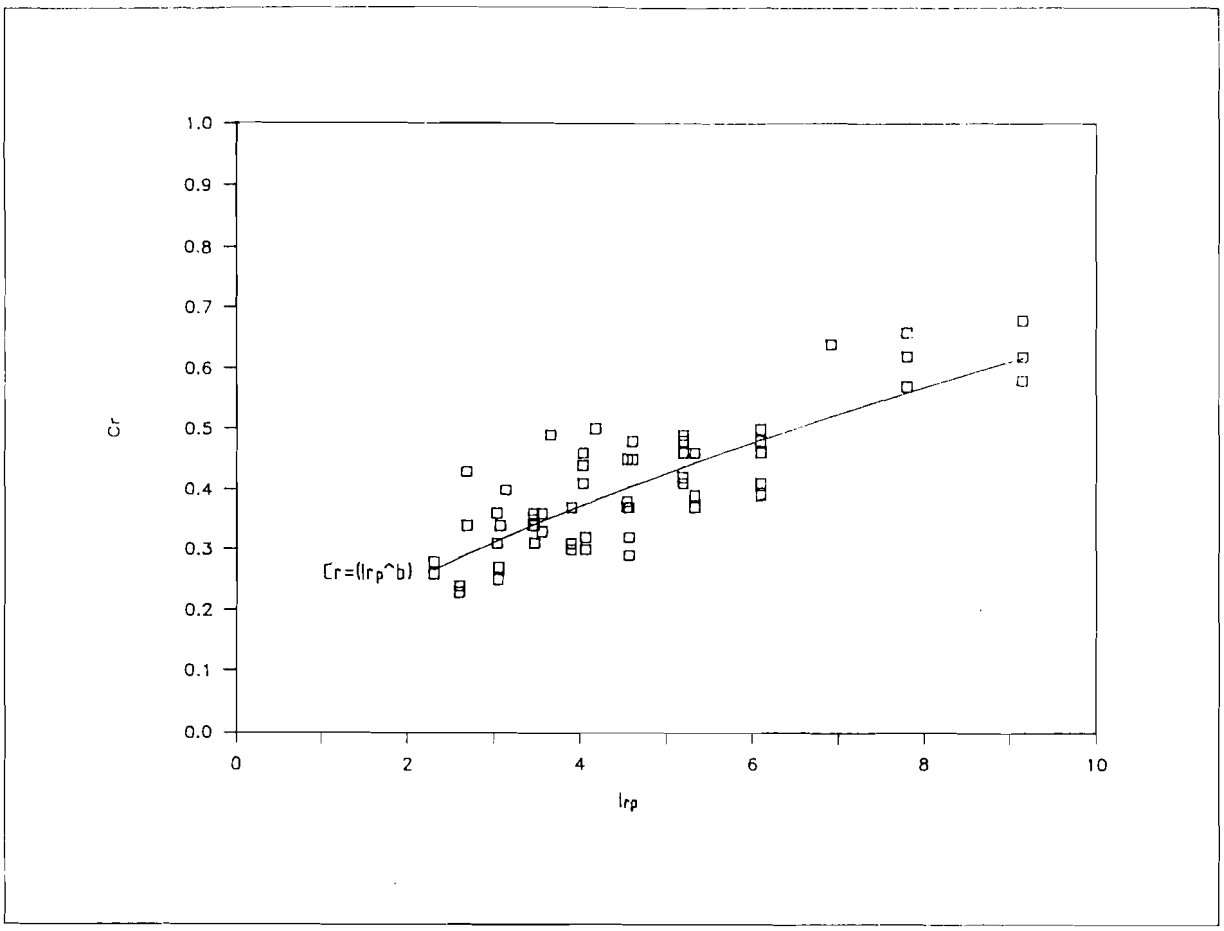

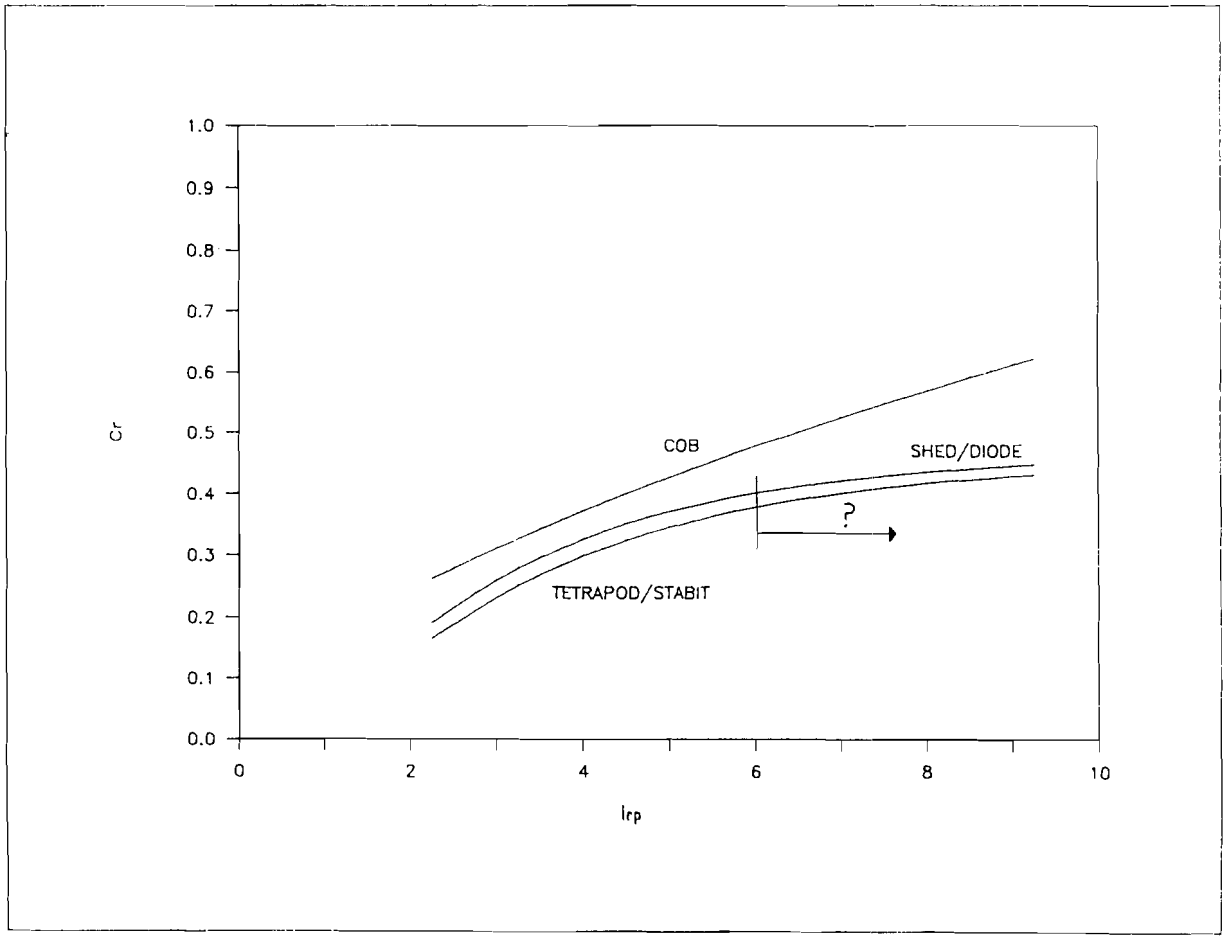

Fig 6.13 Reflection coefficient data, section 1.

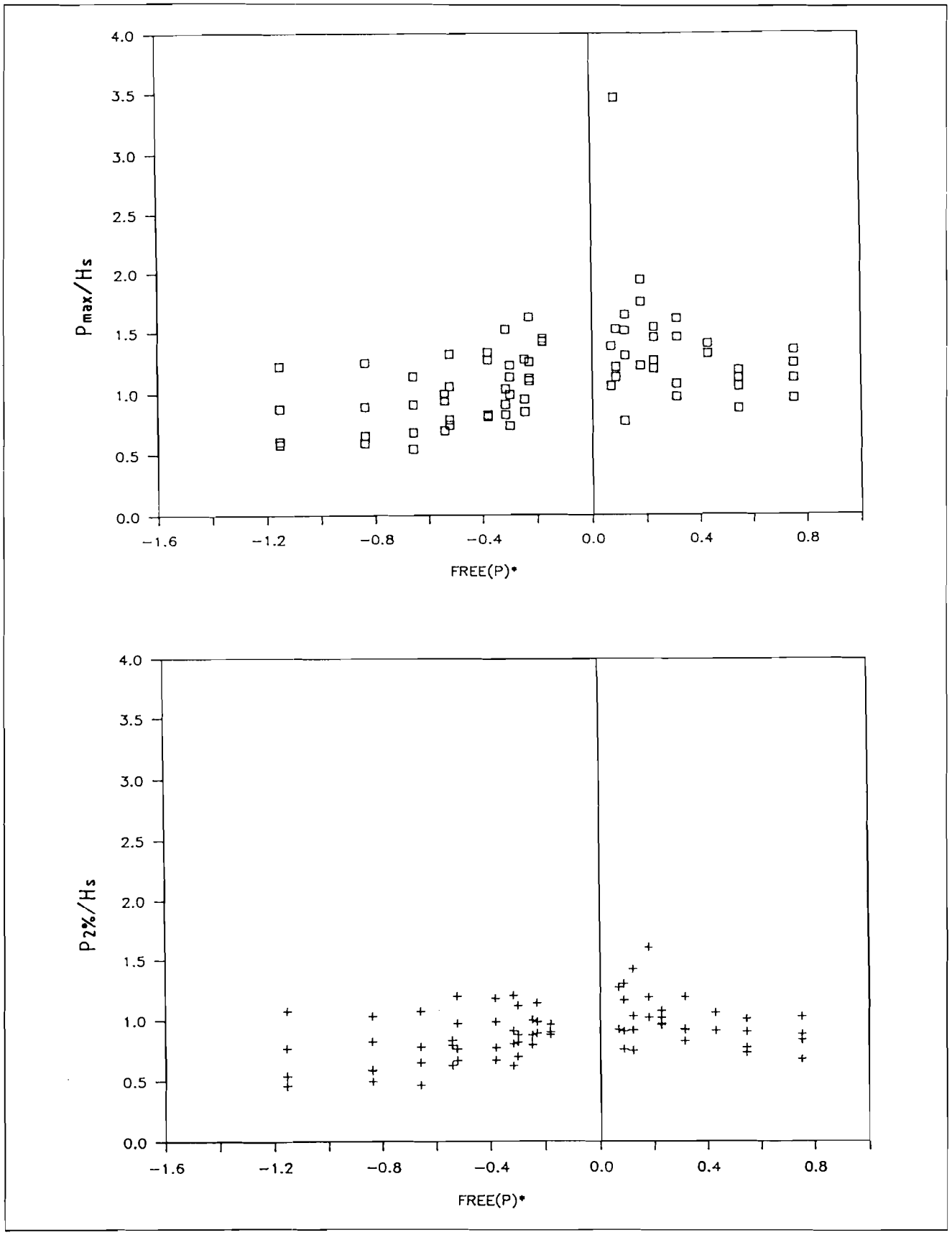

Fig 6.14 Pressure data, section 1, upper limb

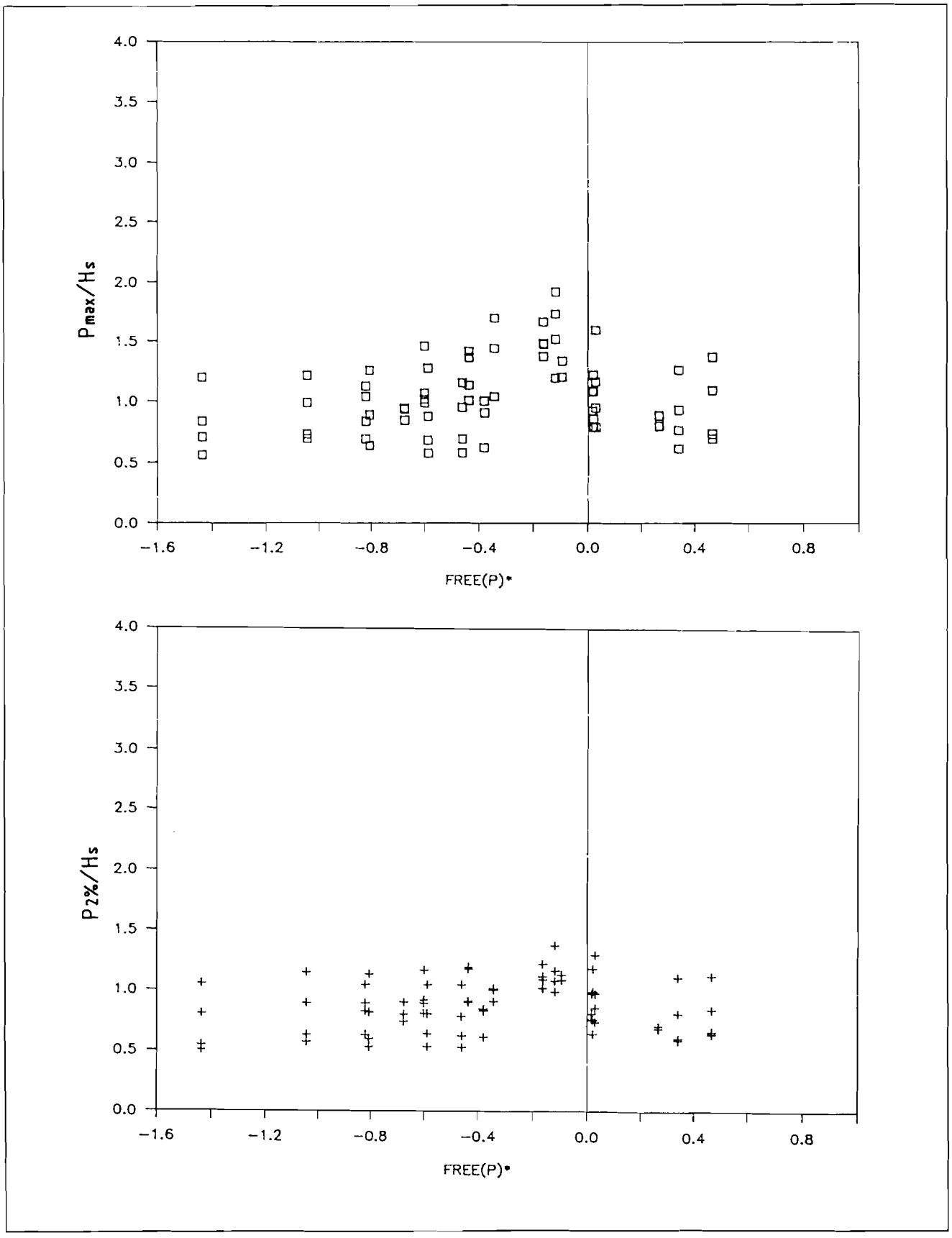

Fig 6.15 Pressure data, section 1, bottom limb

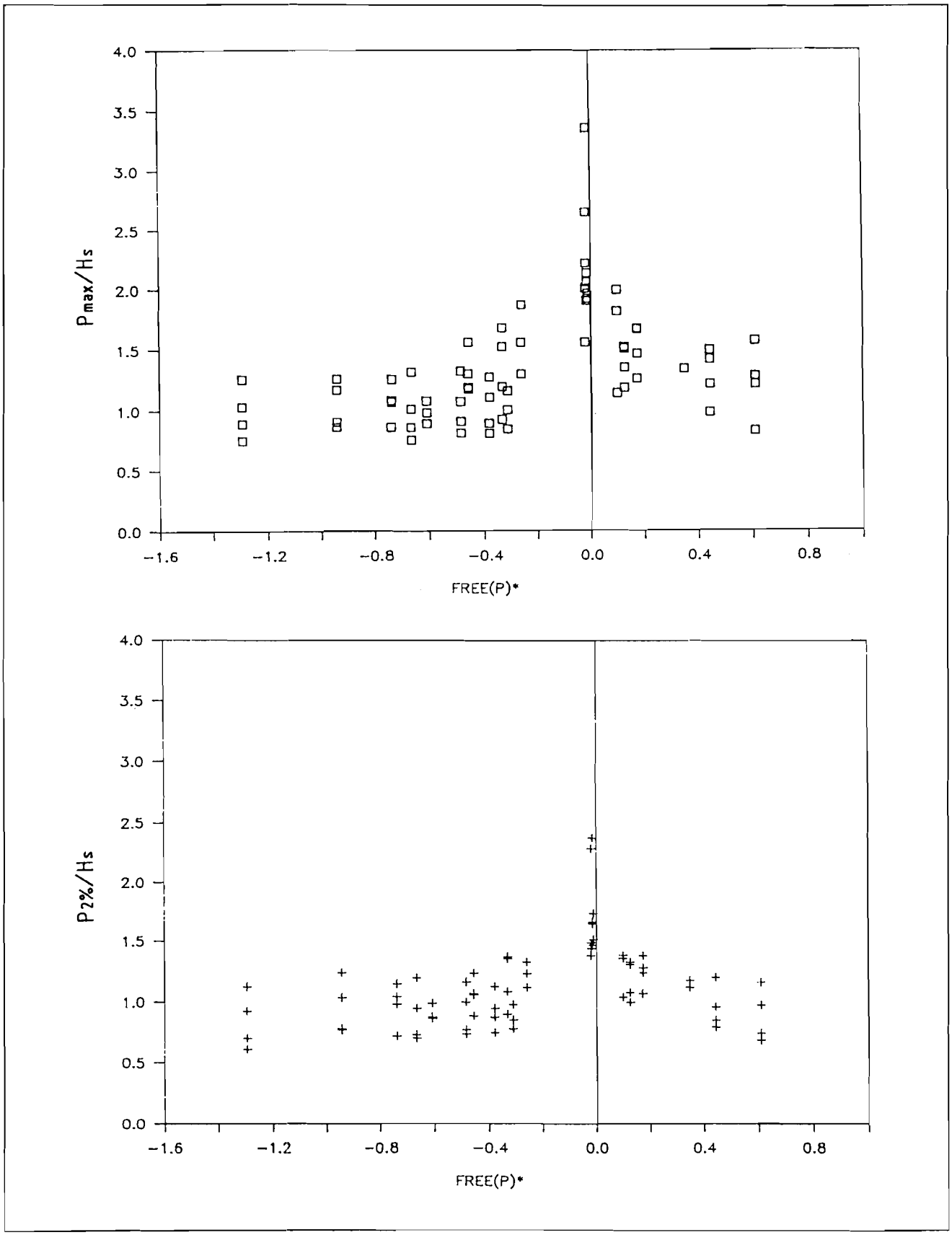

Fig 6.16 Pressure data, section 1, side limb

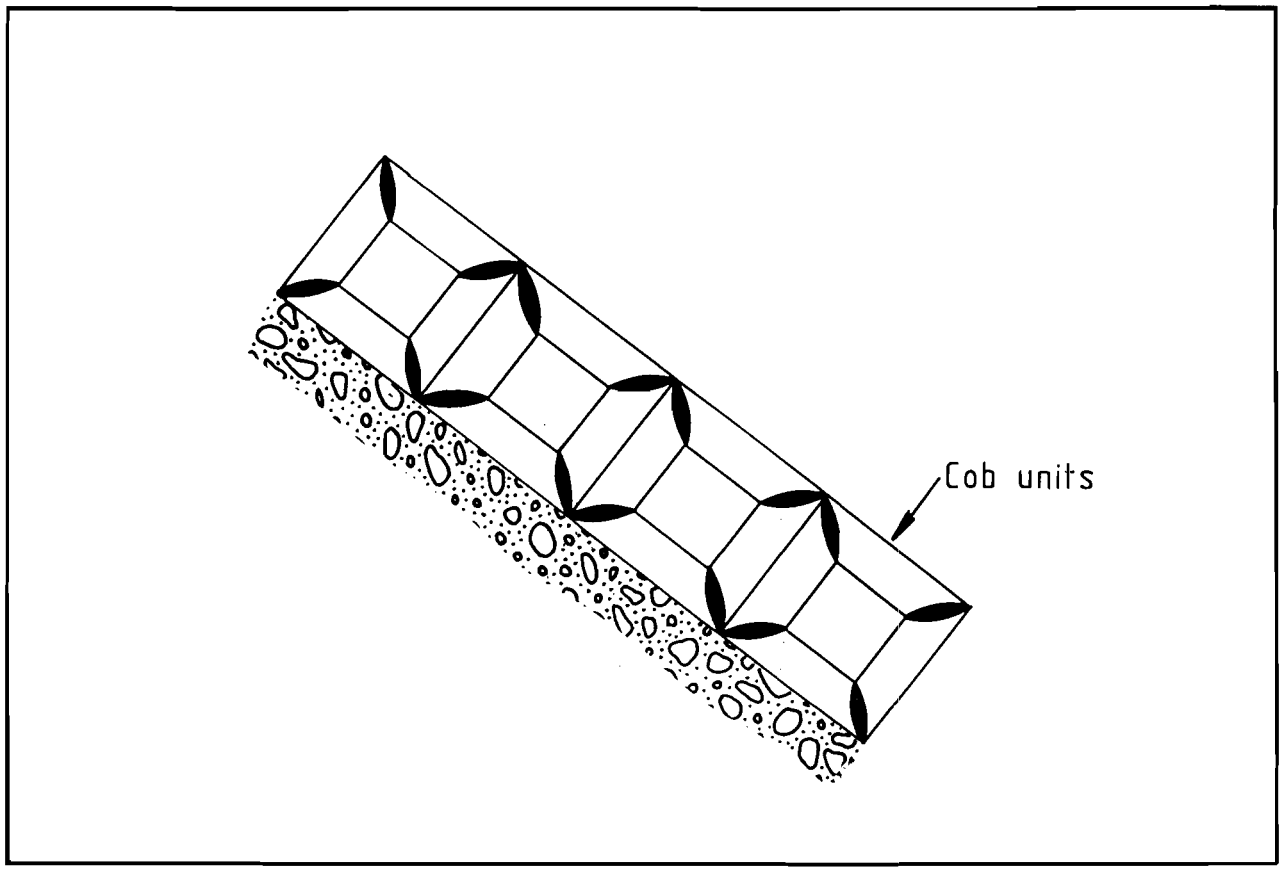

Underlayer prior to testing.

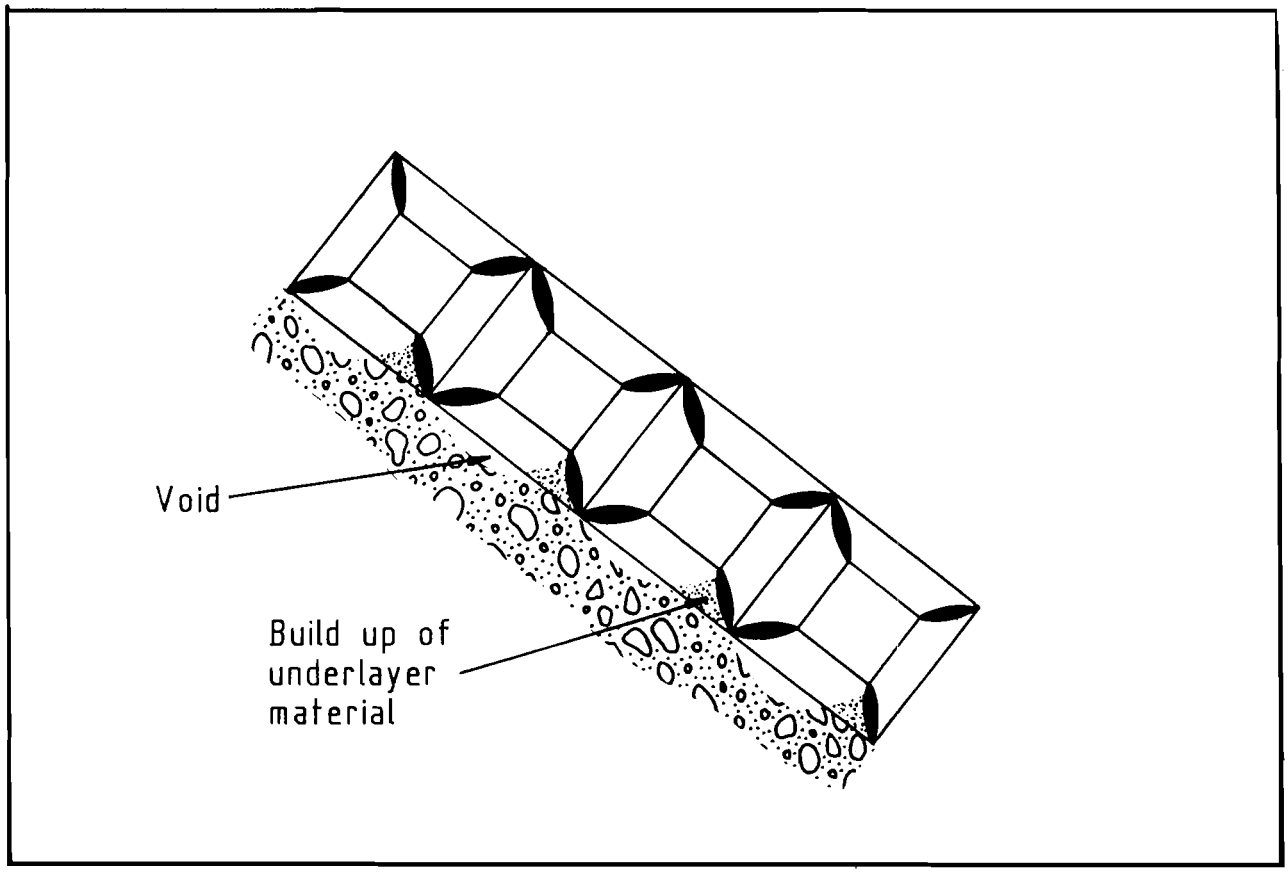

Underlayer after testing.

Fig 6.17 **Underlayer movement.**

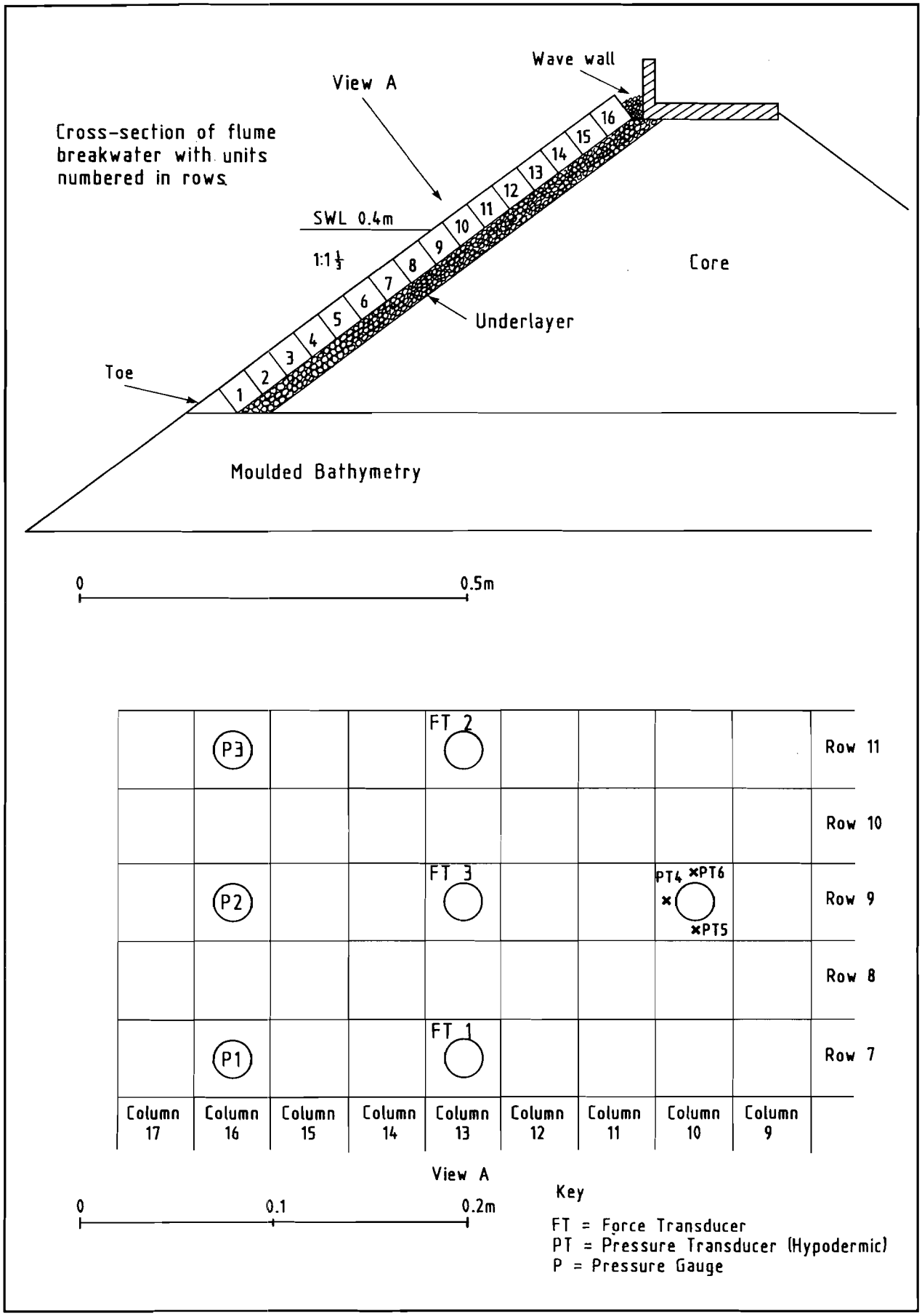

Fig 6.18 Shed breakwater, Section 4.

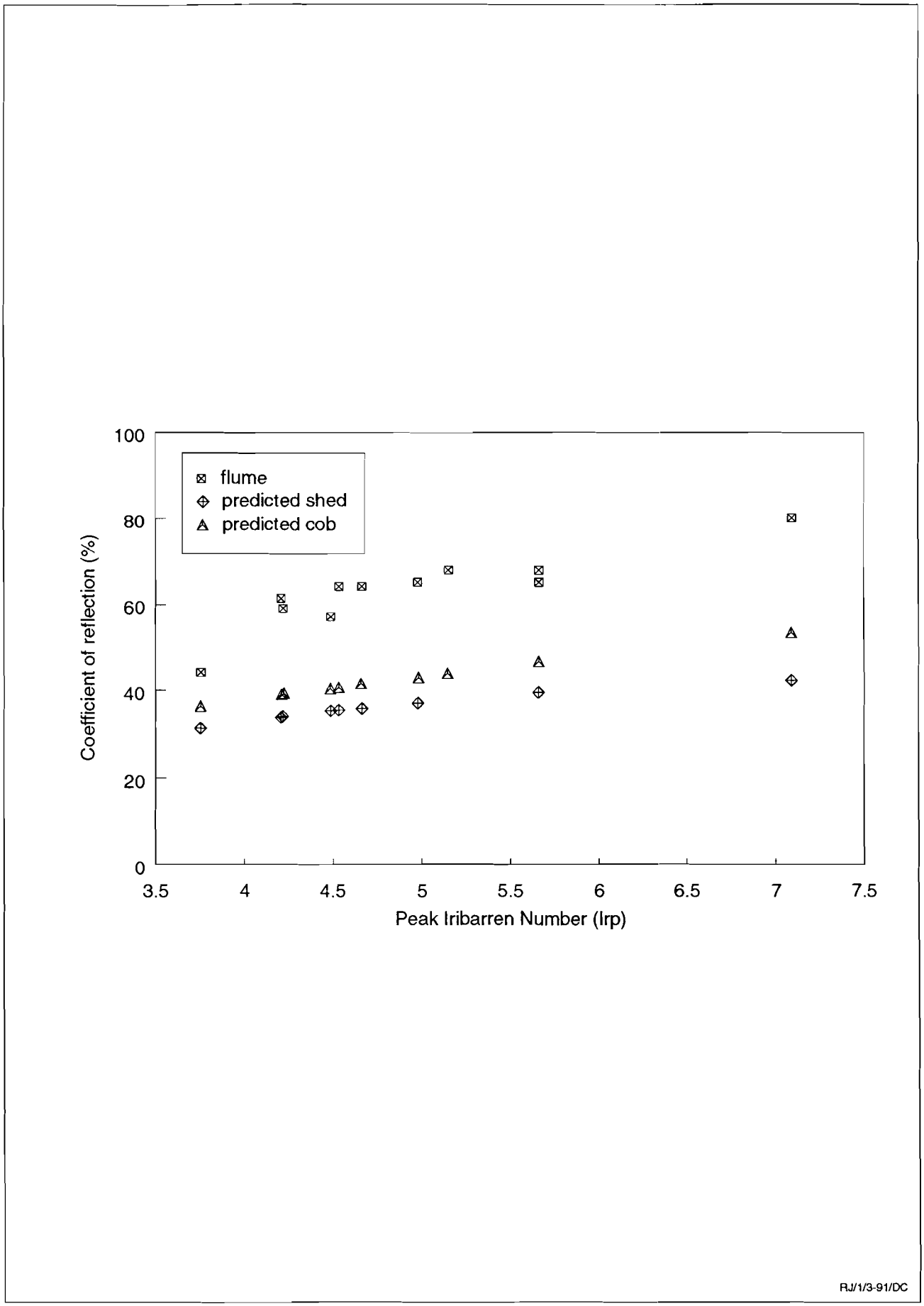

Fig 6.19 Reflection coefficient data, section 4

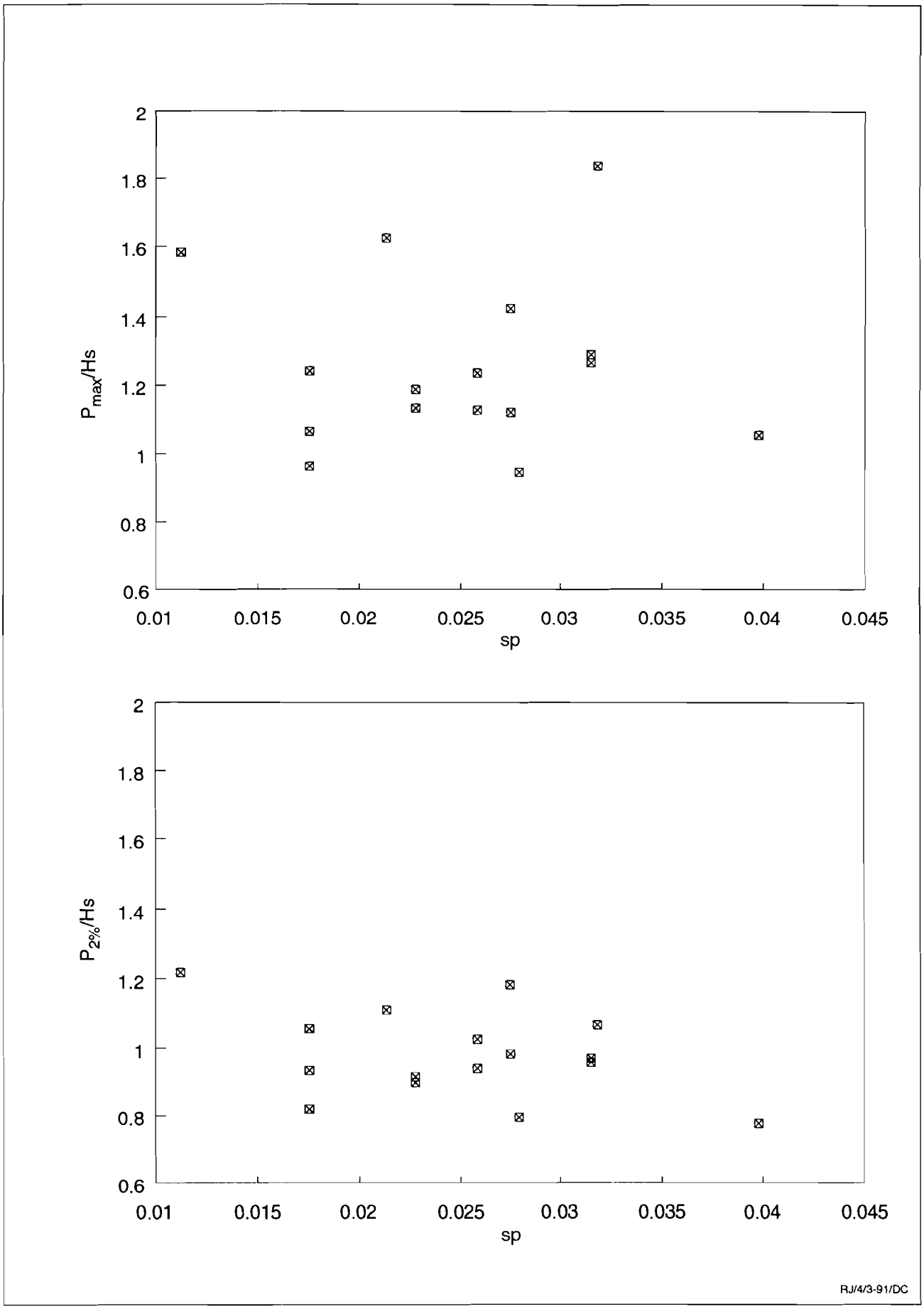

Fig 6.20 Pressure data, upper transducer, free surface, section 4

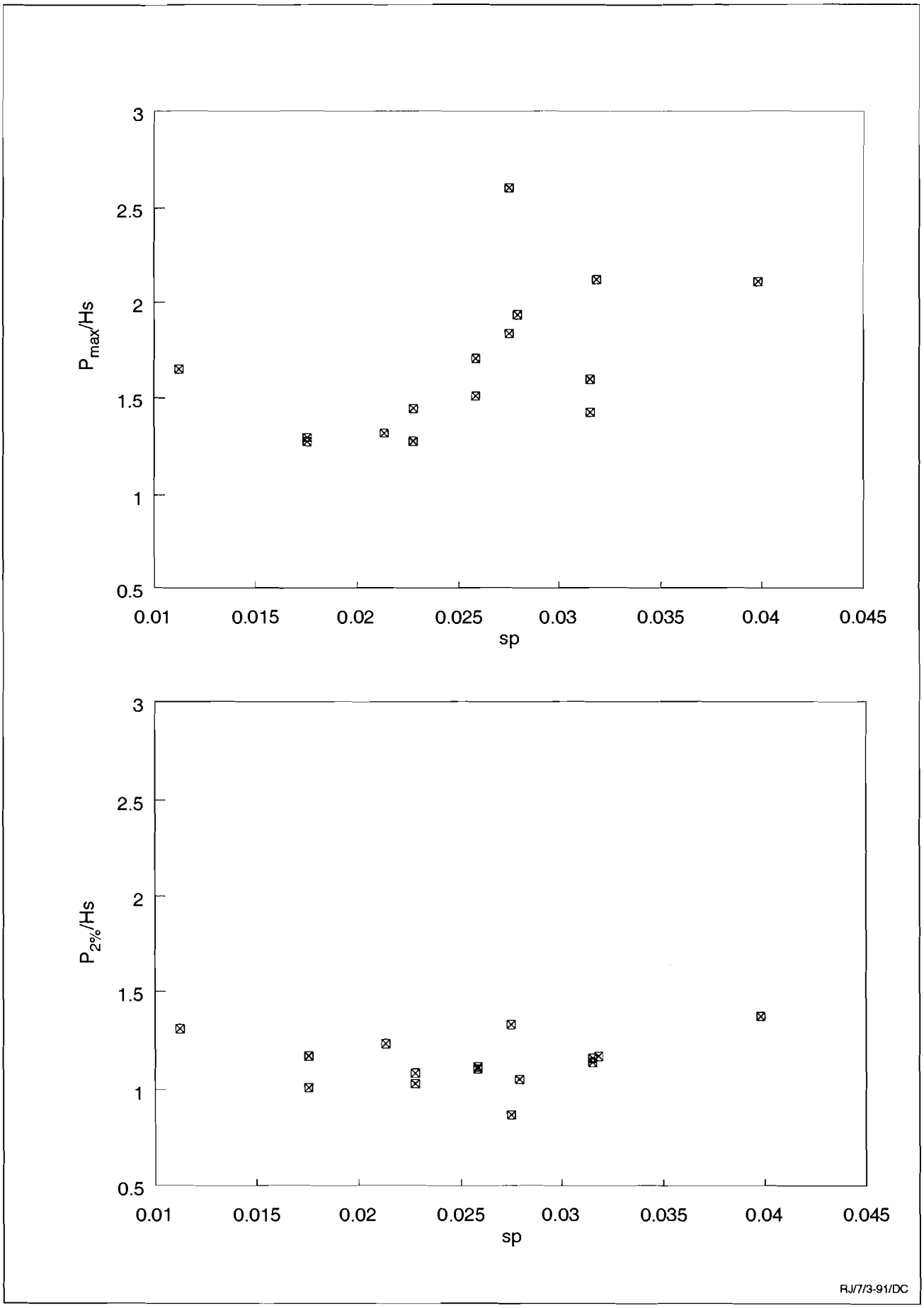

Fig 6.21 Pressure data, middle transducer, free surface, section 4

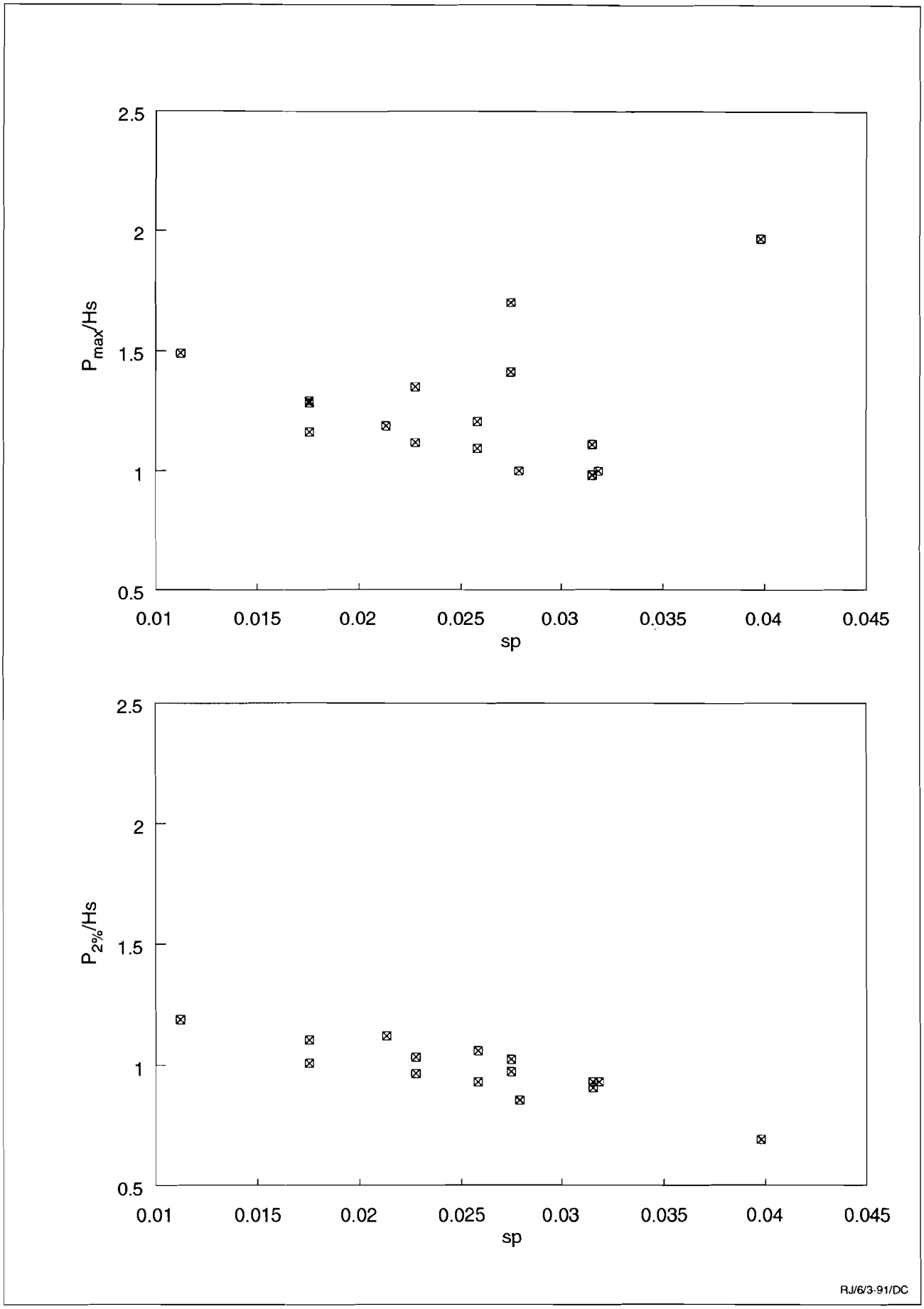

Fig 6.22 Pressure data, lower transducer, free surface, section 4

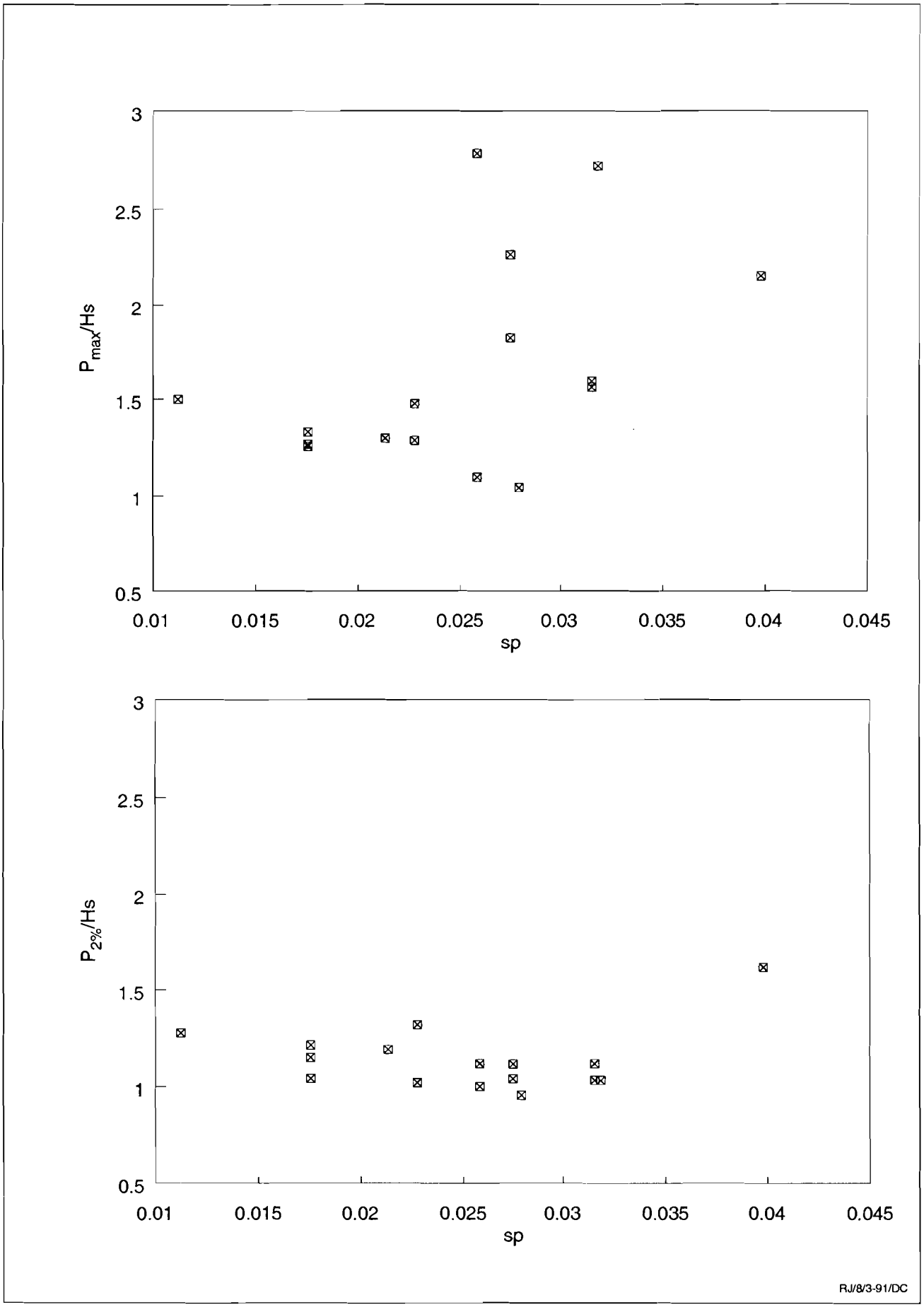

Fig 6.23 Pressure data, upper limb, hypodermic, section 4

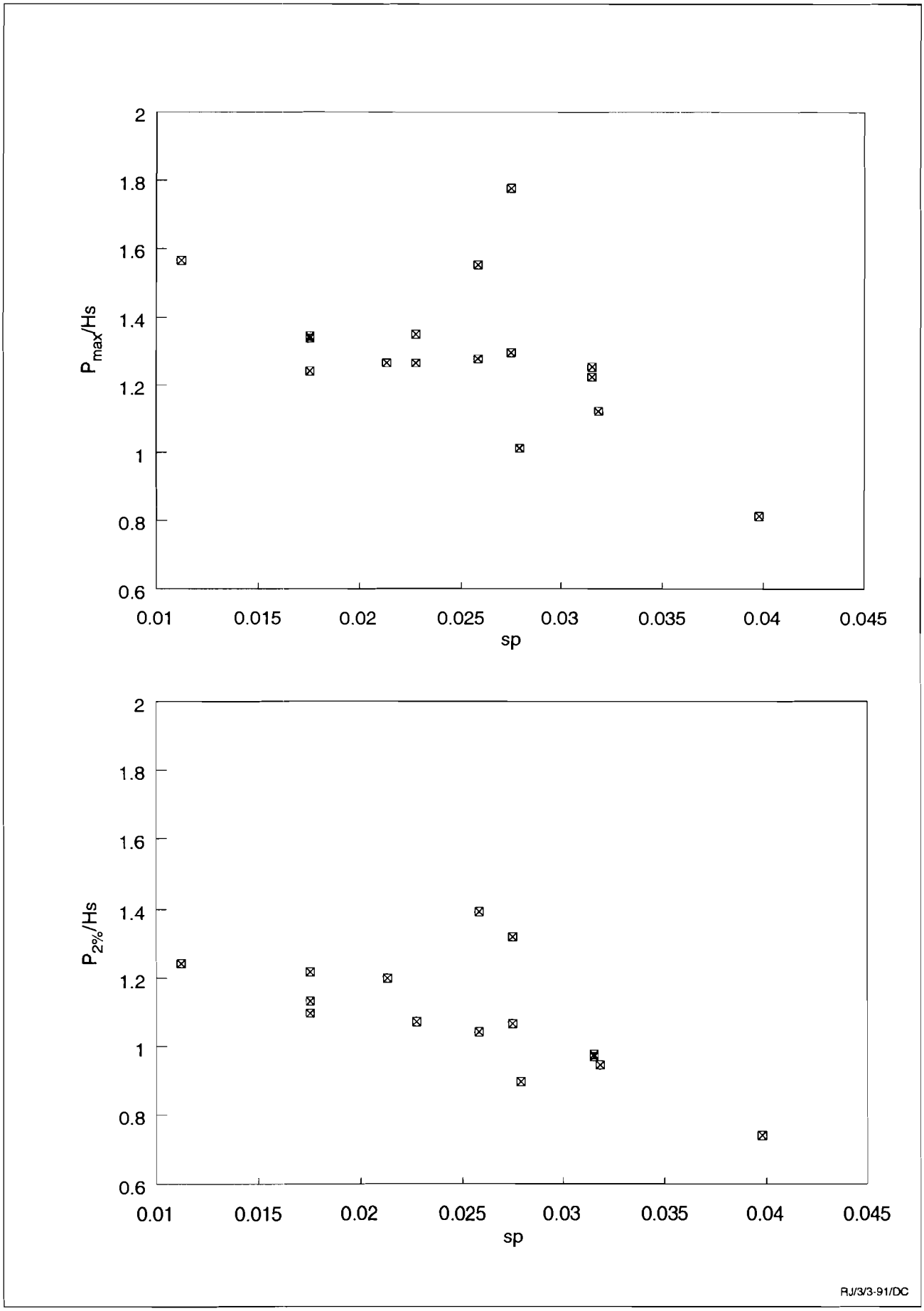

Fig 6.24 Pressure data, side limb, hypodermic, section 4

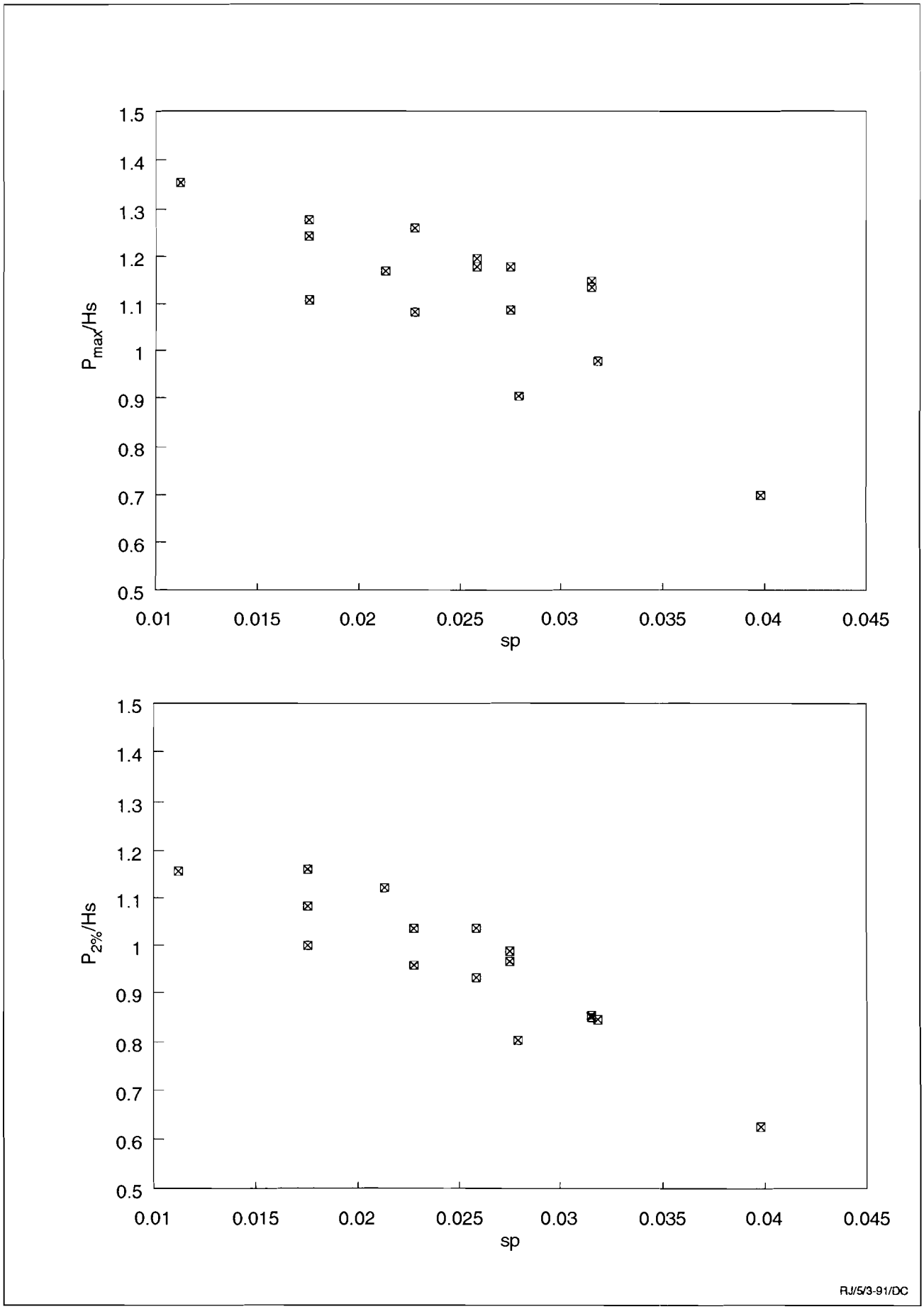

Fig 6.25 Pressure data, lower limb, hypodermic, section 4

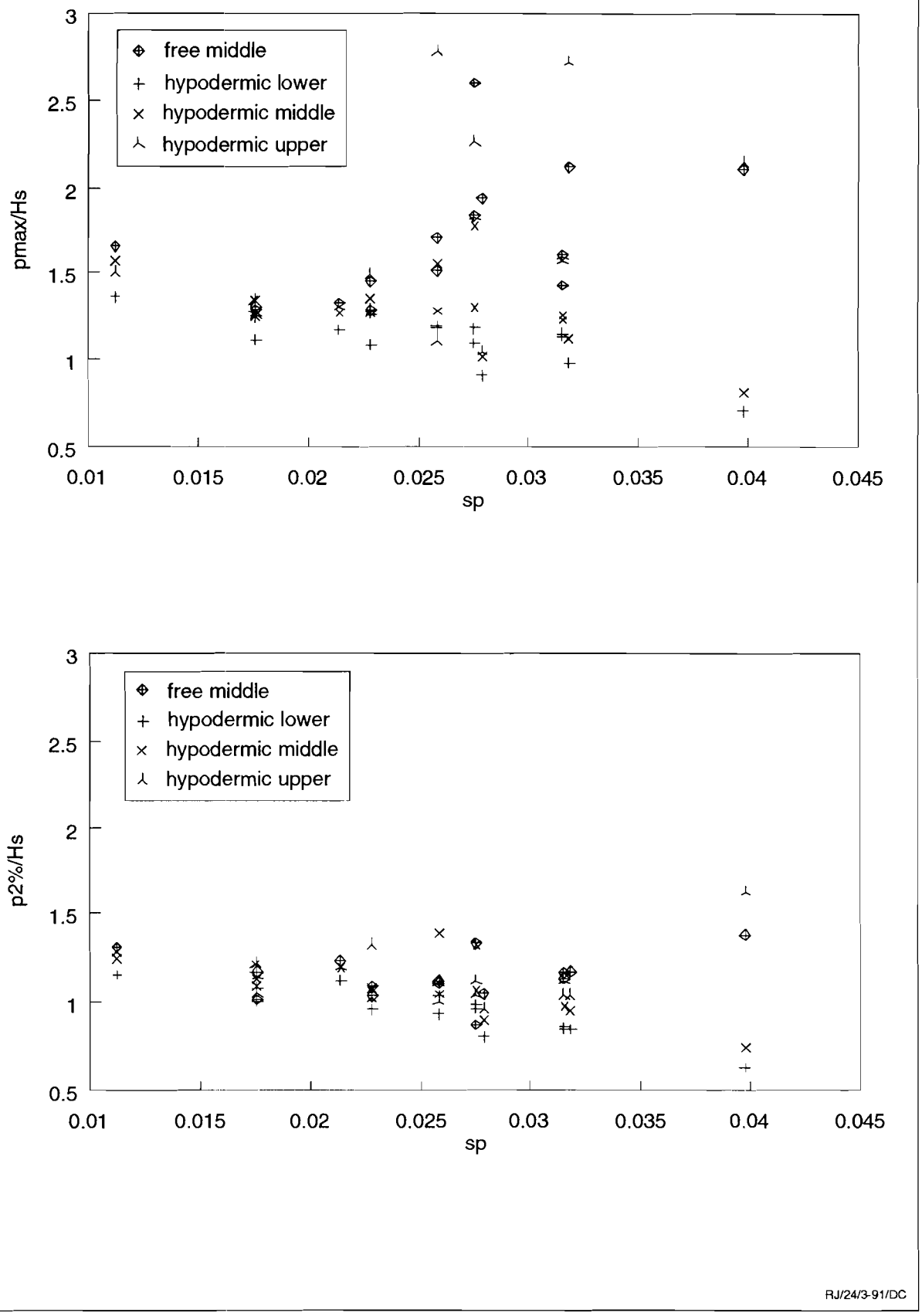

Fig 6.26 Variation in impact pressures, similar elevation, section 4

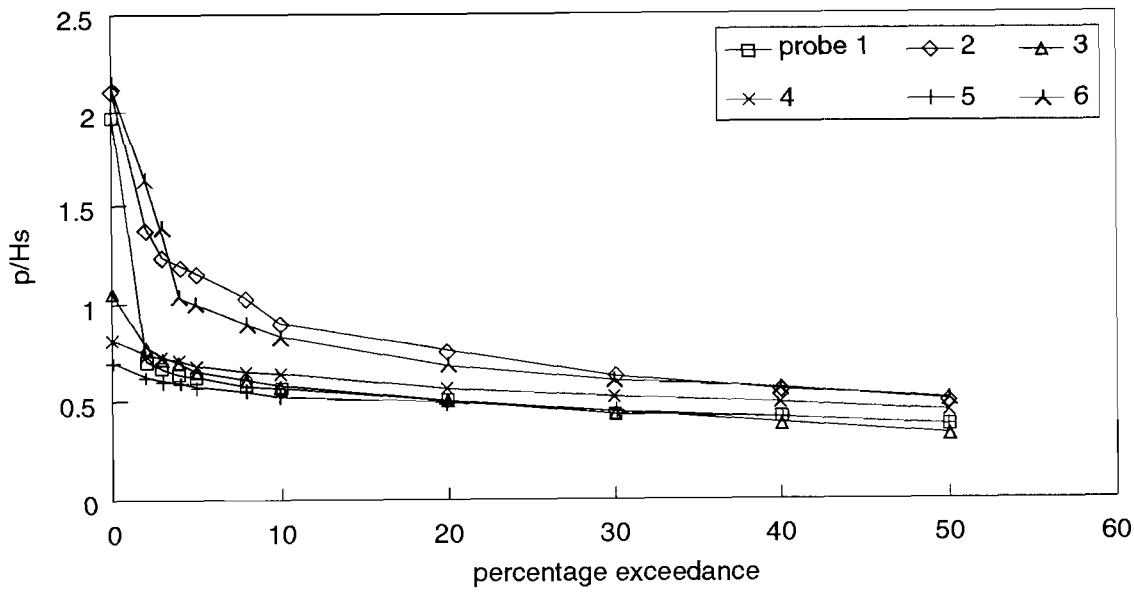

RJ/12/3-91/DC

Fig 6.27 Example of pressure exceedance, section 4

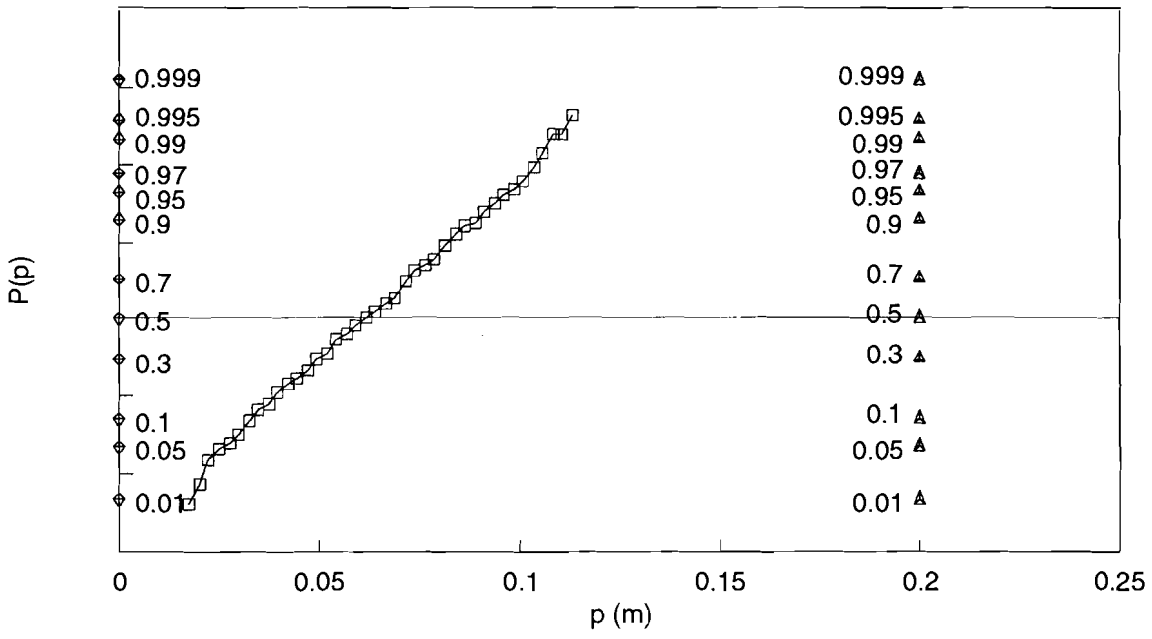

Fig 6.28 Example of Gaussian pressure distribution, section 4

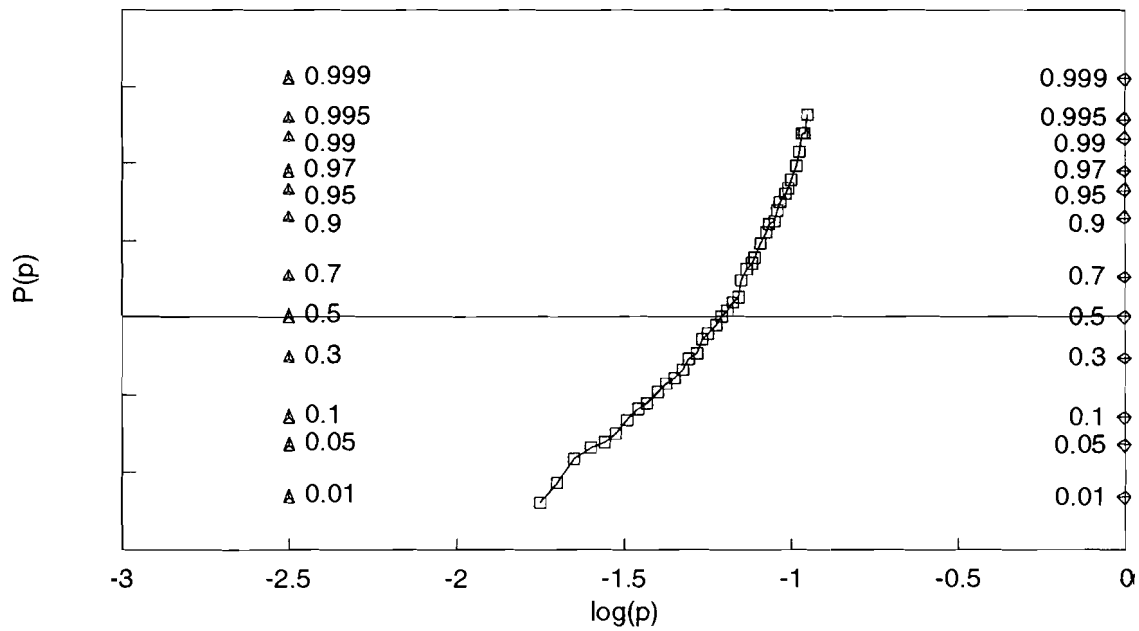

Fig 6.29 Example of log-normal pressure distribution, section 4

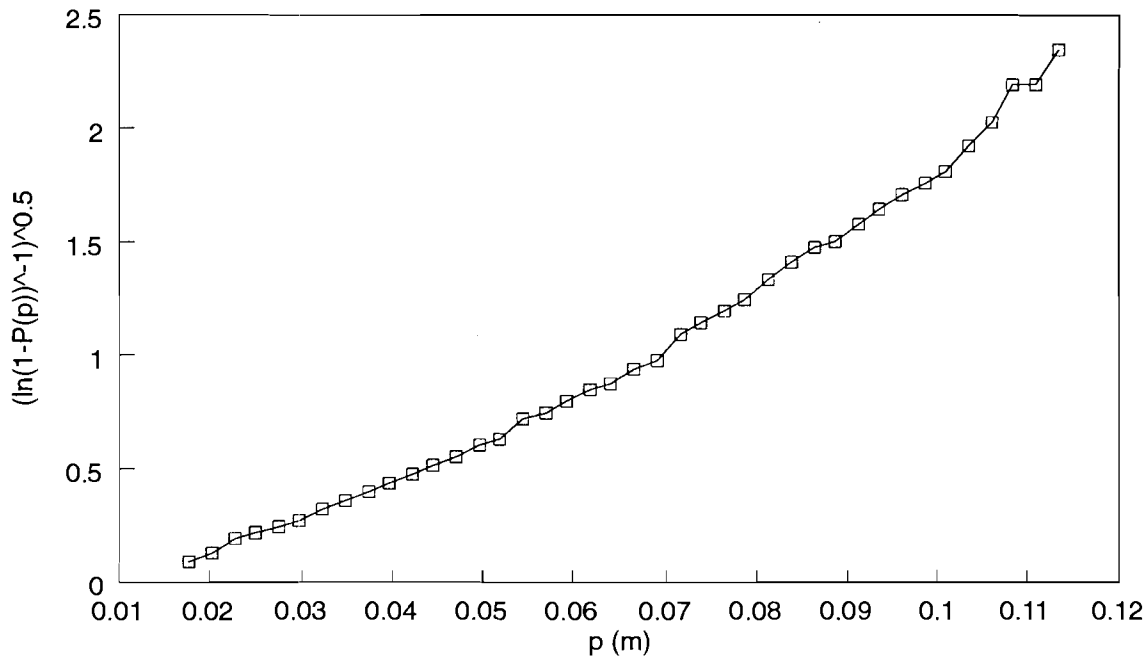

RJ/10/3-91/DC

Fig 6.30 Example of Rayleigh pressure distribution, section 4

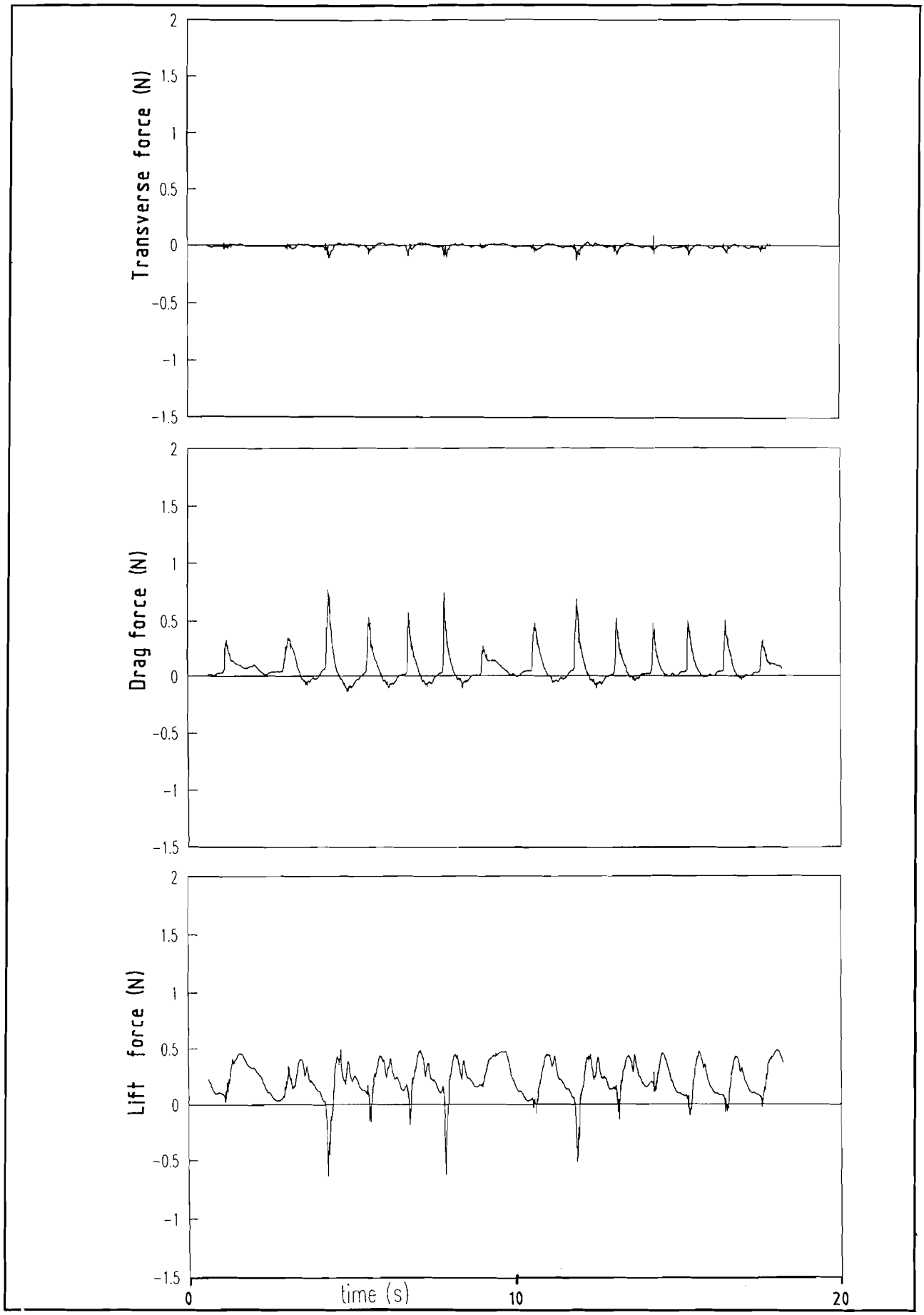

Fig 6.31 Example of force time series, section 4.

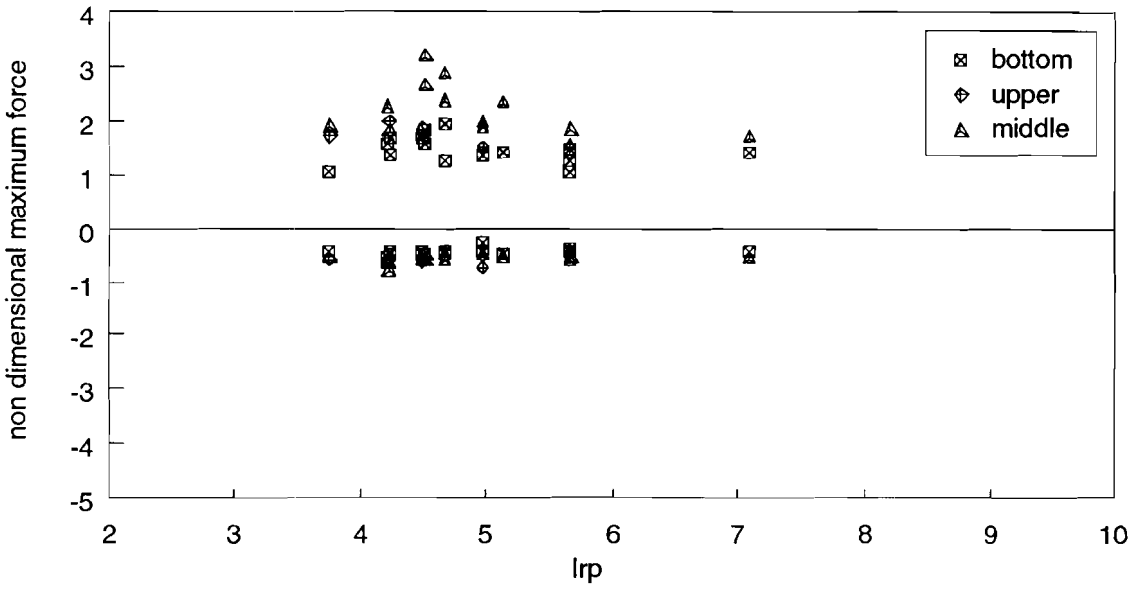

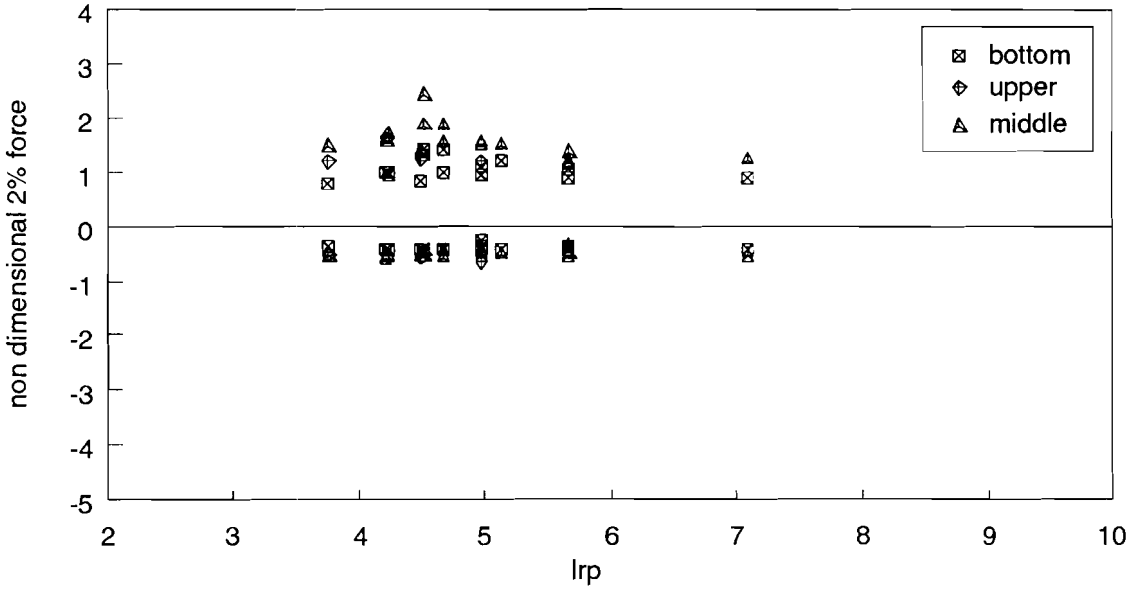

RJ/14/3-91/DC

Fig 6.32 Relative magnitude of non-dimensional drag force, section 4

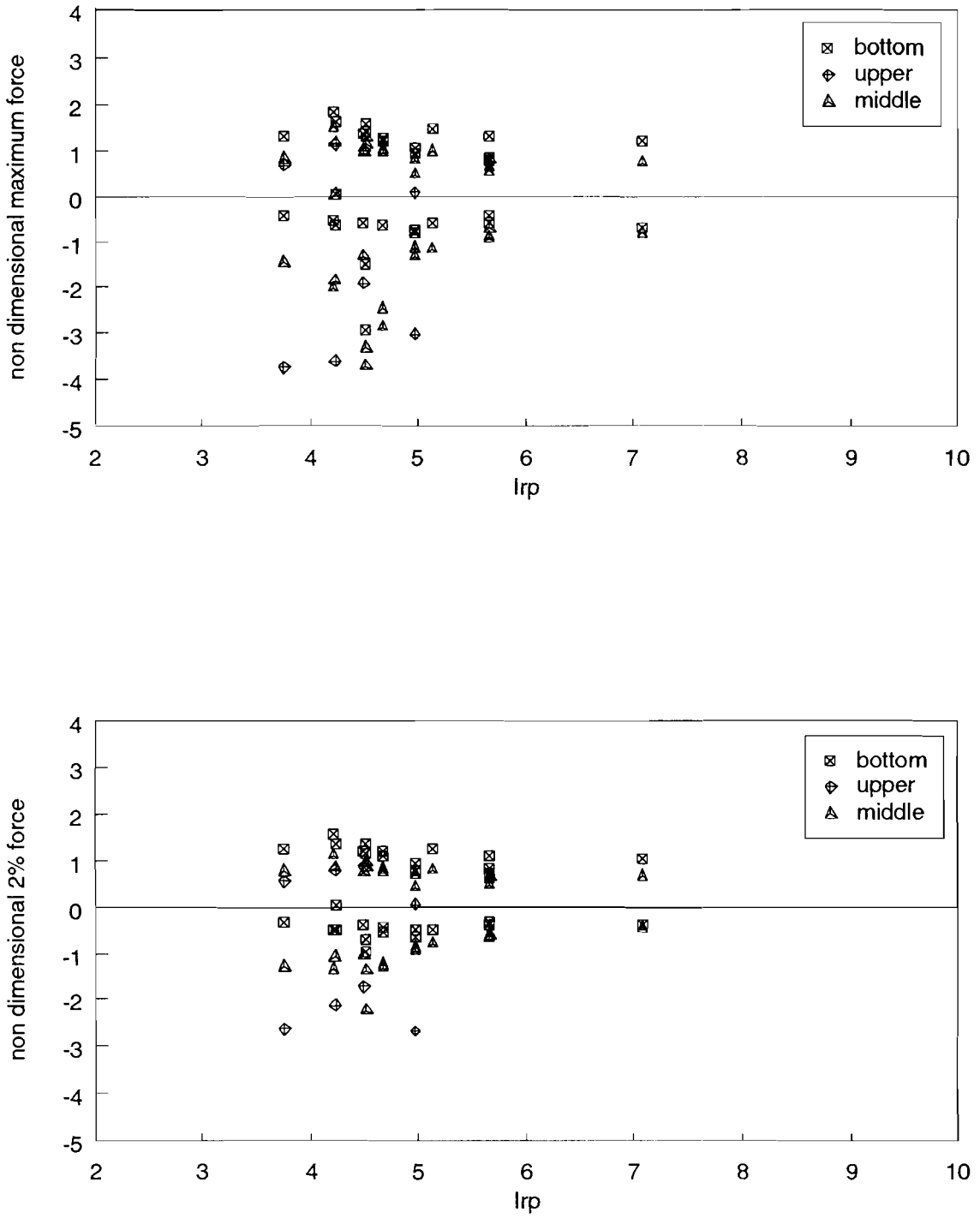

Fig 6.33 Relative magnitude of non-dimensional lift force, section 4

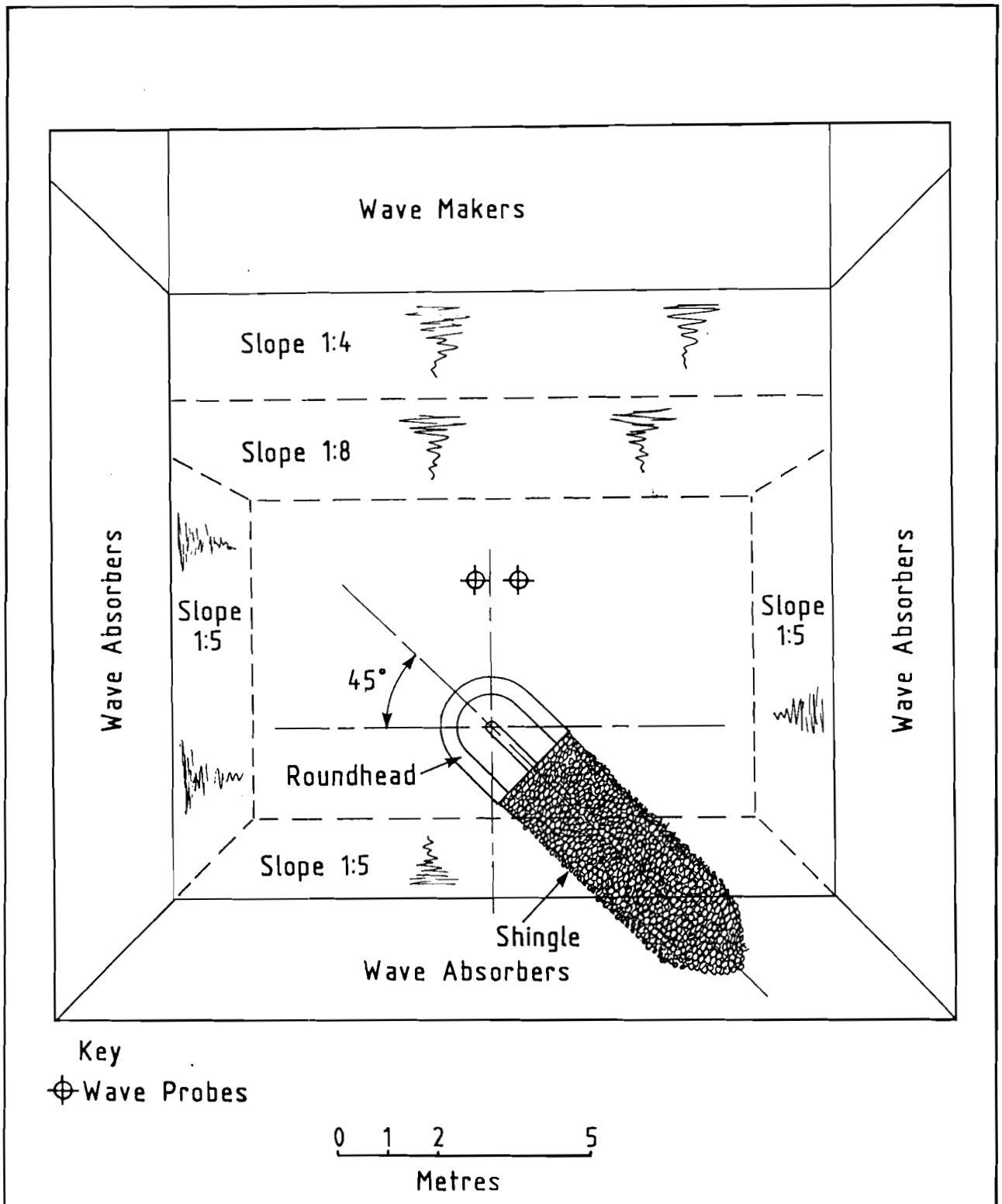

Fig 6.34 Location plan of complex sea basin, showing test section.

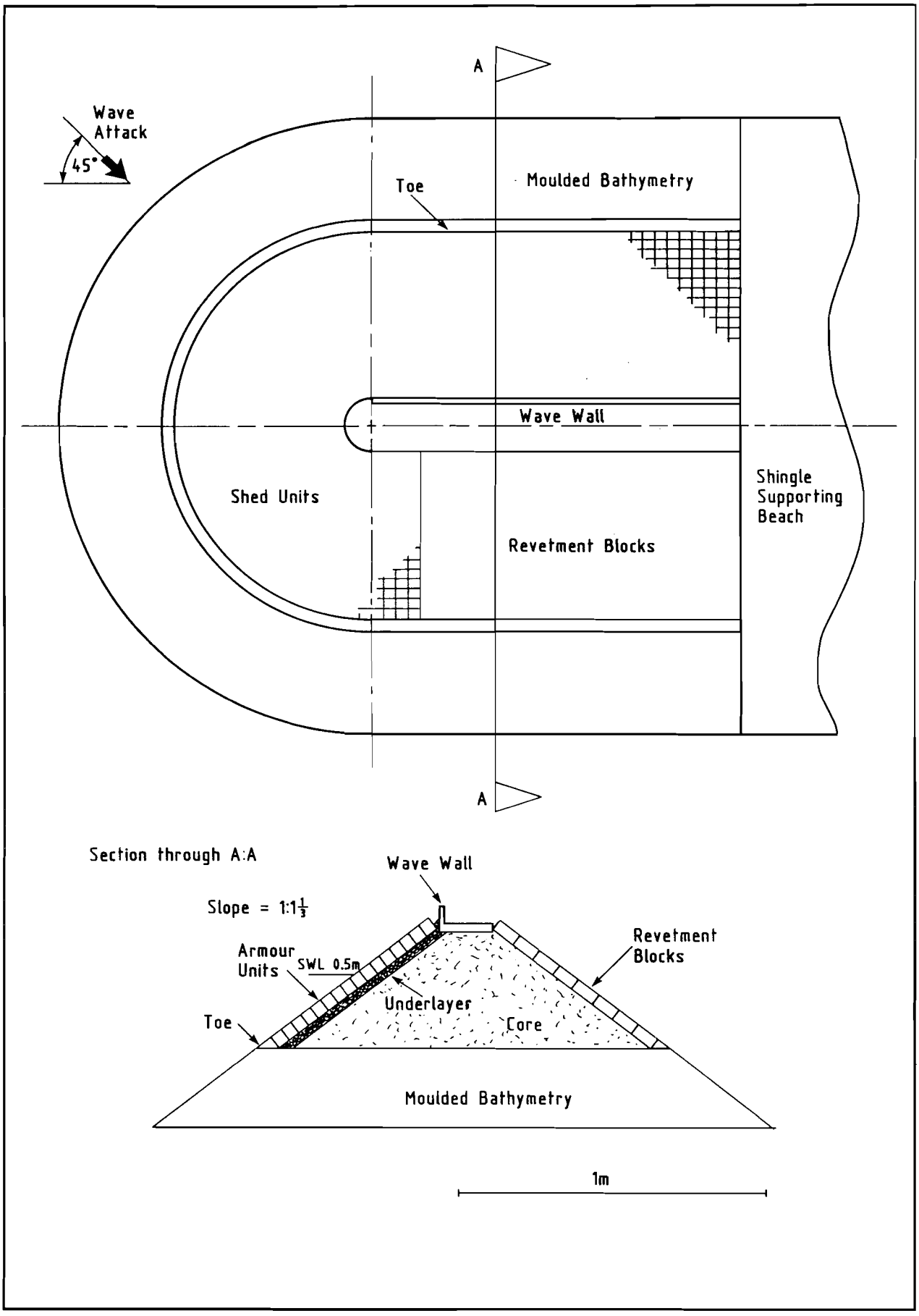

Fig 6.35 Cross-section, test section 5

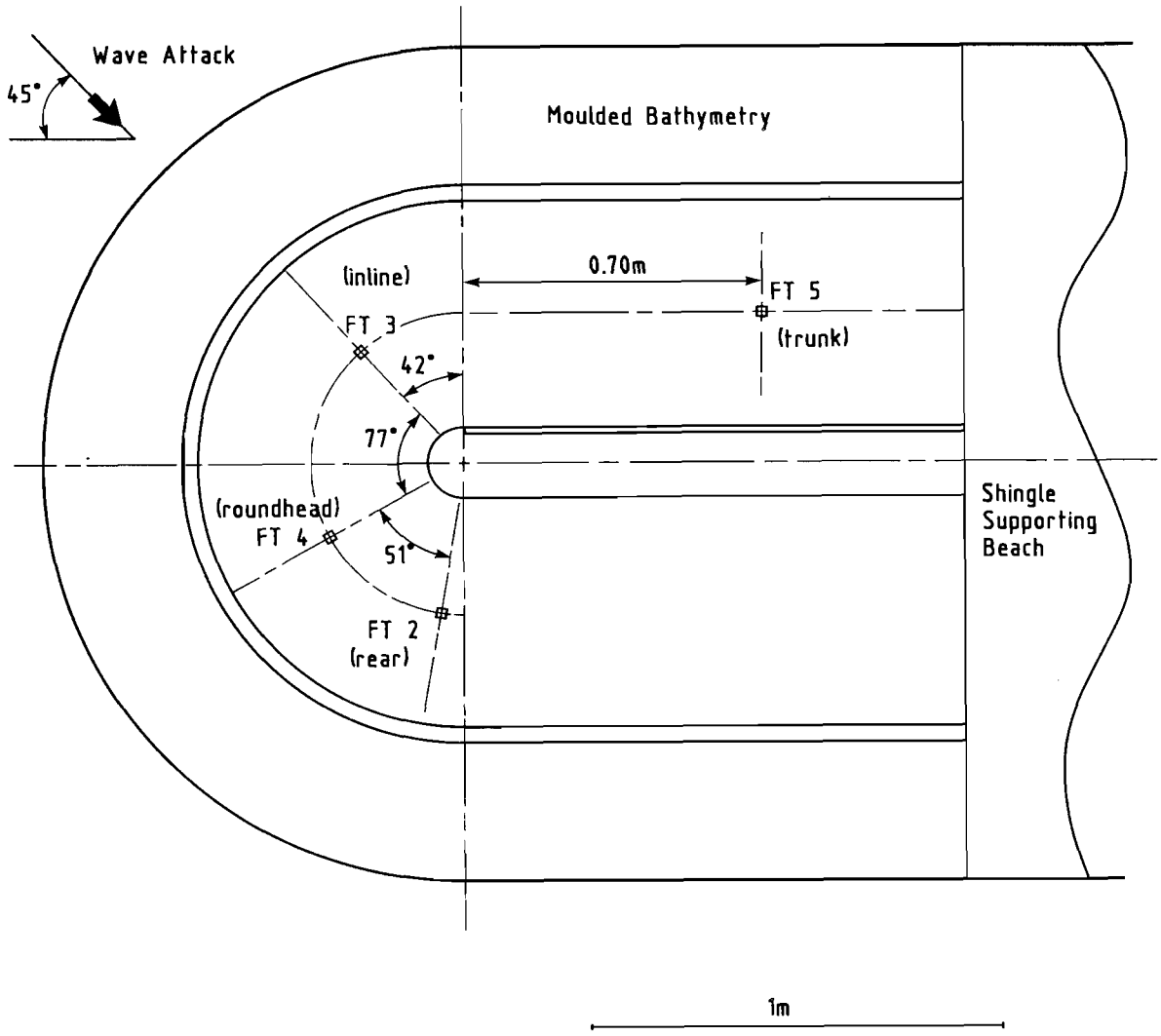

Fig 6.36 Location of force transducers, test section 5.

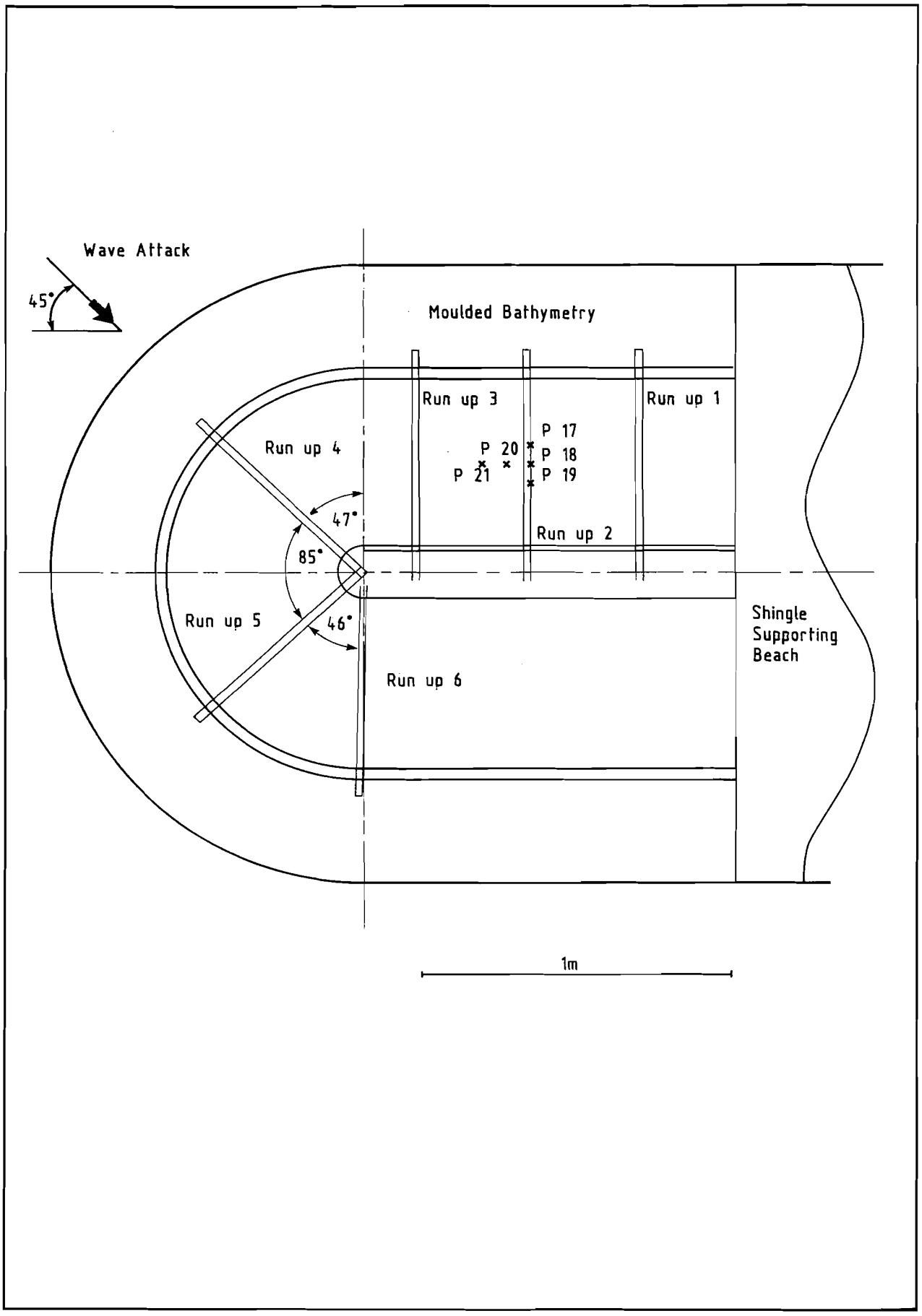

Fig 6.37 Location of pressure transducers and run-up gauges, test section 5.

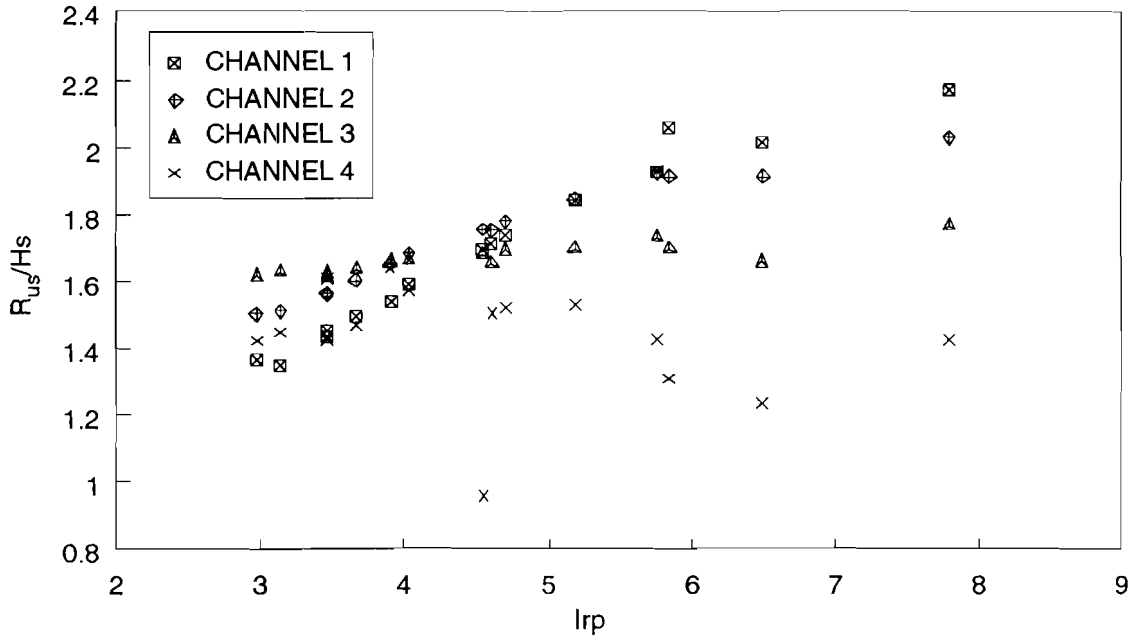

Fig 6.38 Variation in significant relative run-up, test section 5, trunk

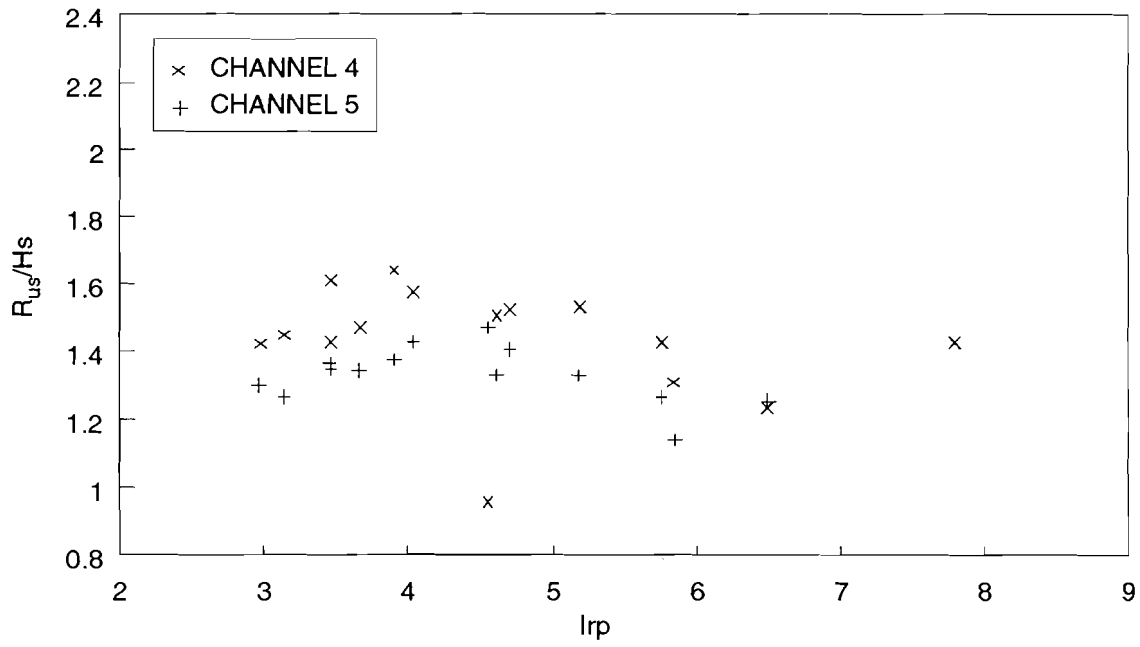

RJ/2/3-91/DC

Fig 6.39 Variation in significant relative run-up, test section 5, roundhead

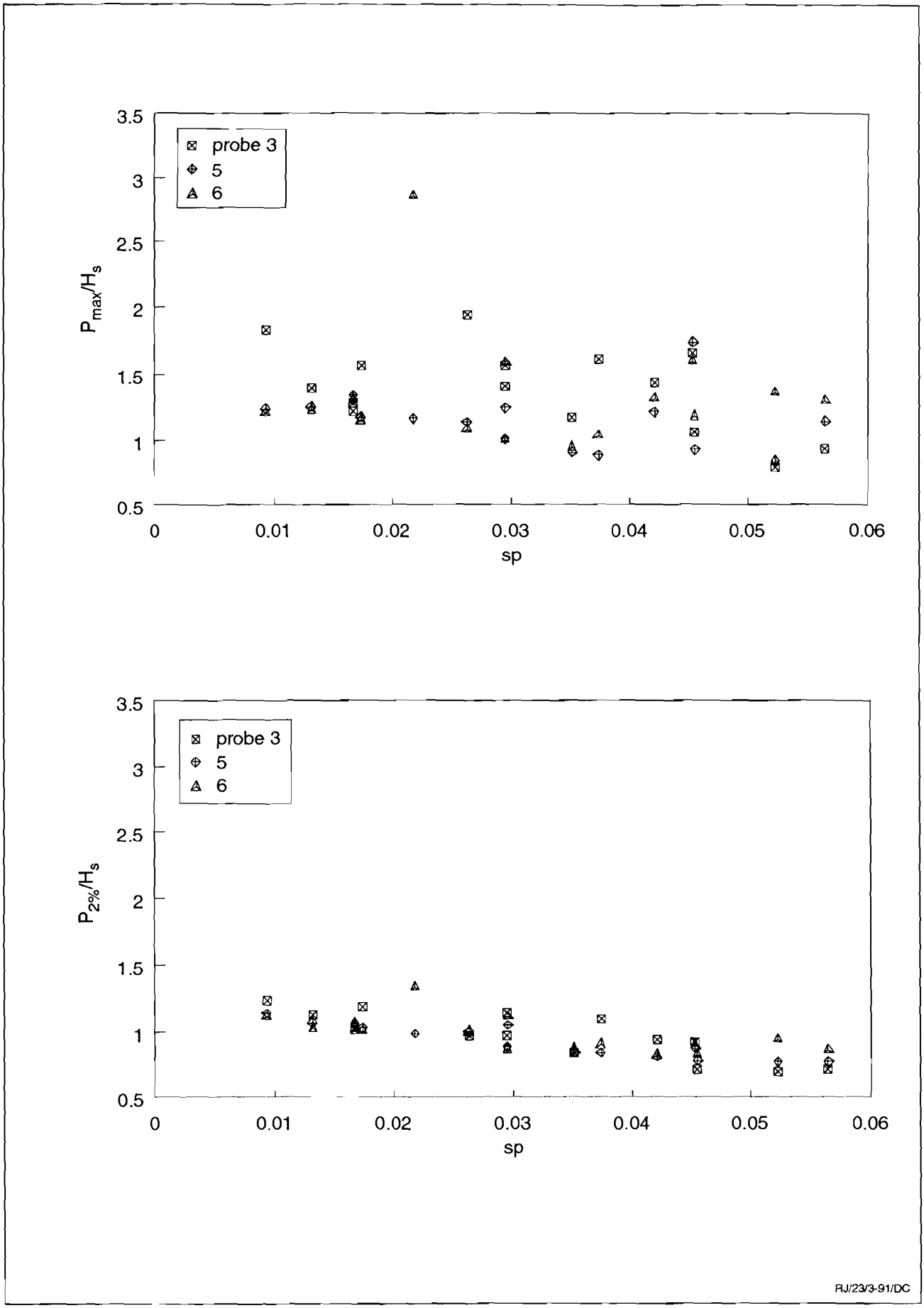

Fig 6.40 Comparison of horizontal pressure transducers, test section 5

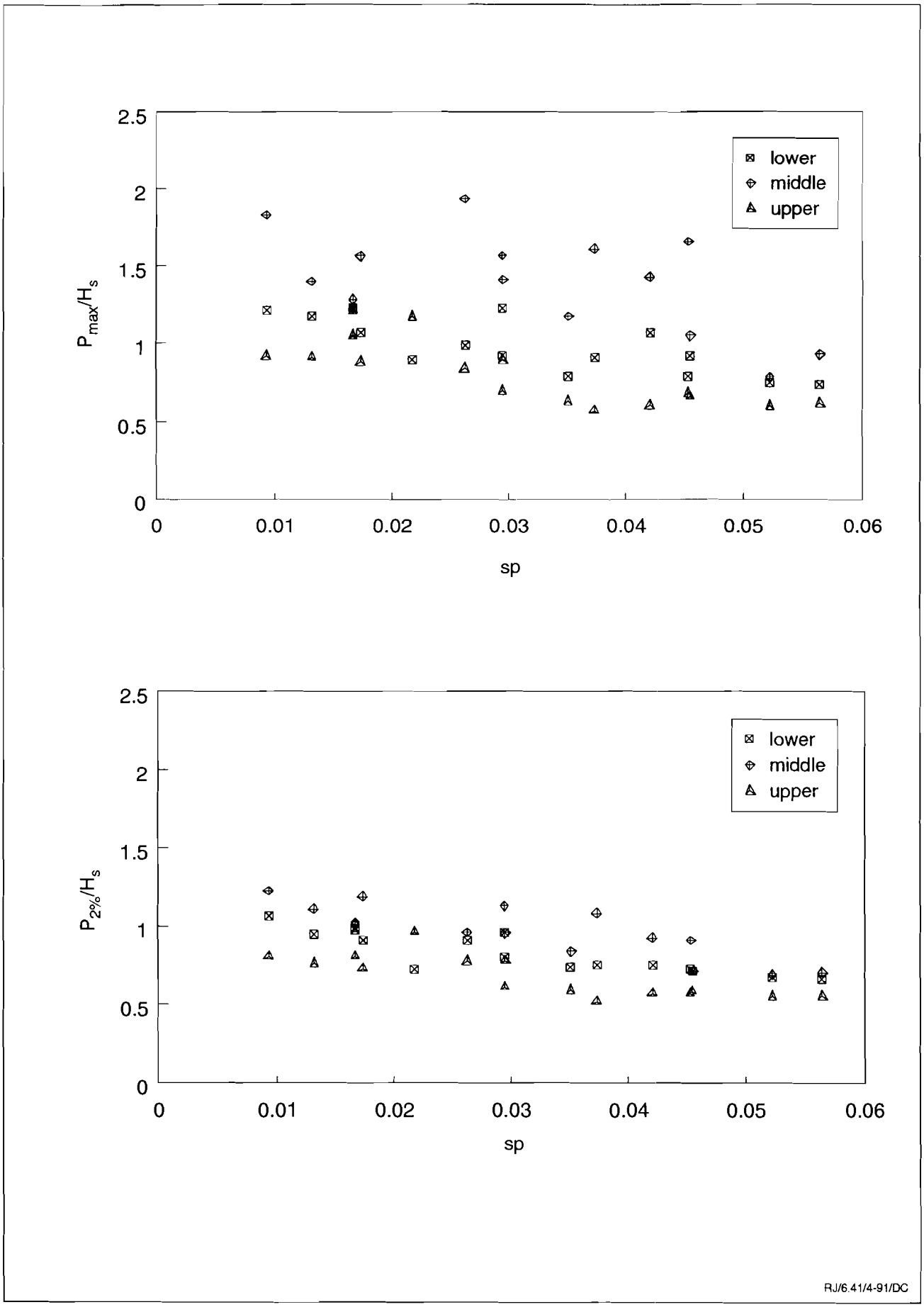

Fig 6.41 Comparison of vertical pressure transducers, test section 5

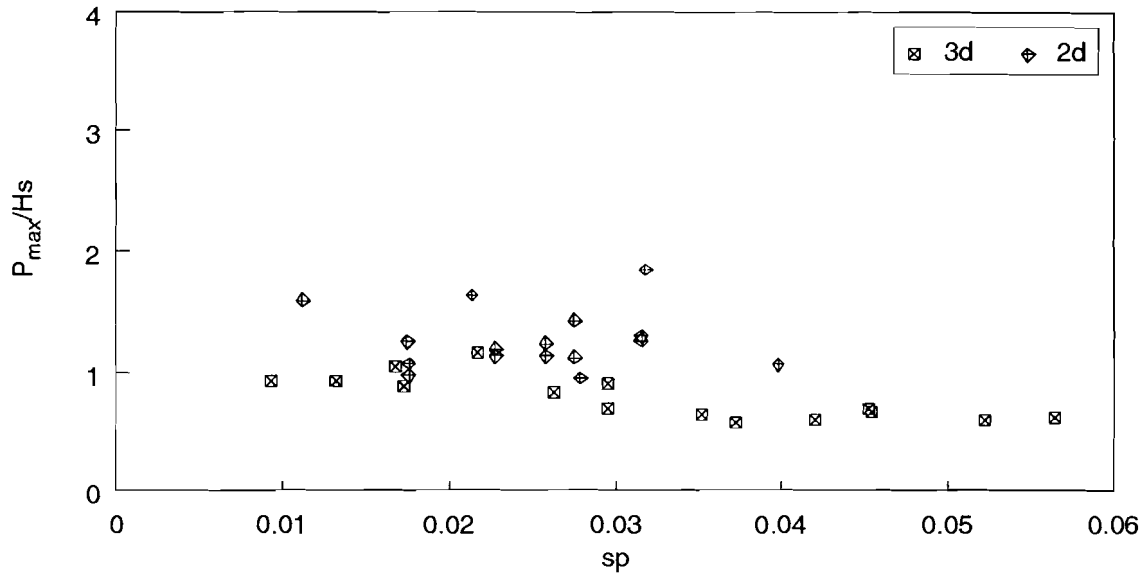

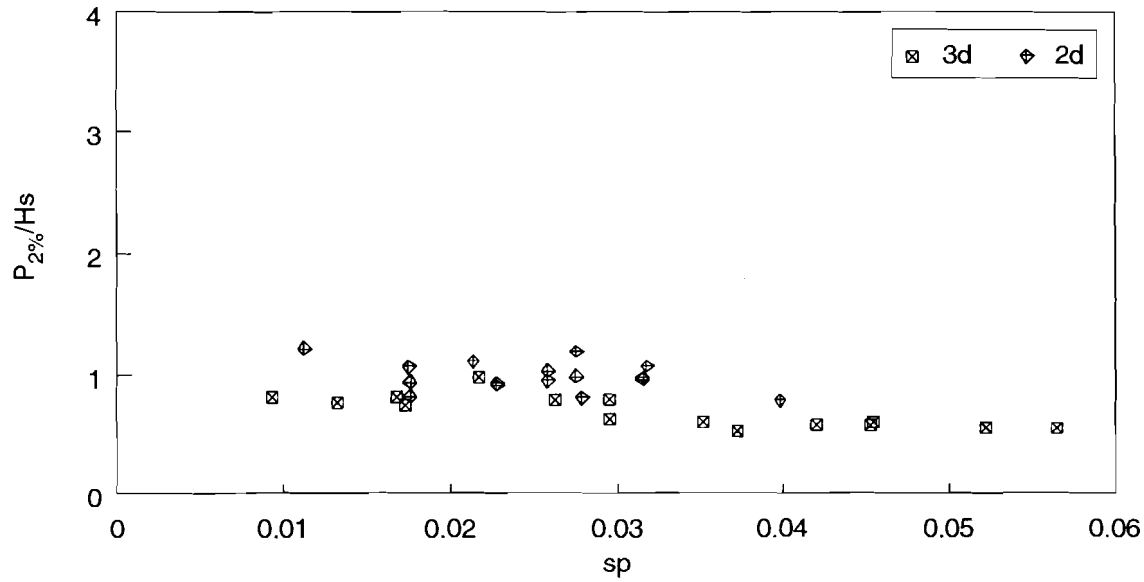

RJ/19/3-91/DC

Fig 6.42 Comparison of upper transducer pressures, test sections 4 and 5

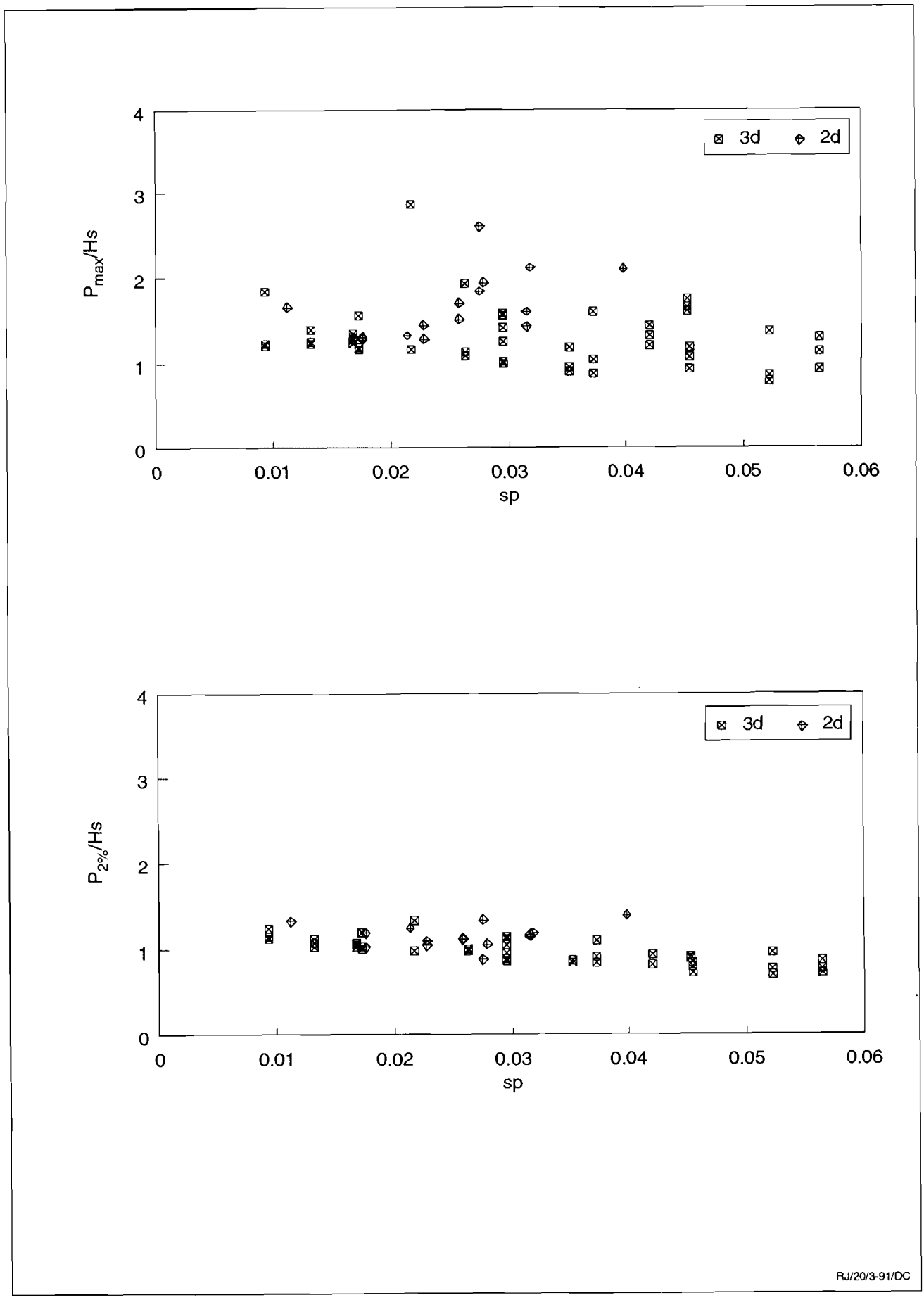

Fig 6.43 Comparison of middle transducer pressures, test sections 4 and 5

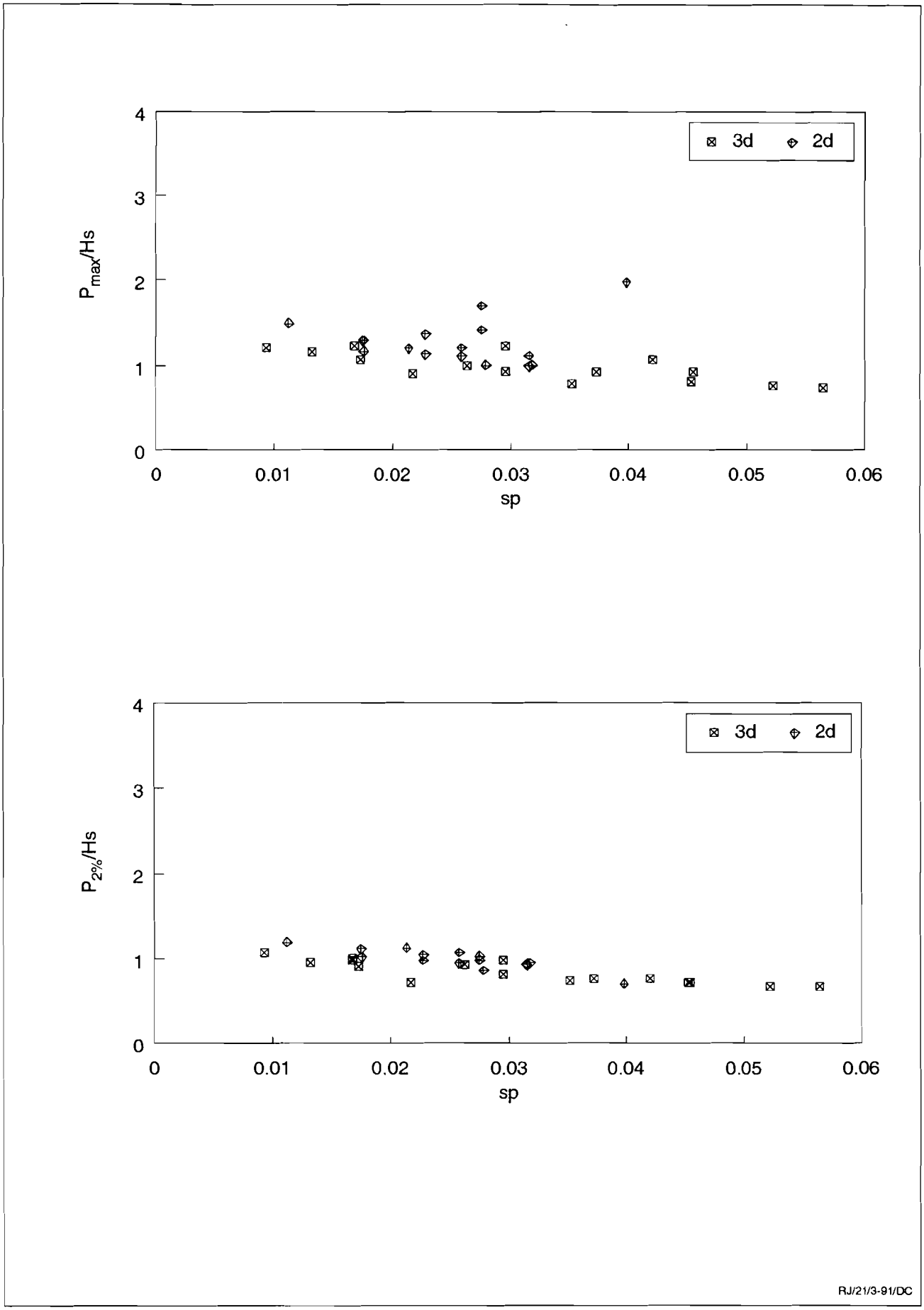

Fig 6.44 Comparison of lower transducer pressures, test sections 4 and 5

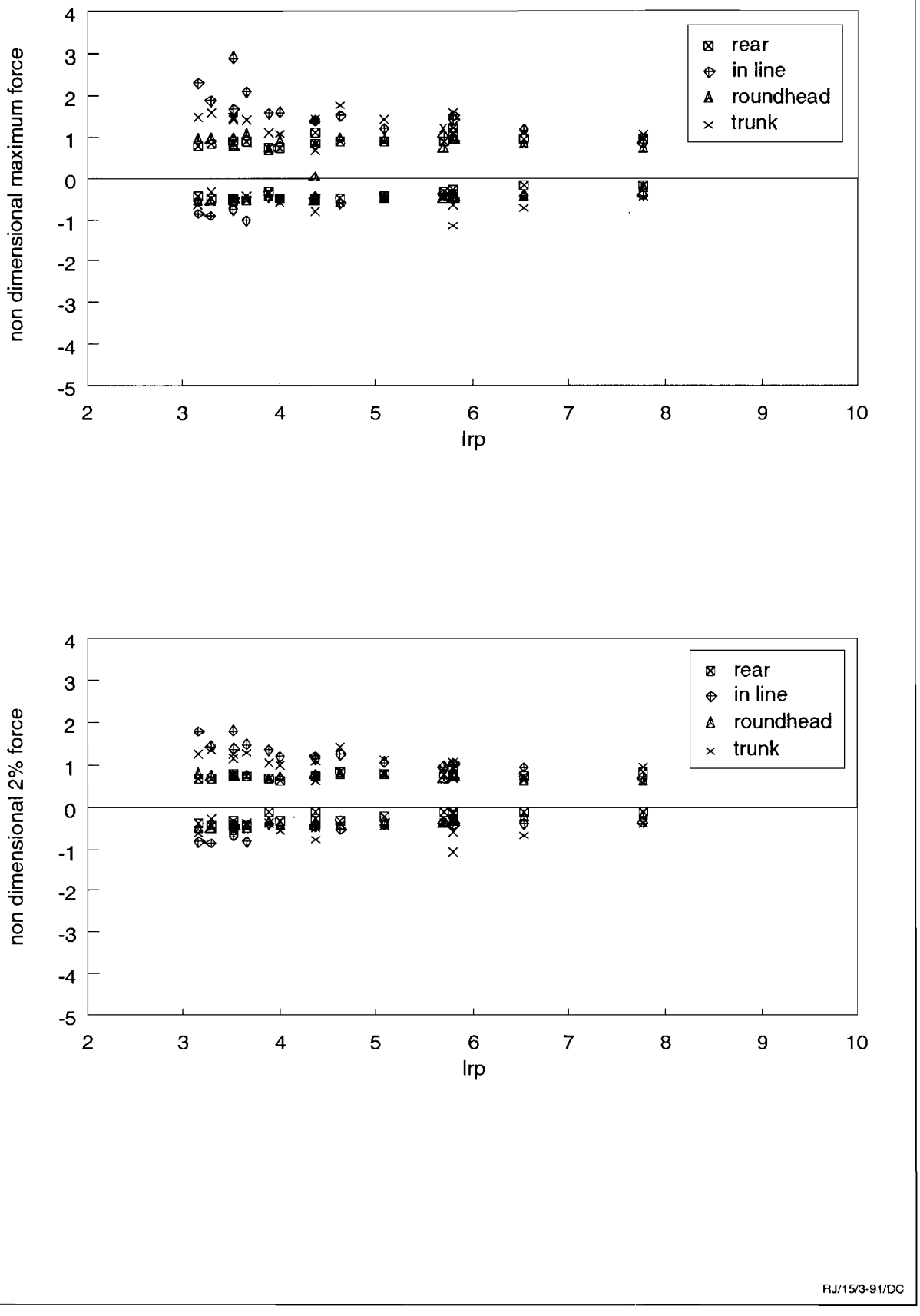

Fig 6.45 Relative magnitude of non-dimensional drag forces, test section 5

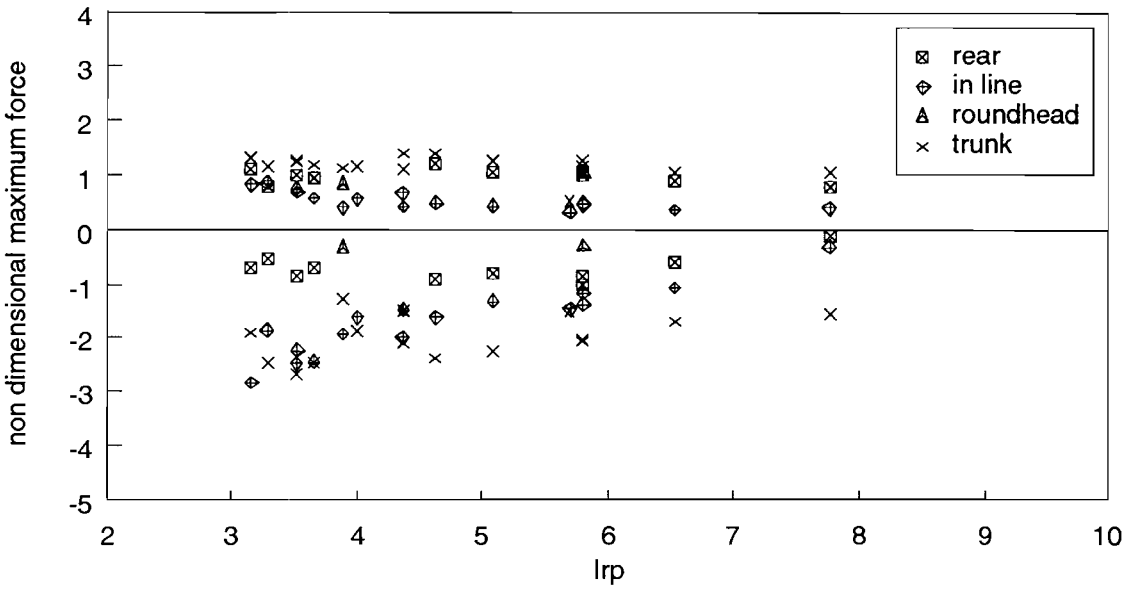

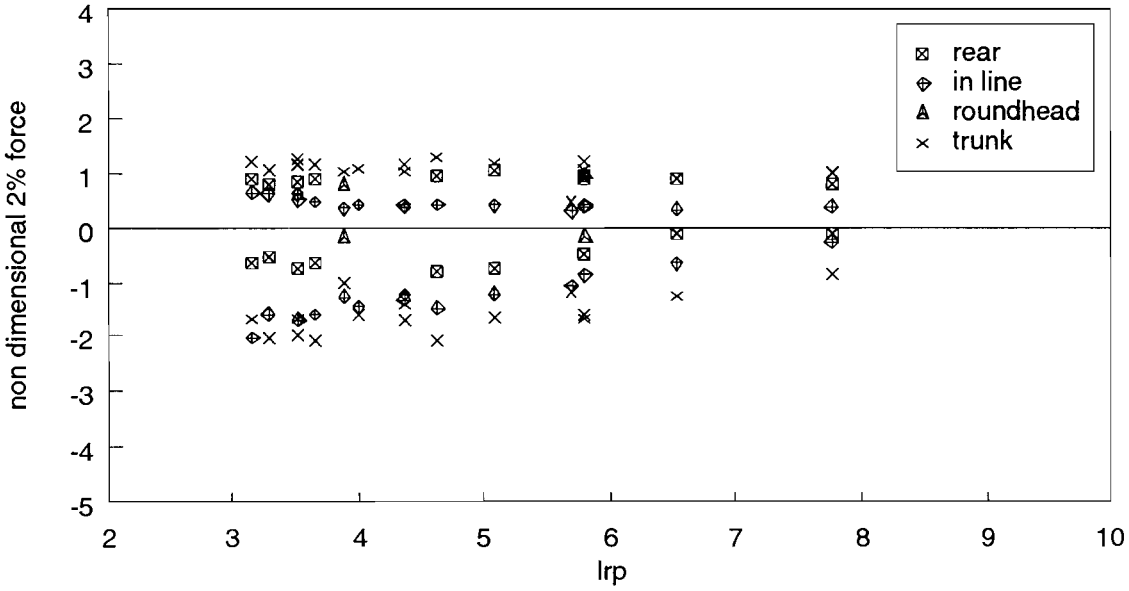

RJ/18/3-91/DC

Fig 6.46 Relative magnitude of non-dimensional lift forces, test section 5

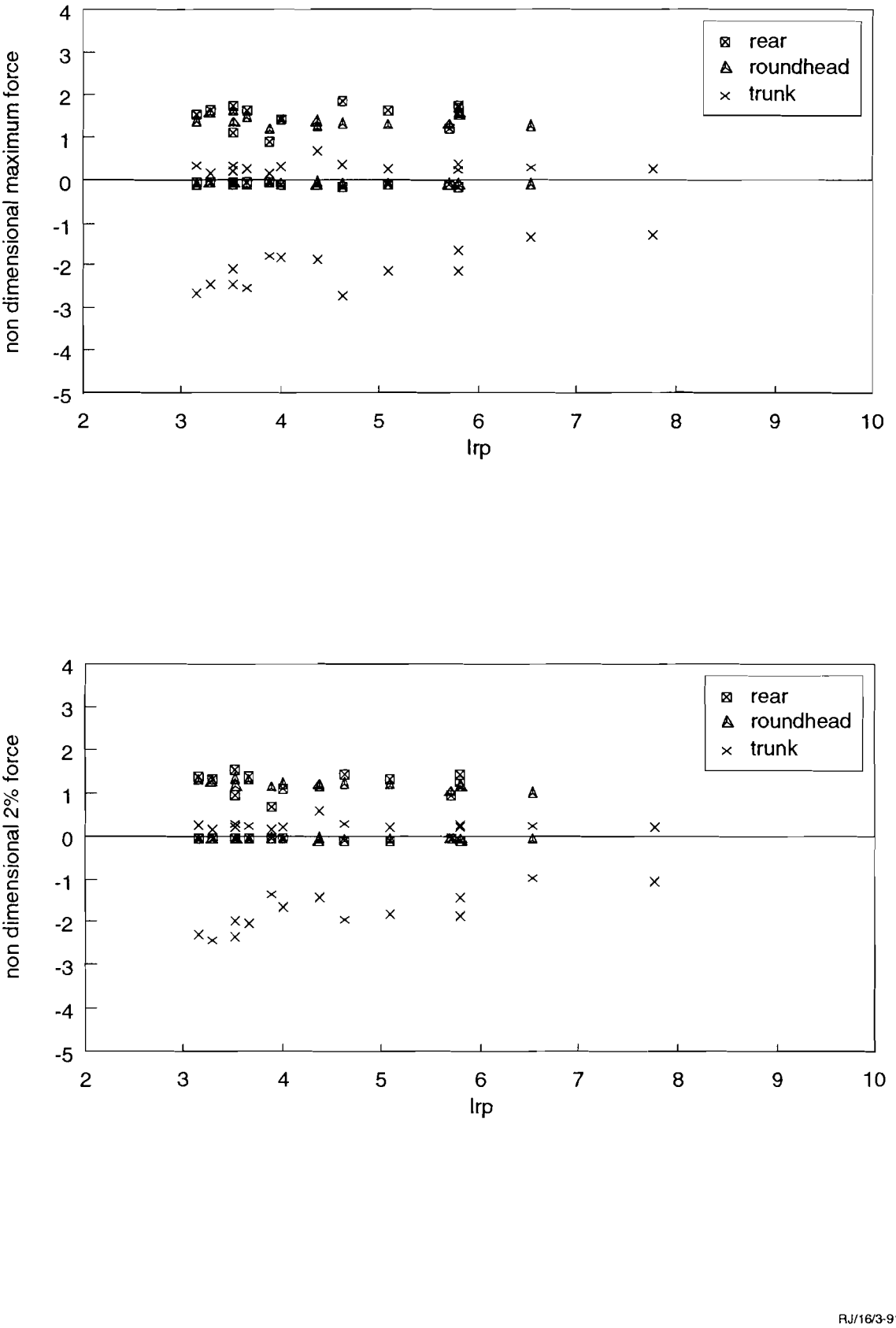

Fig 6.47 Relative magnitude of non-dimensional transverse forces, test section 5

APPENDICES.

APPENDIX 1

Single Layer Armour Research Club - Timetable of main events, June 1986 to April 1991

May 86	Preliminary discussions at Plymouth.
June 86	Exploratory proposal circulated by HR, followed by a series of meetings with potential club members.
Sept 86	Presentation of possible research project made by Allsop at International Conference on Concrete in the Marine Environment, Concrete Society, London.
Oct 86	Initial progress report. Close collaboration established with Bristol and Plymouth. Costs of finite element modelling by practitioner estimated. Funds for initial field trials offered by Shephard Hill, Coode Blizard, HR and Bristol as industrial contributions.
Nov 86	Project statement issued to prospective club members. First research club meeting, at Wallingford. HR agreed to support work at Imperial College 12/86 to 5/87.
Dec 86	Informal meeting at Bristol on numerical modelling of stresses in armour units. Article on proposed project published in Civil Engineering, Nov/Dec edition. Initial discussions with Thompson at Sheffield on numerical model of wave action on slopes.
Jan 87	Field studies working party meeting, at Bristol, to discuss initial trials.
Feb 87	Trial field deployment on La Collette, Jersey
June 87	Research club review meeting (2nd), at Wallingford. Presentation of initial field trial experience and plans for future work.
Aug 87	Second field studies working party meeting, at Plymouth, to discuss winter 87/88 deployment.
Sept 87	Research club meeting (3rd), at Wallingford.
Oct 87	Meeting of industrial members to outline detailed objectives, in London.

Dec 87	Research club meeting (4th), at Wallingford.
Jan 88	Field instrument deployment on La Collette, Jersey.
April 88	Research club meeting (5th), at Wallingford. Publication of article by Clifford on Research Club in Civil Engineering Research Newsletter.
May 88	Presentation by Dunster, Wilkinson, & Allsop to ICE Breakwaters Conference, Eastbourne.
June 88	Presentation by Smallman & Allsop, and by Thompson, on numerical models of wave action on slopes to 21st ICCE at Malaga.
June 88	Fieldwork planning meeting at Bristol.
July 88	Research club meeting (6th), at Wallingford. HR reports IT 311 and IT 318 issued.
Oct 88	Research club meeting (7th), at Wallingford.
Nov 88	Handling and transport stress trials, Shephard Hill and Bristol, Hedsor. Wave flume tests at HR on Cob armoured section.
Jan 89	Research club meeting (8th), at Bristol. M Whastling appointed as analyst. Bristol report UBCE/C/88/6 issued.
April 89	Research club meeting (9th), at Wallingford. HR reports IT 327 and IT 337 issued. J Griffiths appointed as Research Assistant at Plymouth.
July 89	Presentations by Herbert and by Whastling to technical meeting of Research Club in London. Bristol report UBCE/C/89/5 issued.
Sept 89	Research club meeting (10th), at Wallingford. Bristol report UBCE/C/89/5 revised. Third field deployment on La Collette breakwater.
Jan 90	Research club meeting (11th) at Plymouth cancelled due to storm damage. HR report IT 344 issued.
March 90	Research club meeting (11th), at Wallingford. Bristol report UBCE/C/90/8 issued.

Aug 90	Bristol report UBCE/C/90/11 issued.
Sept 90	Research club meeting (11th), at Bristol.
Oct 90	Field equipment recovered from third deployment at Jersey.
Dec 90	Research club meeting (12th), at Wallingford.
Feb 91	Wave basin testing of Shed Armoured roundhead and trunk section at Wallingford. HR report IT 352 on WENDIS issued. Industrial members meeting at Wallingford.
March 91	Presentations by Herbert, Toner, and Bird, at Symposium on developments in coastal engineering at Bristol. Research club meeting (13th), at Wallingford.

Appendix 2

Bibliography of papers and reports

Coode & Partners "Artificial armouring of marine structures" Dock & Harbour Authority, Vol 51, NO 601, November 1970.

Whillock AF "Note on test of Cob blocks as modified by PW Webb" Report EX 622, Hydraulics Research, Wallingford, April 1973, (Restricted).

Whillock AF "High Island water supply, Hong Kong; model tests of a COB block wave protection cover for the inner face of the main dam" Report EX 632, Hydraulics Research, Wallingford, August 1973, (Restricted).

Wilkinson AR "St Helier" Consulting Engineer, Vol 42, No 10, October 1978.

Wilkinson AR & Allsop NWH "Hollow block breakwater armour units" Proc conf Coastal Structures '83, ASCE, Arlington, Virginia, March 1983.

Allsop NWH "The SHED breakwater armour unit, model tests in random waves" Report EX 1124, Hydraulics Research, Wallingford, April 1983.

Shuttler RM "Revetment at Fort Jalali, Oman: a laboratory sea wall study" Report EX 1276, Hydraulics Research, Wallingford, February 1985, (Restricted).

Davis JP, Waldron P, Edwards DJ & Stephens RV "Acquisition of data from single layer armour units in breakwaters using radio telemetry" Proc IABSE Colloquium on Monitoring of Large Structures, Bergamo, 1987.

Allsop NWH "Concrete armour units for rubble mound breakwaters and sea walls; recent progress" Report SR 100, Hydraulics Research, Wallingford, March 1988.

Clifford JE "A research club project on breakwaters" Civil Engineering Research Newsletter, DOE and SERC, April 1988.

Hettiarachchi SSL & Holmes PH "Performance of single layer hollow block armour units" Proc conf Breakwaters '88, ICE, Eastbourne, May 1988.

Dunster JA, Wilkinson AR & Allsop NWH "Single layer armour units" Proc conf Breakwaters '88, ICE, Eastbourne, May 1988.

Allsop NWH, Smallman JV & Stephens RV "Development and application of a mathematical model of wave action on steep slopes" Proc 21st ICCE, Malaga, June 1988 (Also available as Hydraulics Research published paper no. 18).

Stephens RV & Davis JP "Preliminary field work and instrument trials" Report IT311, Hydraulics Research, Wallingford, March 1987, revised July 1988, (Restricted).

Beardsley A, Smallman JV & Stephens RV "Development of a mathematical model of wave action on slopes - recent progress" Report IT318, Hydraulics Research, Wallingford, July 1988, (Restricted).

Toner W & Waldron P "Static testing of two SHED units" Report UBCE/C/88/6, University of Bristol, December 1988, (Restricted).

Stephens RV "Field work on La Collette breakwater, Jersey, January to May 1988" Report IT327, Hydraulics Research, Wallingford, March 1989, (Restricted).

Green APE "Further development of a mathematical model of wave action on slopes" Report IT337, Hydraulics Research, Wallingford, March 1989, (Restricted).

Wastling MA "The effect of self weight loads on SHED and COB units" Report UBCE/C/89/5, University of Bristol, August 1989, (Restricted).

Hewson PJ & Griffiths J "Measurement of air in waves" in proceedings Workshop on wave impacts on coastal structures (Ed NWH Allsop), Hydraulics Research, Wallingford, November 1989.

Wastling MA "The effect of wave forces on individual limbs of single layer armour units" Report UBCE/C/90/8, University of Bristol, March 1990, (Restricted).

Wastling MA "Thermal stress analysis of SHED breakwater armour units" Report UBCE/C/90/11, University of Bristol, August 1990, (Restricted).

Bradshaw AJ & Hill TJF "An investigation into the wave action on single layer breakwater armour units" Internal report submitted in support of BEng degree, University of Bristol, June 1990, (Restricted).

Herbert DM & Hare GR "Physical model testing of a COB armoured structure" Report IT344, Hydraulics Research, Wallingford, January 1990, (Restricted).

Harding GD, Herbert DM & Smallman JV "WENDIS; the wave energy dissipation model" Report IT352, Hydaulics Research Wallingford, January 1991, (Restricted)

Allsop NWH, Herbert DM, Davis JP "Single layer armour units for breakwaters: their design and hydraulic performance" Proc Symp Developments in Coastal Engineering, University of Bristol, March 1991.

Toner WL, Waldron P, & Floyd JA "Structural behavior of single layer concrete breakwater armour units" Proc Symp Developments in Coastal Engineering, University of Bristol, March 1991.

Smallman JV "Developments in numerical modelling of waves" Proc Symp Developments in Coastal Engineering, University of Bristol, March 1991.

Bullock G & Bird P "Field measurements of the wave climate" Proc Symp Developments in Coastal Engineering, University of Bristol, March 1991.

Jones, R J & Herbert, D M. "Physical model testing of a Shed armoured structure" Report IT 361 (Restricted), Hydraulics Research, Wallingford, March 1991.

Allsop NWH & Herbert DM "Single layer armour units for breakwaters" Report SR 259, Hydraulics Research, Wallingford, March 1991.

Clifford JE "Breakwater research - single layer armour units" Dock & Harbour Authority, London, to be published April 1991.

Waldron P & Toner WL "Dynamic loads on concrete breakwater armour units" Proc Conf structural design for hazardous loads, Brighton, 17-19 April 1991.